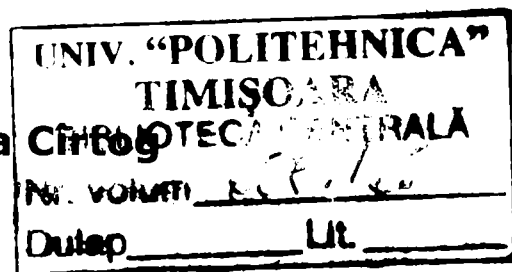


**CONTRIBUTII
LA STUDIUL FENOMENULUI DE
TRECERE
A CALDURII CU SCHIMBARE DE FAZA,
UTILIZAND SISTEME CU TUBURI
PARALELE**

**EXPERIMENTAL INVESTIGATION OF
PARALLEL TUBE HEAT TRANSPORT
DEVICES USING PHASE CHANGE OF
WATER**

Teză destinată obținerii
titlului științific de doctor inginer
al
Universității Politehnica din Timișoara
în domeniul INGINERIE MECANICĂ
de către

Ing. Adina Petronela



Conducători științifici: prof. dr. ing. habil Ioana Ionel
prof. dr. ing. Sadanari Mochizuki
Referenți științifici: conf. dr. ing. Adrian Briggs
prof. dr. ing. Romeo Susan-Resiga
prof. dr. ing. Gheorghe Dumitrașcu

Ziua susținerii tezei: 10.05.2008

Seriile Teze de doctorat ale UPT sunt:

- | | |
|------------------------|---|
| 1. Automatică | 7. Inginerie Electronică și Telecomunicații |
| 2. Chimie | 8. Inginerie Industrială |
| 3. Energetică | 9. Inginerie Mecanică |
| 4. Ingineria Chimică | 10. Știința Calculatoarelor |
| 5. Inginerie Civilă | 11. Știința și Ingineria Materialelor |
| 6. Inginerie Electrică | |

Universitatea „Politehnica” din Timișoara a inițiat seriile de mai sus în scopul diseminării expertizei, cunoștințelor și rezultatelor cercetărilor întreprinse în cadrul școlii doctorale a universității. Seriile conțin, potrivit H.B.Ex.S Nr. 14 / 14.07.2006, tezele de doctorat susținute în universitate începând cu 1 octombrie 2006.

Copyright © Editura Politehnica – Timișoara, 2008

Această publicație este supusă prevederilor legii dreptului de autor. Multiplicarea acestei publicații, în mod integral sau în parte, traducerea, tipărirea, reutilizarea ilustrațiilor, expunerea, radiodifuzarea, reproducerea pe microfilme sau în orice altă formă este permisă numai cu respectarea prevederilor Legii române a dreptului de autor în vigoare și permisiunea pentru utilizare obținută în scris din partea Universității „Politehnica” din Timișoara. Toate încălcările acestor drepturi vor fi penalizate potrivit Legii române a drepturilor de autor.

România, 300159 Timișoara, Bd. Republicii 9,
tel. 0256 403823, fax. 0256 403221
e-mail: editura@edipol.upt.ro

Foreword

The present research work was done during my doctoral study in the Department of Mechanical Systems Engineering at Tokyo University of Agriculture and Technology in collaboration with „Politehnica” University of Timisoara. Fortunately, I was granted by the Government of Japan a Monbukagakusho scholarship for a period of three and a half years (from October 2004 till March 2008) and this made possible for me to accomplish my study.

The research topic which makes the subject of the present dissertation is of a high international interest nowadays due to the rapid advancement of technology. High heat disipation equipments require high performant cooling devices. Heat transfer with phase change is a very attractive cooling process. Although many types of heat transport devices (HTD) have been developed in the past decades, a more performant cooling system is still needed. Therefore, a new concept of HTD was developed and experimentally investigated during my PhD study. The project was succesfully ended and the two new devices described in this dissertation, proved to be more efficient than the conventional HTD.

I would like to take this opportunity to express my deepest gratitude to my supervisors, prof. dr. eng. Sadanari Mochizuki from Tokyo University of Agriculture and Technology and prof. dr. eng. Ioana Ionel from „Politehnica” University of Timisoara, for their guidance and support. I will always be thankful for the kind advices, the patience and the time they spent for me.

Appreciation is also expressed to prof. dr. eng. Akira Murata, prof. N. Arai, prof. M. Kameda and prof. N. Nishiwaki for their valuable comments and suggestions related to the present research. For his professional help, discussions and suggestions regarding my study I would like to express my deepest gratitude to dr. Jaroslav Hemrle. I also appreciate very much his kindness and the time he spent to help me with daily life issues. I am thankful to Mr. Hiroshi Saito for his help regarding technical matters. For their friendship and kind attitude, I would like to thank to all laboratory members. Thanks to them, the atmosphere around me was always a warm and comfortable one.

I would like to thank to the reviewers, dr. Adrian Briggs, prof. dr. eng. Gheorghe Dumitraşcu and prof. dr. eng. Romeo Susan-Resiga, for the time they dedicated reading my dissertation and for the precious advices. Also, I must thank to prof. dr. ing. Stoian Petrescu, for his valuable comments related to the present study and for his kind intentions to collaborate in continuing this research.

I would like to express my gratitude to the chairman of the committee, prof. dr. eng. Liviu Bereteu, the dean of the Faculty of Mechanical Engineering at „Politehnica” University of Timisoara and to all members of the TMTAR department.

Special thanks go to my family and friends who always supported and encouraged me, and gave the strength to move forward. Although this study took me away from them, they have been always understanding and happy for my success. Not at last, I am truly grateful to my dear fiancé David Ross, for providing me with love, patience and understanding during all this time.

Timișoara, May 2008

ing. Adina P. Cîrtog

Cîrtog, Adina Petronela

Contribuții la studiul fenomenului de trecere a căldurii cu schimbare de fază, utilizând sisteme cu tuburi paralele

Experimental investigation of parallel tube heat transport devices using phase change of water

Teze de doctorat ale UPT, Seria 9, Nr. 28, Editura Politehnica, 2008, 130 pagini, 98 figuri, 1 tabel.

ISSN: 1842-4937

ISBN: 978-973-625-646-2

Cuvinte cheie:

Flux termic, schimbare de fază, dispozitiv cu tuburi paralele, investigații experimentale, agent de lucru apă, performanța ridicată, tub termic, optimizarea transferului de căldură.

Rezumat:

Lucrarea de față tratează modalități de îmbunătățire a sistemelor de transport a căldurii. Datorită nevoilor actuale de protecție a echipamentelor electrice și electronice, au fost concepute diverse modalități de înlăturare a energiei degajate sub forma de căldură. În urma studiului literaturii de specialitate s-a constatat că deși actualele sisteme de transport a căldurii au fost studiate și îmbunătățite de-a lungul ultimelor decenii, încă este o nevoie acută de dezvoltare a unor sisteme cât mai eficiente. Analizând informațiile existente în literatură referitoare la avantajele și dezavantajele actualelor sisteme, precum și a nivelului actual de cunoaștere în domeniu, s-a conturat ideea construirii noului sistem de transmitere a căldurii descris în lucrarea de față. Rezultatele prezentate sunt bazate pe experimente efectuate în laborator utilizând instalații pilot de scară redusă, fiind special concepute pentru elucidarea problemelor și atingerea scopurilor de cercetare impuse de tematica tezei. Datele obținute au fost comparate cu cele ale echipamentelor de răcire convenționale existente și s-a constatat că, instalațiile pilot concepute s-au dovedit mult mai performante. De asemenea, eficiența acestora este explicată și argumentată de unicitatea fenomenelor observate.

Teza originală a fost redactată în limba engleză iar un rezumat în limba română al lucrării este anexat la sfârșit.

CONTENT

Abstract	7
Nomenclature	9
1. Chapter: INTRODUCTION	11
1.1 Background of research	11
1.1.1 Thermosiphon	12
1.1.2 Heat Pipes	13
1.1.3 Meandering Closed Loop	14
1.1.4 Concept of PT-HTD	16
1.2 Objectives of the present study	17
1.3 Organization of the thesis	18
2. Chapter: PT-HTD with two tubes of different diameter.	19
2.1 Experimental set up and Procedure	19
2.2 Data Reduction and Measurements Uncertainly	21
2.3 Results and Discussions	23
2.3.1 Performance of the present HTD	23
2.3.2 Mechanism of fluid flow	24
2.3.2.1 Pressure measurements	24
2.3.3.2 Flow visualizations results	26
2.3.3 Effect of device orientation	29
2.3.4 Effect of tubes length	34
2.3.5 Effect of working fluid filling ratio	36
2.4 Flow visualization analysis	42
2.4.1 Flow velocity estimation method	42
2.4.2 Flow visualization analysis	46
2.5 Conclusions	50
Appendix - 2.....	51
3. Chapter: PT-HTD with five parallel tubes	57

3.1 Experimental set up and Procedure	57
3.2 Data Reduction and Measurements Uncertainly	61
3.3 Results and Discussions	62
3.3.1 Vertical orientation	62
3.3.1.1 Performance of the 5-PT-HTD	62
3.3.1.2 Relationship between tube wall temperature measurements and the fluid phase inside the tubes	65
3.3.2 Horizontal orientation.....	67
3.3.3 Bent tubes	69
3.3.2.1 Performance of present test section	69
3.3.2.2 Inner flow behaviour and performance	70
3.4 Conclusions	75
Appendix – 3	76
4. Chapter: Summary and General Conclusions	99
References	102
Author’s publications	107
Japanese summary	109
Romanian summary	111

ABSTRACT

High-performance cooling techniques for high density energy dissipation are nowadays required. Heat transfer with phase change is a very attractive cooling process. The need for a more compact and efficient heat transport device (HTD) led to the development of the new devices presented in this thesis. The characteristics of the novel devices consist in their different structure as compared with the conventional HTDs. The devices consist of parallel tubes connected to an evaporator (hot header) and a condenser (cold header). The new HTDs have the advantage of the tubes being open to both headers and therefore, the resistance in the flow existing in case of a meandering closed loop (MCL) is avoided. The tubes are simple, without any internal structure (wick) and compared with conventional heat pipes (HP), the performance of the new devices is not limited by the capillary limit.

(I.) The first device introduced in this thesis consists of two different diameter tubes arranged in parallel which connect an electrically heated evaporator and a water cooled condenser. There are various parameters that affect the fluid flow and heat transport characteristics of the device. They are (a) geometrical properties (diameter and length of the tubes), (b) orientation of the device (c) type of working fluid (d) amount of charged working fluid and (e) evaporator and condenser temperatures. Experiments were conducted systematically using water as the working fluid. Time-dependent temperatures and pressures at the evaporator and the condenser were continuously measured and recorded. The heat transport rate was obtained from the temperature rise and mass flow rate of cooling water flowing through the condenser. Flow visualization was also performed and the inner flow behaviour was analysed using the video recordings by high-speed-camera.

From the present study it was found that the new HTD had much higher performance as compared to conventional HPs of similar sizes, and this was attributed to the unique mechanism of fluid flow. One-way recirculation was maintained to occur, with vapour up-flow from evaporator to condenser through the larger diameter tube, and condensate return flow from condenser back to evaporator through the smaller diameter tube. Through the separation of the two phases of the fluid into the two different tubes, the entrainment limit existing in

conventional HP (due to the two streams flowing in opposite directions in one tube) was avoided. In the range of experiments performed for this device, it was found that, (1) the present device can transport three to four times more heat (800W) than a conventional HP of similar sizes; (2) the optimum orientation was vertical with the evaporator at the bottom, (3) the optimum filling ratio was found to be 40% of the total inner volume of the test core, and (4) the optimum length of the tubes was 530mm.

(II.) For further improvements of HTDs, a new test section was designed, manufactured and tested under different conditions. The second test section introduced in this study consists of five parallel tubes of same diameter. The geometry of the headers differs from the previous test section. Based on the results obtained in the first investigated test section, the new experimental conditions were established, in order to increase the heat transport performance. A series of test were run under certain conditions, to determine the relation between the mechanism of fluid flow and the heat transport performance.

In the range of experiments performed and presented in this study, it was found that, the inner flow behaviour changes with temperature and that gravity plays an important role for the fluid recirculation (i.e. reflected in the efficiency of heat transport). The performance of the present device compared with that of conventional HP was found to be much higher. The effective thermal conductivity was 200 times higher than that of copper. Also, through flow visualizations, the method of estimating the fluid phase inside the copper tubes by measuring the tube wall temperature was proved to be reliable.

Nomenclature

A_t	total cross sectional area of the tubes (based on inner diameter) [m^2]
c_p	specific heat at constant pressure [$\text{J}/(\text{kg}\cdot\text{K})$]
k_{eff}	effective thermal conductivity [$\text{W}/(\text{m}\cdot\text{K})$]
l	distance from evaporator to condenser [m]
P_{co}	pressure inside condenser [kPa]
P_{ev}	pressure inside evaporator [kPa]
\dot{Q}	heat transport rate [W]
$T_{w, in}$	inlet temperature of cooling water [$^{\circ}\text{C}$]
$T_{w, out}$	outlet temperature of cooling water [$^{\circ}\text{C}$]
T_{ev}	temperature inside evaporator [$^{\circ}\text{C}$]
T_{co}	temperature inside condenser [$^{\circ}\text{C}$]
T_{fco}	fluid temperature inside condenser [$^{\circ}\text{C}$]
T_{fev}	fluid temperature inside evaporator [$^{\circ}\text{C}$]
T_{wev}	evaporator wall temperature [$^{\circ}\text{C}$]
T_{wco}	condenser wall temperature [$^{\circ}\text{C}$]
T_e	tube wall temperature close to evaporator [$^{\circ}\text{C}$]
T_m	tube wall temperature at the middle of the tube [$^{\circ}\text{C}$]
T_c	tube wall temperature close to condenser [$^{\circ}\text{C}$]
ΔT	temperature difference between evaporator and condenser [$^{\circ}\text{C}$]
\dot{V}	volumetric water flow rate [m^3/s]
γ	working fluid volume fraction [-]
θ	inclination angle, [$^{\circ}$]
ρ	density [kg/m^3]

1. INTRODUCTION

1.1 Background of research

The rapid development of electronic equipments lead to an increase of heat dissipation and therefore, high-performance cooling techniques are nowadays required. Heat sinks and fans attached to the heat generating components are commonly employed for relatively low power dissipation systems such as personal computers. However, for components with higher heat dissipation, the conventional air-cooled heat sinks may encounter problems because of its bulky size, noise and insufficient cooling performance. One of the proposed solutions for dissipating high heat fluxes is the use of cooling techniques with phase change. Two-phase heat transfer is a very attractive cooling process, as high heat fluxes can be achieved through vaporization of the fluid in an evaporator attached to or enclosing the heat source. An inconvenience which appears in this case is that the process of the vapour condensation and the returning of the condensate to the evaporator, adds complexity in the system. In order to achieve high heat transport performance, many kinds of heat transport devices (HTD) with phase change have been developed in the recent decades. Above all, thermosyphons [3, 8, 12, 30, 33, 37], heat pipes (HP) [2, 7, 10, 15, 29, 31, 34, 36], and meandering closed loops (MCL) [1, 4, 5, 6, 9, 11, 17, 18, 19, 20, 22, 23, 24, 32, 35] are well known. An example of common CPU cooling using heat pipes can be seen in Fig. 1.1

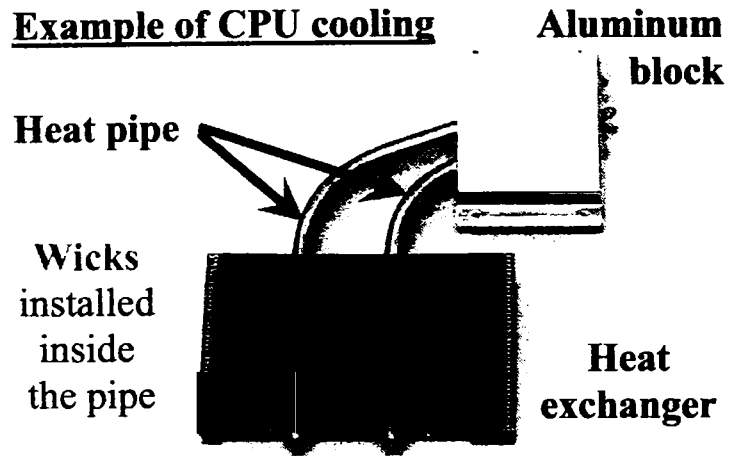


Fig. 1.1 Example of CPU cooling using heat pipes

1.1.1 Thermosiphon

Thermosiphon heat exchangers are sealed systems that consist of an evaporator, a condenser, interconnecting piping, and an intermediate working fluid that is present in both liquid and vapor phases. Two types of thermosiphon are used—coil type and sealed tube type. In the sealed tube thermosiphon, the evaporator and the condenser are usually at opposite ends of a bundle of straight, individual thermosiphon tubes, and the exhaust and supply ducts are adjacent to each other (this arrangement is similar to that in a heat pipe system). In coil-type thermosiphons, evaporator and condenser coils are installed independently in the ducts and are interconnected by short lengths of working fluid piping (this configuration is somewhat similar to that of a coil loop system). In thermosiphon systems, a temperature difference and gravity cause the refrigerant to circulate between the evaporator and condenser.

Advantages

- passive heat exchange with no moving parts,
- relatively space efficient,
- the cooling or heating equipment size can be reduced in some cases,
- the moisture removal capacity of existing cooling equipment can be improved,
- no cross-contamination between air streams with coil type.

Disadvantages

- adds to the first cost and to the fan power to overcome its resistance,
- requires that the two parts be placed so that the liquid condensate can return to the evaporator part by gravity,
- may require a significant temperature difference to initiate boiling,

Although similar in form and operation to heat pipes, thermosiphon tubes are different in two ways: (1) they have no wicks and hence rely only on gravity to return the condensate to the evaporator, whereas heat pipes use capillary forces; and (2) thermosiphon tubes depend, at least initially, on nucleate boiling, whereas heat pipes vaporize the fluid from a large, ever-present liquid vapor interface. As a result, thermosiphon heat exchangers may require a significant temperature difference to initiate boiling. Thermosiphon tubes require no pump to circulate the working fluid. However, the geometric configuration must be such that liquid working fluid is always present in the evaporator section of the heat exchanger.

Few typical examples of thermosiphon applications are: collection and utilization of solar energy; domestic heating and cooling; thawing of snow on major roads; thermal control of food storage units and commercial fisheries; thermal treatment of exterior coating in auto industries [8].

1.1.2 Heat Pipes

The rapid evolution of technology from the past decades led to further development of HTDs and improvement of their performance. For example, most commonly used for CPU cooling and for space crafts are the so called heat pipes (HP). A heat pipe is a heat transfer mechanism that can transport large quantities of heat with a very small difference in temperature between the hotter and colder interfaces. They are capillary driven heat transport devices and have the advantage of not being depended on gravity. Though, the wick providing the capillary action for the condensate return to evaporator adds complexity of construction and introduces a limitation for the heat transport. The reducing in size of electronic components results in a need to reduce the size of cooling devices as well which means, reducing the heat transfer area. One of the problems encountered in the HP design is that reducing the inner diameter, the capillary limit in heat transport rate decreases rapidly below a value needed for the heat spreader [7]. Therefore, a lot of research in this field has been done and many type of wick structure where investigated.

Beside the type of wick, other parameters (diameter and length, temperature range, working fluid, container material, etc.) where considered as well. At present, there exists a large variety of HP. A simple schematic of a HP structure can be seen in Fig. 1.2. A typical heat pipe consists of a sealed hollow tube. A thermo-conductive metal such as copper or aluminum is used to make the tube. The pipe contains a relatively small quantity of a "working fluid" or coolant (such as water, ethanol or mercury) with the remainder of the pipe being filled with vapor phase of the working fluid, all other gases being excluded. On the internal side of the tube's side-walls a wick structure exerts a capillary force on the liquid phase of the working fluid. The wick structure is typically a sintered metal powder or a series of grooves parallel to the tube axis, but it may in principle be any material capable of soaking up the coolant. Inside a heat pipe, at the hot interface a fluid turns to vapor and the gas naturally flows and condenses on the cold interface. The liquid falls or is moved by capillary action back to the hot interface to evaporate again and repeat the cycle [29].

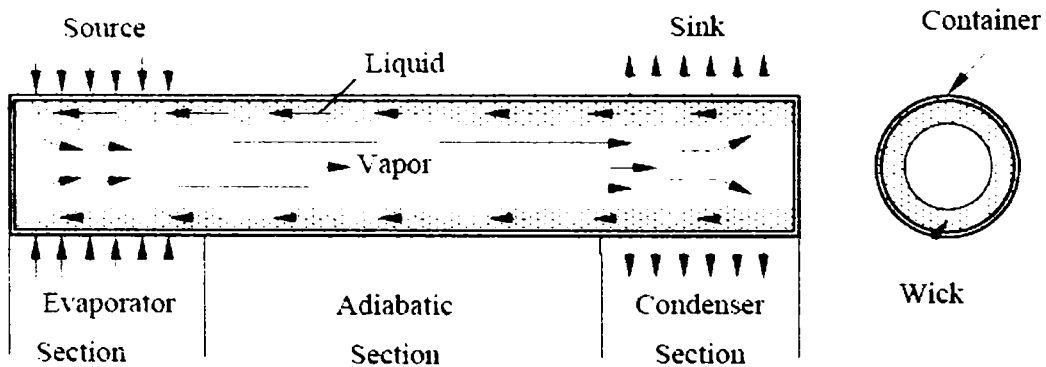


Fig. 1.2 Structure of a typical heat pipe

1.1.3 Meandering Closed Loops (MCL)

Another type of heat transport device introduced by Akachi [1] in the recent years consists in a closed meandering loop in which heat is transported from the hot end to the cold end by oscillating motion of liquid column and vapor plugs. Schematic of a meandering closed loop is shown in Fig. 1.3. The liquid and vapor slug/bubble transport is caused by the thermal induced pressure pulsations inside the device and no external mechanical power is required [18, 19, 20].

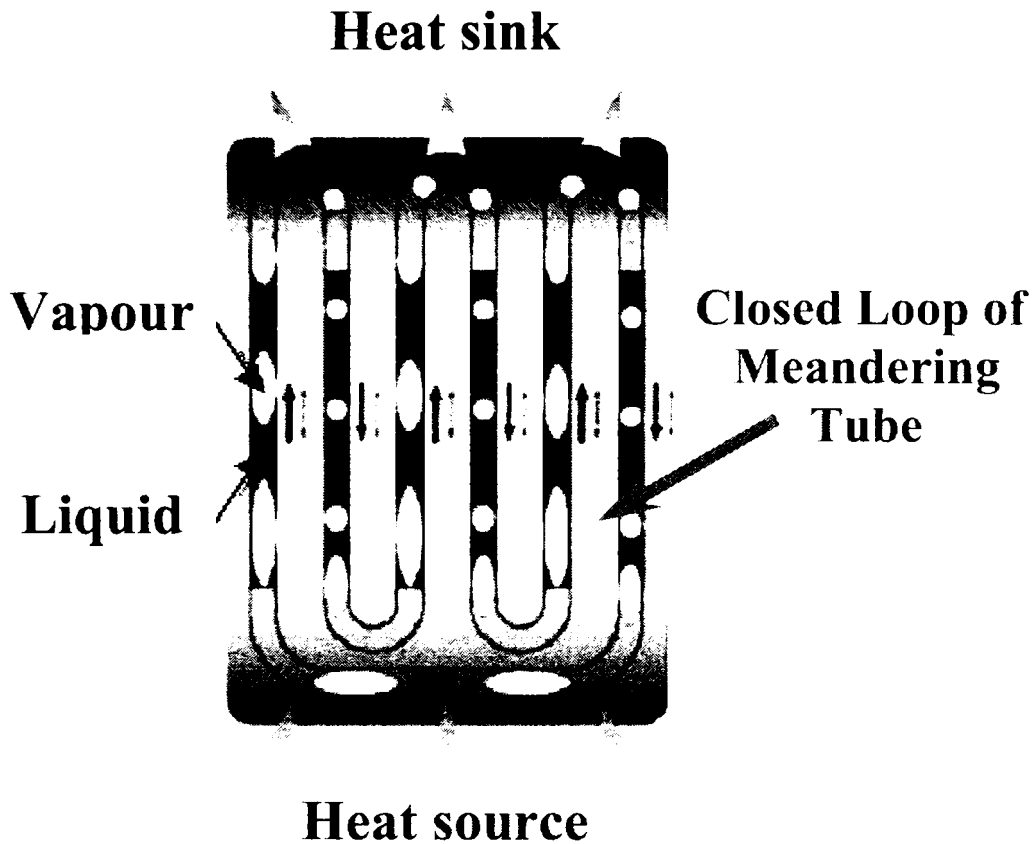


Fig. 1.3 Meandering Closed Loop

Compared with the traditional heat pipes, the pulsating heat pipes present a number of features:

- (1) higher driving force; thermally driven pulsating flow combining with a capillary force;
- (2) lower pressure drops: parallel flows and no wick structure in most of the fluid paths;
- (3) higher heat transfer coefficients: evaporating/condensing heat transfer combining with forced convection [22]

One of the MCL limitations consists in the maximum inner diameter above which the vapor plug can not be formed [25]. Many research works were conducted to investigate the characteristics of pulsating heat pipe [1, 4, 5, 6, 9, 11, 17, 18,

19, 20, 22, 23, 24, 32, 35] and still, the mechanism governing the pulsating phenomena have not been fully understood yet [22].

1.1.4 Concept of Parallel Tubes HTD (PT-HTD)

A newly developed HTD in our laboratory is the Parallel Tube HTD which compared to the MCL was the advantage of the tubes open to the headers and proved to have two times higher performance than same diameter and same number of turns MCL. [27]. A typical representation of a PT-HTD can be seen in Fig. 1.4, where the cold and hot headers are connected by parallel tubes of same diameters. Many test cores where investigated, based on different parameters (like, headers geometry, numbers of tubes and diameter of tubes) [28]. The reciprocating motion of the vapor and liquid plugs in the capillary tubes was considered to be responsible for the high heat transport performance of the PT-HTD.

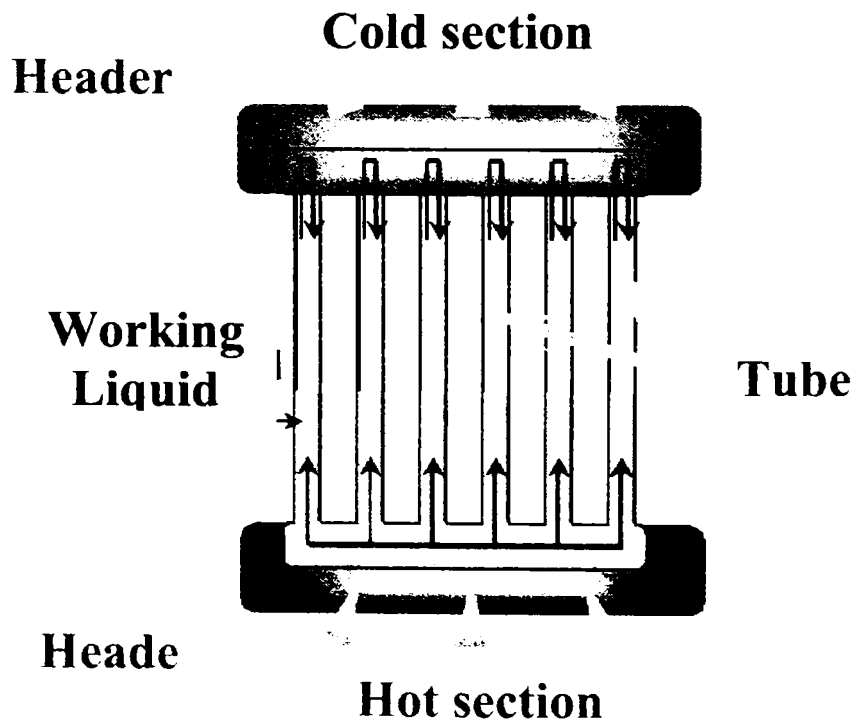


Fig. 1.4 Parallel Tubes Heat Transport Device

1.2 Objectives of the present study

From the above brief introduction, and the researcher work available in the literature [1-37], it can be concluded that, the existing HTDs, although used in many application, do have some limitations. Also, there are still many unclear issues regarding the correlation between some of the observed phenomena and the performance of the corresponding HTD. Further investigations on this issue are required.

Nowadays rapid development of electronic equipments implies a need for more compact and efficient heat transport device, able to coop with the high density of heat dissipation. This led to the design and investigation of the novel device which makes the subject of the present study. Heat transport with phase change is a very attractive way to carry heat from one place to the other. There are various parameters that affect the flow and heat transport performance. The understanding of the mechanism of fluid flow and its relation to the heat transport performance is crucial for a further improvement of HTD.

Many characteristics of the conventional HTDs were considered before designing the novel device. As compared to previous HTDs introduced in 1.1, the new developed HTD has the advantage of higher heat transport performance achieved through a simple structure with self pump mechanism. The device consists of an evaporator and a condenser chamber connected by two parallel tubes of different diameter. The tubes are simple without a wick structure and therefore, no capillary limit is present in the novel device as compared to HPs. The advantage over the MCL consists in providing the headers, the hot and cold header respectively, to which both tubes are opened. In this regard, the new HTD is more close to a thermosiphon-loop. The key point of the novel device structure consists in the combination of two different diameter tubes. The target beyond this design was to establish a recirculation of the fluid with high efficiency in heat removing and avoiding of evaporator dry-out. This was though to be achieved by separating the vapor flow through the larger diameter tube and the condensate return through the smaller diameter tube, avoiding in this way the entrainment limit (due to the two fluids flowing in opposite directions).

657.165



1.3 Organization of the thesis

The present dissertation is revealing a new concept of HTD for which two different test sections were investigated. The background of research and the literature review are introduced in the first chapter. Chapter 2 is related to a novel HTD with two parallel tubes of different diameters for which various parameters were investigated. The effect of each parameter is treated in a separate subchapter. The common experimental set up and details of the test section are introduced only once at the beginning of respective chapter. Chapter 3 is introducing the second test section for which the conditions of experiments were decided based on the results presented in Chapter 2, aiming a further improvement in the HTD performance. Chapter 4 summarizes the main findings of present research, contributions in the related field and link for the continuity (approach to applications). The Nomenclature for both test cores, is introduced only once at the beginning of the thesis. Appendixes for auxiliary details are provided for each chapter. All references are listed in a section at the end of the thesis.

2. Parallel tube heat transport device (PT-HTD) with two tubes of different diameter.

2.1 Experimental setup and procedure

A schematic of the experimental setup is shown in Fig. 2.1. The test section consists of two cylindrical chambers (40 mm in diameter and 20 mm in axial length) and two 215-mm-long (initial length) copper tubes. The two tubes are arranged in parallel and have a different inner diameter of 3.5 mm and 6.5 mm. An electrical ceramic heater (50x50) is attached on the backside of the evaporator and it is connected to a regulated electric power source.

Water cooling coils are installed inside and backside of the condenser. The coils are connected to a constant head water reservoir to insure a steady cooling water flow rate. The cooling water flow rate was measured using a graduate cylinder and a stop watch. Providing a constant head for the reservoir of the cooling water, there was no significant fluctuation of the volume flow rate. The flow rate was checked for each point of measurements and the corresponding value was input into the LabView program.

After the test core was evacuated to around 2 kPa through a vacuum pump, it was charged with a given amount of working fluid using a graduated syringe.

Thermocouples were used for measuring the temperatures of (1) inlet and outlet cooling water of condenser (2) working fluid inside the evaporator and condenser and (3) the ceramic heater attached to the evaporator. For measuring the temperature of cooling water inlet and outlet ($T_{w,in}$ and $T_{w,out}$), thermocouples were placed in the stream of the cooling water inlet to condenser (just before the branching to condenser back-wall and the copper coil), as well as in the stream of cooling water outlet, just after the mixing chamber (MC, see Fig.1 and Fig.2A-6). The two outlets of cooling water (one from the coil inside condenser chamber, and one from the backside wall) were connected to a small chamber to provide the mixture of the two streams. Two types of mixing chambers were used and the two results were in good agreement. The thermocouples outputs were fed to a DAQ card and the measured temperatures were recorded continuously during the experiments.

For each point of measurements, the corresponding temperature in time was measured, recorded and used in the further computation of the heat transport performance. The temperatures inside condenser chamber, T_{co} and inside evaporator chamber, T_{ev} were measured by the sheath-type thermocouples placed in the middle of each chamber and they were in contact with the working fluid in liquid and vapor phase. To reduce heat losses, thermal insulation is placed around the external surface of the evaporator and the copper tubes.

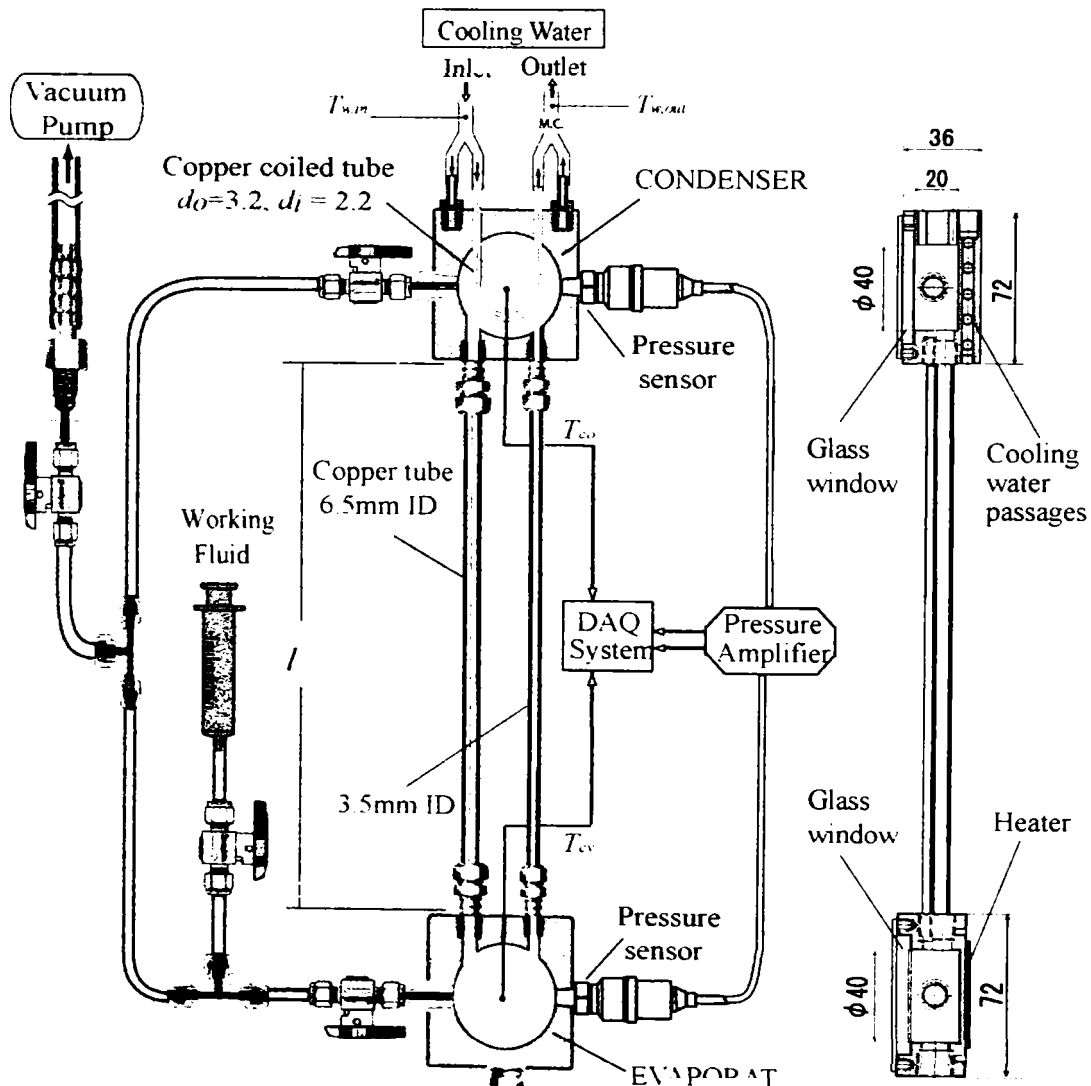


Fig. 2.1 Schematic of experimental setup

Two high precision pressure sensors (-100~100 kPa, 1 ms response time) were attached to both, the evaporator and condenser chambers.

Experiments were conducted systematically using pure water as working fluid. The effect of various parameters such as: (1) orientation angle of the device, (2) tube length, (3) amount of charged working fluid, and (4) heat input to the evaporator, on the fluid flow and heat transport characteristics were examined. The orientation angle θ is defined as indicated in Fig. 1.

Time-dependent temperatures and pressures at the evaporator and the condenser were continuously measured and recorded. The temperature and the pressure data were fed to a data acquisition (DAQ) system and were analyzed using LabView software. The LabView interface allows one to see the variation in time of all measured parameters, and to determine the steady state. Raw data from beginning to the end of experiments were recorded (including transient stage) as well as average values at the steady state of each point of measurements. Each value of Q shown in the present manuscript was obtained from the average of 6000 readings (or more), during the steady state, for an interval of minimum 10 minutes.

Inner flow behaviour was observed through the sight glasses attached to the front side of both the evaporator and condenser and it was recorded by digital high-speed video camera (DHSVC). For the flow visualization inside the tubes, the copper tubes were replaced by Teflon tubes.

2.2 Data reduction and Measurements uncertainty

The heat transport rate was obtained from the temperature rise and mass flow rate of cooling water flowing through the condenser. It was calculated by:

$$\dot{Q} = \rho c_p \dot{V} (T_{w,out} - T_{w,in}) \quad (1)$$

where $T_{w,in}$, $T_{w,out}$ and \dot{V} are the condenser inlet, outlet temperatures and the volume flow rate of the cooling water, respectively.

In the present study, an effective thermal conductivity, k_{eff} , was introduced as a measure of the heat transport performance of the device. It was defined by the following equation:

$$k_{eff} = \frac{\dot{Q}l}{A_t(T_{ev} - T_{co})} \quad (2)$$

where l is the tube length (distance between the evaporator and condenser) and A_t is the total of the inner cross sectional areas of the two tubes; T_{ev} and T_{co} are the working fluid temperature inside evaporator and condenser chamber

The overall thermal resistance, R_{total} , between the heater and the cooling water was calculated using the following relationship:

$$R_{total} = \left[T_{heater} - (T_{w,in} + T_{w,out})/2 \right] / \dot{Q} \quad (3)$$

Measurements Uncertainty

For the temperature measurements the accuracy of the thermocouples readings was of $\pm 0.2^\circ\text{C}$. Two methods were used to measure accurately the temperature of the cooling water outlet and the comparison resulted in a good agreement. The uncertainty of Q was estimated using the method of Kline and McClintock [21]. The error range was between 15% and 3%, for low and high heat input respectively. The majority of the experimental errors were less than 10%. Only at the lowest heat input the uncertainty was high as the error range relative to the low temperature difference of the cooling water resulted in a higher percentage error. For the pressure measurements, the accuracy was $\pm 2\text{kPa}$.

2.3 Results and Discussions

2.3.1 Performance of present device

For a better estimation of the PT-HTD performance, the heat transport rate was compared with the one of a heat pipe of similar size (diameter and length), same working fluid (water) and same orientation (vertical with evaporator at the bottom). Figure 2.2 shows the heat transport rate \dot{Q} versus evaporator temperature T_{ev} , and the performance of a conventional heat pipe [15] which has comparable dimensions ($l=150\text{mm}$, and $\phi=6.35\text{mm}$) with the preset two-tube system is also shown as a reference. From Fig.2.2 it can be seen that:

- (1) \dot{Q} increases with an increase in T_{ev} .
- (2) Although for relatively low T_{ev} , conventional HP shows higher \dot{Q} than the present HTD, for larger T_{ev} the present HTD shows superior performance, which is three to four times higher in \dot{Q} than the conventional HP.
- (3) The present device can transport more than 800W for T_{ev} below 100°C.

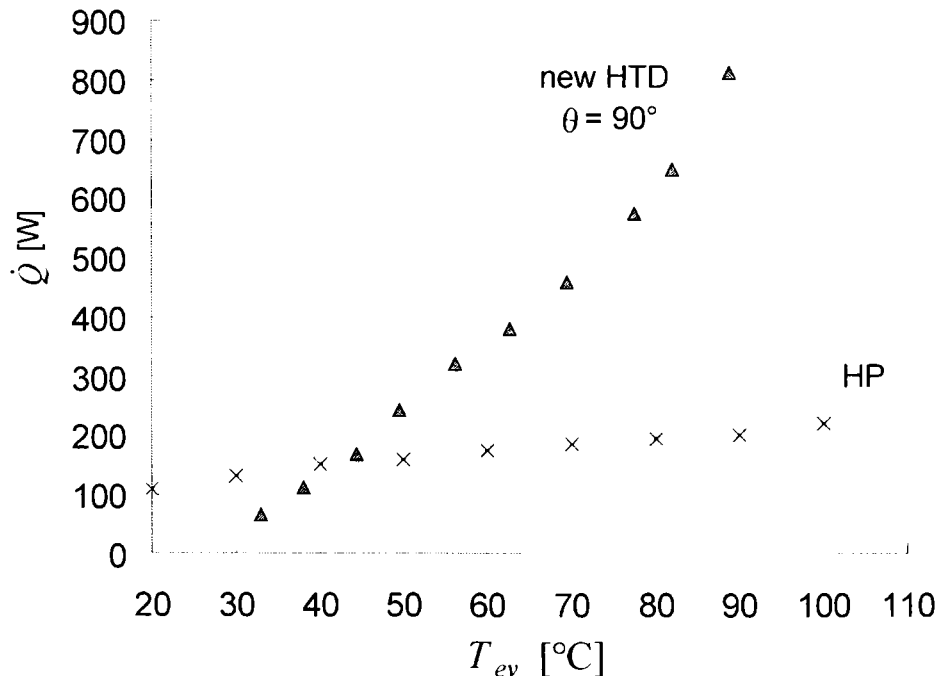


Fig. 2.2 Heat transport rate vs. evaporator temperature, compared with the performance of a conventional HP [15]

2.3.2 Mechanism of fluid flow

2.3.2.1 Pressure measurements

Figures 2.3 and 2.4 show the time-averaged evaporator and condenser pressure, $P_{ev,m}$ and $P_{co,m}$ versus evaporator and condenser temperature, T_{ev} and T_{co} , respectively, with γ as a parameter. The inclination angle is 90° . The saturation pressure curves are also indicated in the figures for comparison. From these two figures it is confirmed that the general trend of both $P_{ev,m}$ and $P_{co,m}$ agree fairly well with the corresponding saturation curve irrespective of the values of γ . However, by comparing the two figures closely, one can observe that the measured evaporator pressure, $P_{ev,m}$, is lower than the saturation curve while the measured condenser pressure, $P_{co,m}$, is slightly higher than the saturation curve. This will be discussed later.

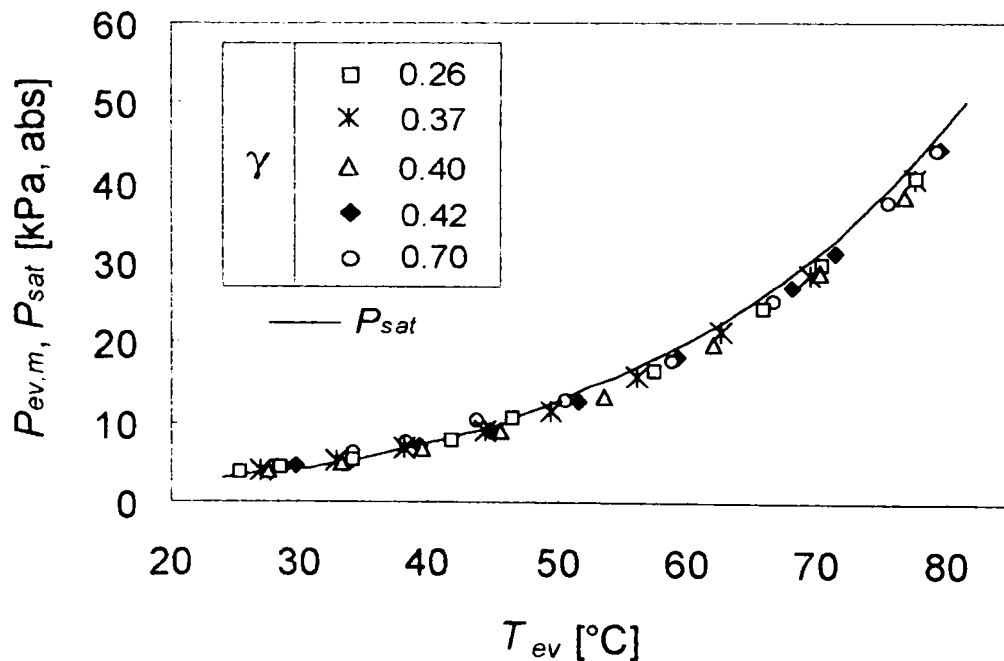


Fig. 2.3 Time averaged evaporator pressure, $P_{ev,m}$ vs. evaporator temperature, T_{ev} , in comparison with the saturation curve for different charging ratio, γ .

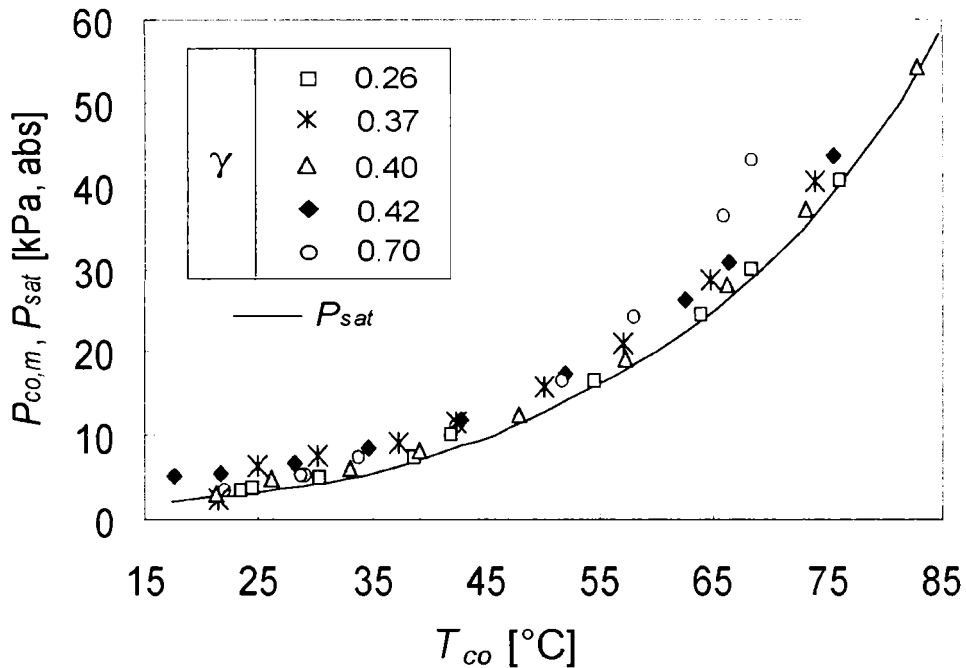


Fig. 2.4. Time averaged condenser pressure, $P_{co,m}$ vs. condenser temperature, T_{co} , in comparison with the saturation curve for different charging ratio, γ .

Figure 2.5 shows typical examples of the variation of evaporator and condenser pressure, P_{ev} and P_{co} , with time. One can see from the figure that: (1) Both P_{ev} and P_{co} oscillate periodically. (2) Oscillation amplitude of P_{co} is larger than that of P_{ev} . (3) Time averaged pressure is higher for P_{ev} than that for P_{co} . (4) When P_{co} reaches its peaks during the oscillation period, the value of P_{co} is almost the same or sometimes even higher than P_{ev} .

Above observations clearly indicate the existence of dynamic effect which is considered to be the main cause of the recirculation of the working fluid in the present devise. If the phenomenon were steady, no recirculation would occur because the temperature at the evaporator is always higher than that of condenser, and therefore the condenser pressure would be always lower than that of the evaporator resulting in no motive force to drive the condensate back to the evaporator. But in reality, boiling and bubble growth occurs intermittently by its very nature and it gives high momentum instantaneously to the vapour flow inside the larger-diameter tube. When the fluid is jetted out into the condenser this

momentum induces directly the pressure rise in condenser, with the pressure drop in evaporator at the same time. This situation causes the higher time averaged pressure than the saturation pressure in condenser and slightly lower pressure in evaporator as was indicated in Figs. 2.3 and 2.4.

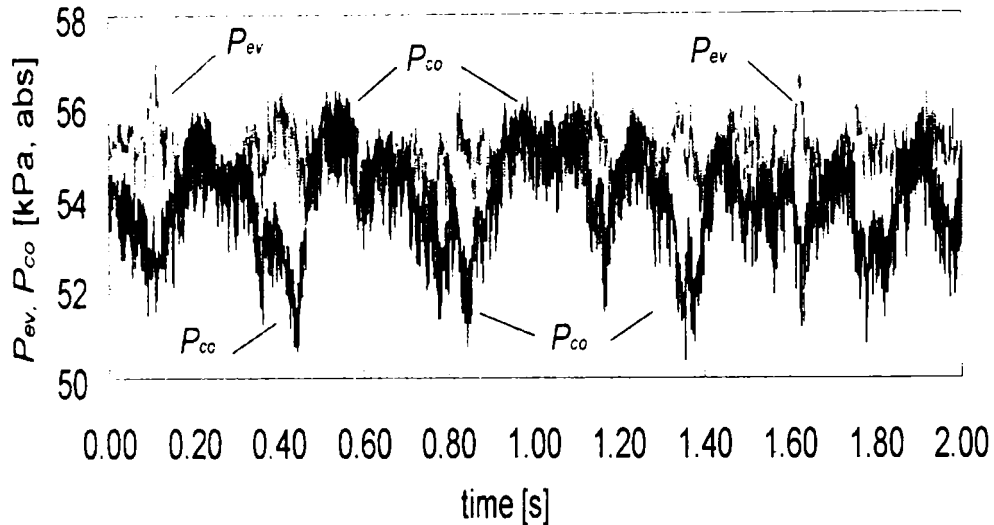
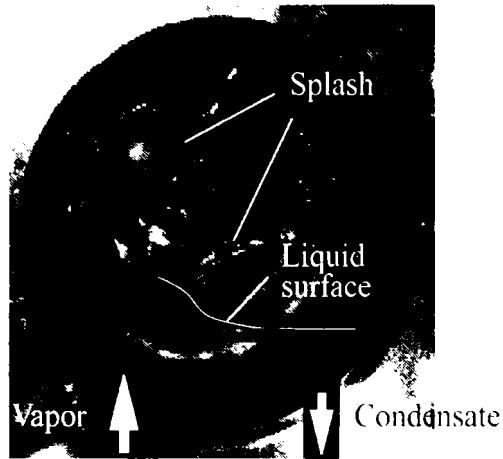


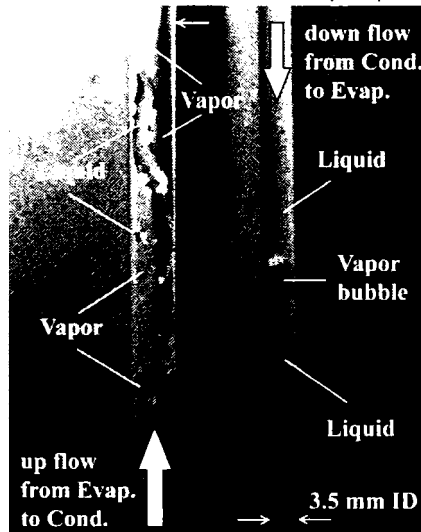
Fig. 2.5. Time-dependent change of evaporator and condenser pressure P_{ev} , P_{co} , for $\gamma=0.4$ and $\theta=90^\circ$.

2.3.2.2 Flow visualization

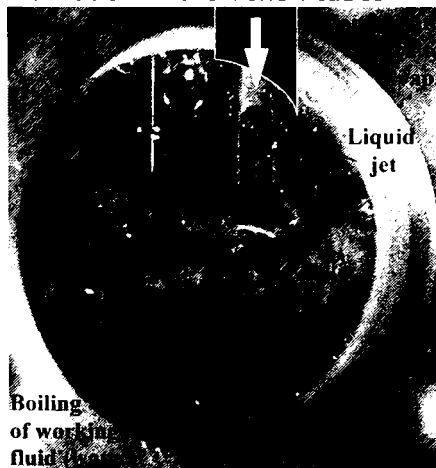
The flow through the larger-diameter tube from evaporator to condenser and the return of condensate from condenser to evaporator through the smaller diameter tube were confirmed when transparent Teflon tubes were used instead of copper tubes. By observing the fluid behaviour inside the tubes (especially of the larger diameter tube) and that inside the evaporator and condenser through the sight glass, one can clearly see that (1) periodic generation, growth and coalescence of vapour bubbles in the evaporator push the fluid inside the larger-diameter tube into the condenser, and (2) intermittent churn flow [13] is a typical two-phase flow pattern inside the larger-diameter tube.



2.6 Fluid flow in condenser chamber, captured by DHSVC.



2.7 Flow visualization in the Teflon tubes



2.8 Capture of the return flow inside evaporator chamber

Fig. 2.6 shows a representative movie frame of the flow inside the condenser obtained by a high speed digital video camera. The photo indicates the instant when the vapour jet coming out from the larger-diameter tube is penetrating the accumulated condensate inside the condenser forming a splash. Fig. 2.7 shows a typical frame of high speed movie records of the flows inside the tubes. Through slow motion re-play of the movie, one can observe the intermittent upward flow of vapour through the larger diameter tube from evaporator to condenser and the return flow of the condensate through the smaller diameter tube from condenser to evaporator. A clearer view of the liquid return is shown in Fig. 2.8 where a continuous jet of condensate entering the evaporator chamber can be seen.

As it was described above, the recirculation flow phenomenon was intermittent and its frequency increased with the evaporator temperature. The one-way recirculation was observed for all the orientation angles of the device and also for different charging ratio of the working fluid.

Mechanism of flow recirculation

The frequency of the intermittent jet flowing into the condenser (jetting) was examined by analyzing the recorded high-speed video-movie frames. The results were compared with the pressure oscillation records. It was found that the frequency of vapour jets entering the condenser chamber agreed very well with the frequency of pressure variations. For example, the frequency was about 4.5 Hz for both the jetting and the pressure oscillation for $T_{ev} = 85^{\circ}\text{C}$, $T_{co} = 82^{\circ}\text{C}$, $\gamma = 0.4$ and $\theta = 90^{\circ}$. The result leads to the conclusion that the pressure rise in condenser is directly induced by the incoming momentum of the vapour flow brought about by the intermittent jet from larger-diameter tube. The periodical abrupt increase of condenser pressure plus gravity (except the case of $\theta = 0^{\circ}$) drive the condensate back to evaporator through the smaller diameter tube, establishing the one-way recirculation of the flow.

2.3.3 Effect of device orientation

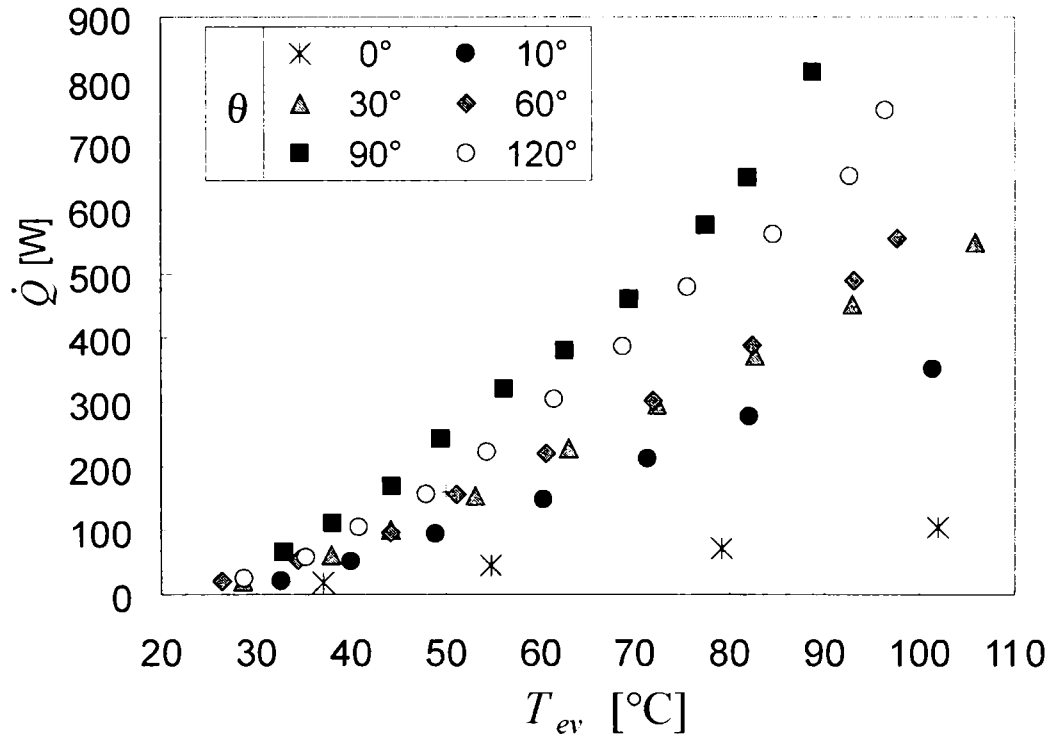


Fig. 2.9 Effect of device inclination on heat transport performance

There are many parameters which are affecting the performance of the present device. The gravity seems to play an important role in the fluid recirculation, which results in the efficiency of heat transport. Fig. 2.9 shows the variation of \dot{Q} with evaporator temperature with θ =the inclination angle as a parameter. It can be seen from the figure that:

- (1) \dot{Q} increases with an increase in T_{ev} irrespective of the inclination angles.
- (2) Inclination angle has significant effect on the heat transport performance. For a given evaporator temperature, vertical orientation ($\theta=90^\circ$) gives the highest performance and the horizontal orientation ($\theta=0^\circ$) gives the lowest. The heat transport characteristics do not coincide for the two cases, $\theta=60^\circ$ and 120° . This is because the contact area between the liquid working fluid and the heating surface in the evaporator, and that between the vapour and the cooling surface in the

condenser, are not the same for the two cases. From the side view of the test section, in Fig.2.1, one can see that the two cases are not symmetrical.

The main reason for the high heat transport performance of the present device may be attributed to the unique mechanism of fluid flow. Through the separation of vapor flow and condensate liquid flow in the two individual tubes, one-way recirculation of the fluid was established and the shear force at the vapor-liquid interface which exists in the conventional heat pipes was avoided eliminating the entrainment limit. In the range of the present study, the one-way recirculation was observed for all inclinations of the device. As one can observe in Fig. 2.9, the highest performance was achieved for the vertical orientation ($\theta = 90^\circ$) with \dot{Q} reaching a value of more than 800 W for an evaporator temperature below 100°C .

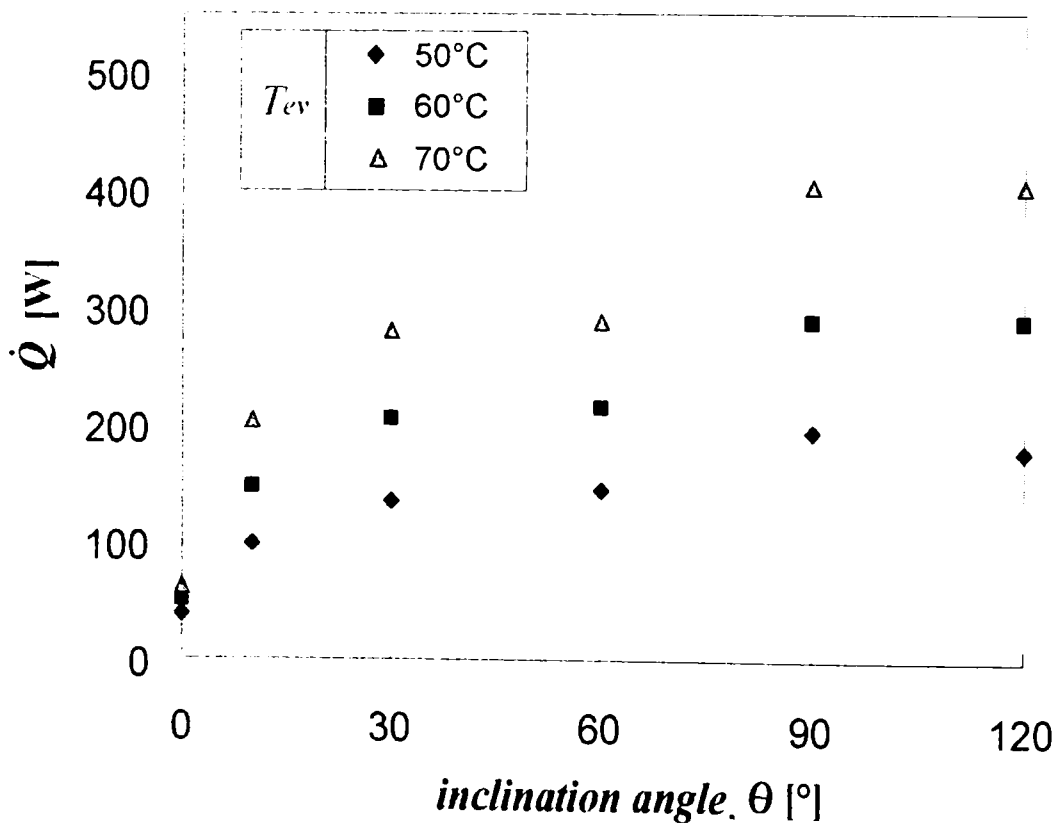


Fig. 2. 10 \dot{Q} vs. inclination angle with T_{ev} as a parameter

Fig. 2.10 shows \dot{Q} vs. θ for three different evaporator temperatures, T_{ev} . One can observe that, in all three cases, the highest value of \dot{Q} is achieved for the vertical orientation (90°). The horizontal orientation (0°) gives the minimum heat transport rate. For the same evaporator temperature, a small increase in the inclination from 0° to 10° brings an abrupt rise in the heat transport rate, \dot{Q} being up to three times higher. After \dot{Q} reaches the maximum at the vertical orientation ($\theta = 90^\circ$), the performance decreases with a further increase in the inclination angle. The difference between the 60° and 120° cases occurs because the structure of the test section is not symmetrical with respect to the centre plane as shown in Fig. 2.1. The contact area between the liquid working fluid and the hot surface of the evaporator, and the one between the vapor and the cold surface of condenser, changes with the inclination angle. This plays a certain role on the characteristic of heat transport phenomenon and influences the performance of the present device. Both, the boiling and the condensation are important in the entire process of transporting the heat efficiently. The higher performance of the 120° case compared to the 60° case indicates that the condenser is more dominant than the evaporator in the present system.

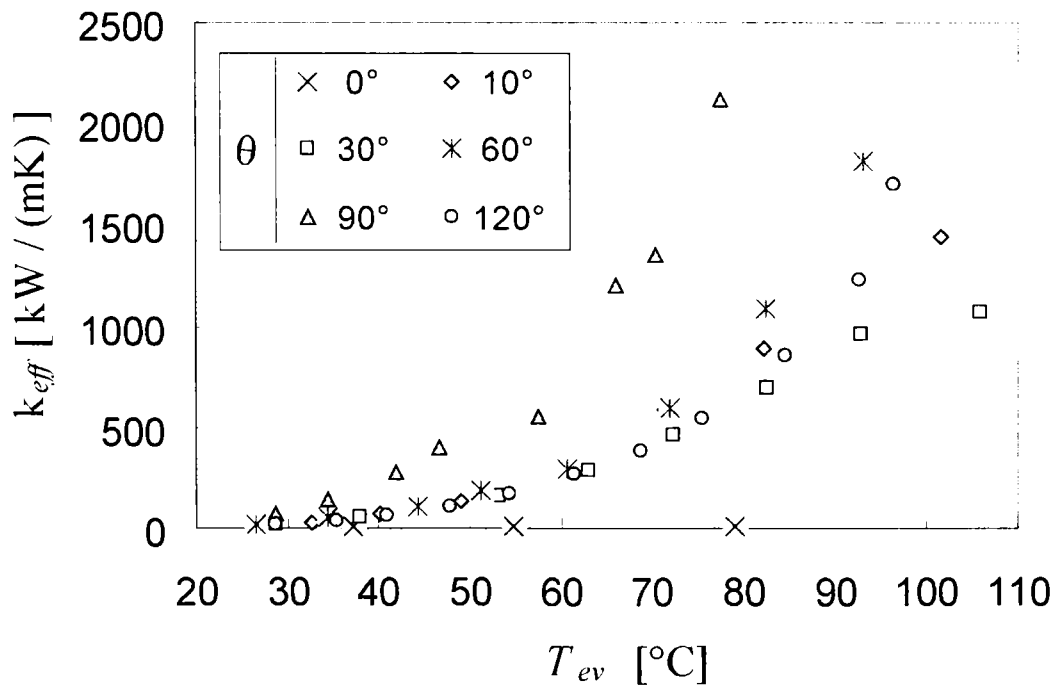


Fig. 2.11 Effective thermal conductivity, k_{eff} vs. evaporator temperature T_{ev} .

Figure 2.11 shows the effective thermal conductivity k_{eff} versus evaporator temperature T_{ev} with the inclination angle θ as a parameter. It can be seen from the figure that, k_{eff} is increasing with a rise of heat input. The highest value of k_{eff} obtained in the present experiment is about 2×10^6 W/(m·K) which is more than 5000 times higher than the thermal conductivity of copper, $k_{copper} \sim 400$ W/(m·K).

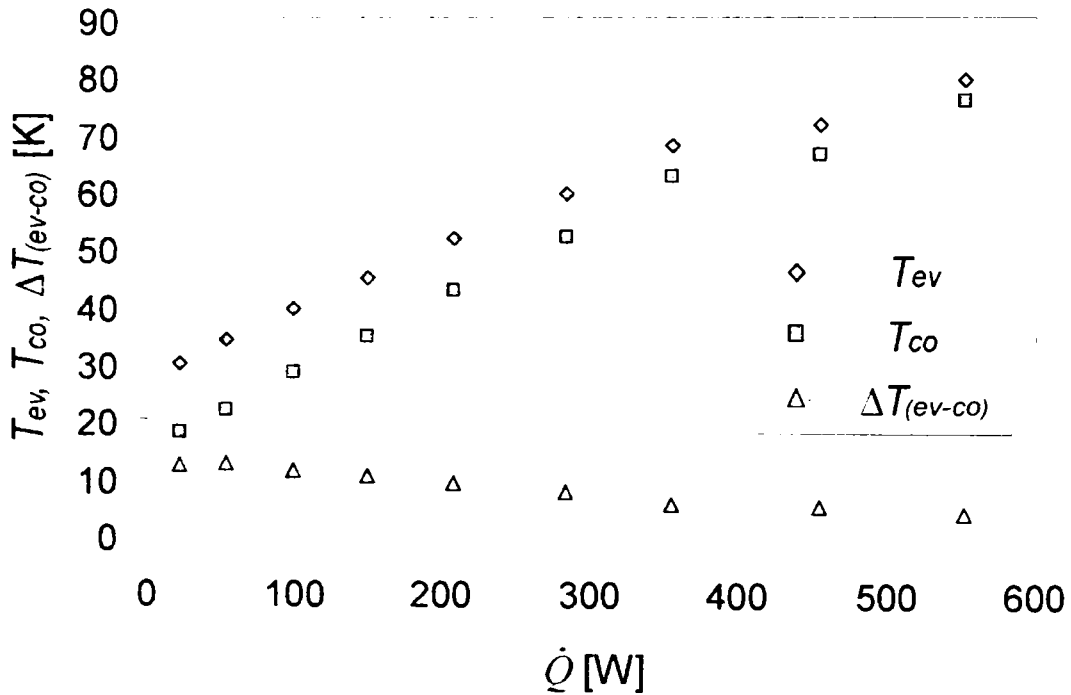


Fig. 2.12 Change of evaporator and condenser temperature, T_{ev} , T_{co} and their differences, $\Delta T_{(ev-co)}$, with heat transport rate, \dot{Q} , for $\gamma=0.4$ and $\theta=90^\circ$.

Figure 2.12 shows representative results of the temperature change in evaporator and condenser, T_{ev} and T_{co} , and their differences, ΔT_{ev-co} , with heat transport rate, \dot{Q} , for the vertical orientation. One can see from the figure that both T_{ev} and T_{co} increase while the difference between them decreases with an increase in \dot{Q} . This means that the heat transport efficiency (the heat transport rate, \dot{Q} , divided by the temperature difference, ΔT_{ev-co}) or the effective thermal conductivity, k_{eff} , increases rapidly as the heat transport rate increases as was observed in Fig. 2.11.

One can observe in Fig. 2.13 the results for the overall thermal resistance, R_{total} plotted against T_{ev} with the inclination angles as parameter. In this figure it is shown that R_{total} decreases with an increase in T_{ev} and that for an evaporator temperature larger than 50 °C, in case of $\theta = 90^\circ$, the values of the thermal resistances become as low as 0.2 °C/W. For the horizontal orientation, the thermal resistance is much higher, irrespective of T_{ev} .

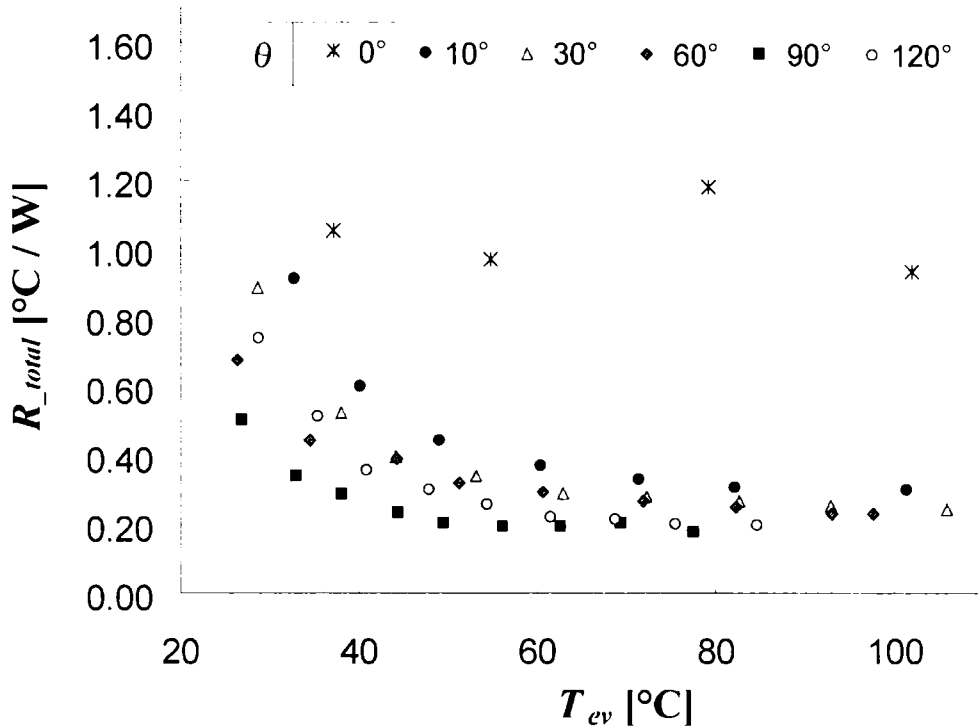


Fig. 2.13 Total thermal resistance vs. evaporator temperature, with θ as a parameter.

It can be concluded from this subchapter that, gravity plays an important role in the performance of the present device and therefore, the vertical orientation of device, $\theta = 90^\circ$, gives the highest performance.

2.3.4 Effect of tube length

In the present subchapter, a stress is put on the effect of tubes length on the heat transport performance. Experiments were performed for 6 different lengths of the tubes ranging from 215 to 750 mm.

Fig. 2.14 shows the variation of \dot{Q} as a function of tube lengths, l , for three different evaporator temperatures, T_{ev} . It is seen from the figure that \dot{Q} rises initially with an increase in l , reaches the maximum at $l=530\text{mm}$ and then decreases with further increase in l . Increasing the tube length brings an increase in gravity head that will enhance condensate return. Increase in gravity head, on the other hand may gradually cause reduction in pumping ability which is created by intermittent boiling. This is considered to be the reason for the existence of an optimum tube length.

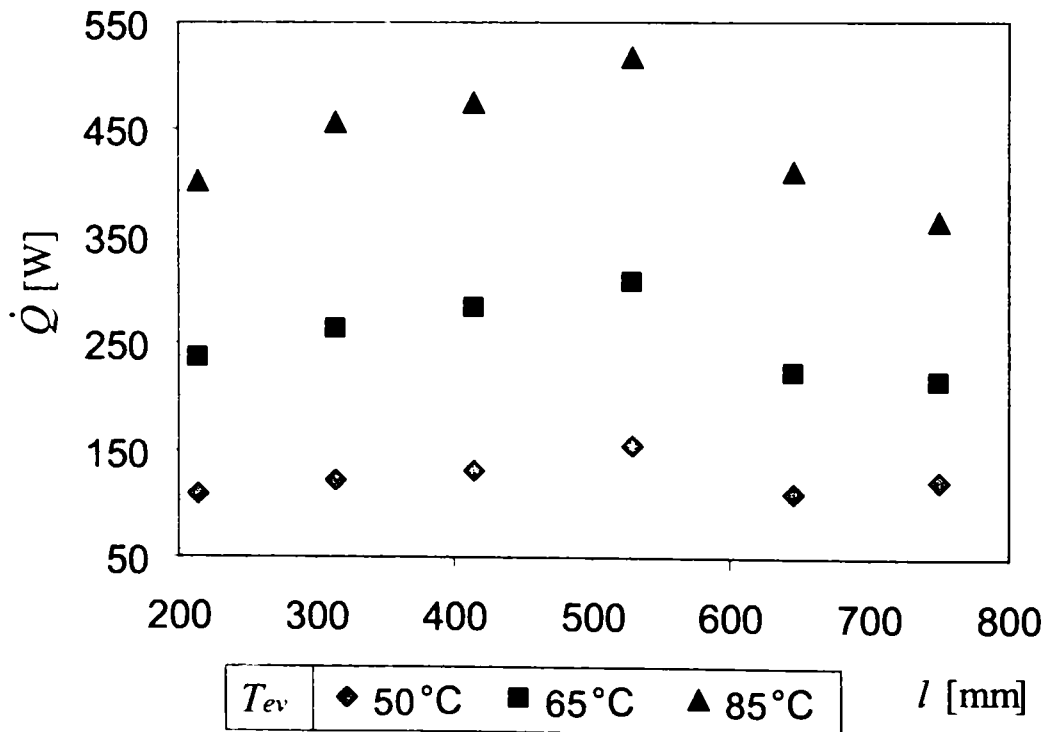


Fig. 2.14 \dot{Q} versus tube length, for 3 different evaporator temperatures

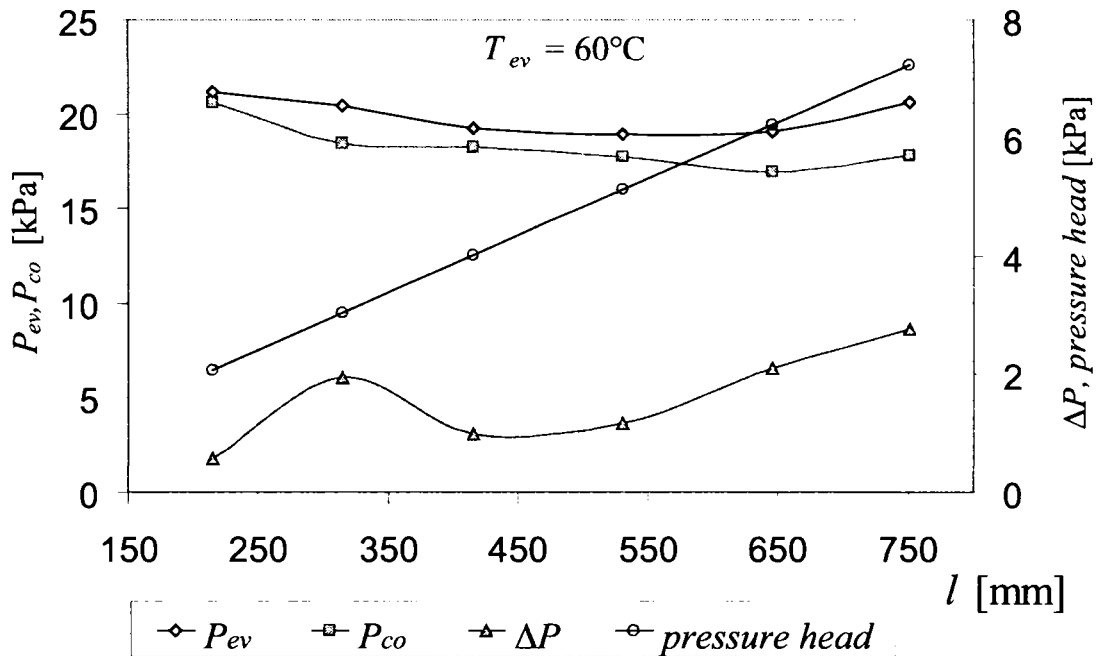


Fig. 2.15 Pressures variations with l

A better understanding of above explanation can be obtained by observing the pressure change with l as shown in Fig.2.15.

In Fig.2.16, \dot{Q} and ΔT_{ev-co} are plotted against T_{heater} for $l=530$ mm and $\gamma=0.4$, where ΔT_{ev-co} is temperature difference between evaporator and condenser. It is shown in the figure that with an increase in T_{heater} , \dot{Q} increases while ΔT_{ev-co} decreases, causing a rapid increase in effective thermal conductivity ($k_{eff} = \dot{Q} l / A \Delta T_{ev-co}$). In the present case it reached a value more than 5000 times higher than that of copper.

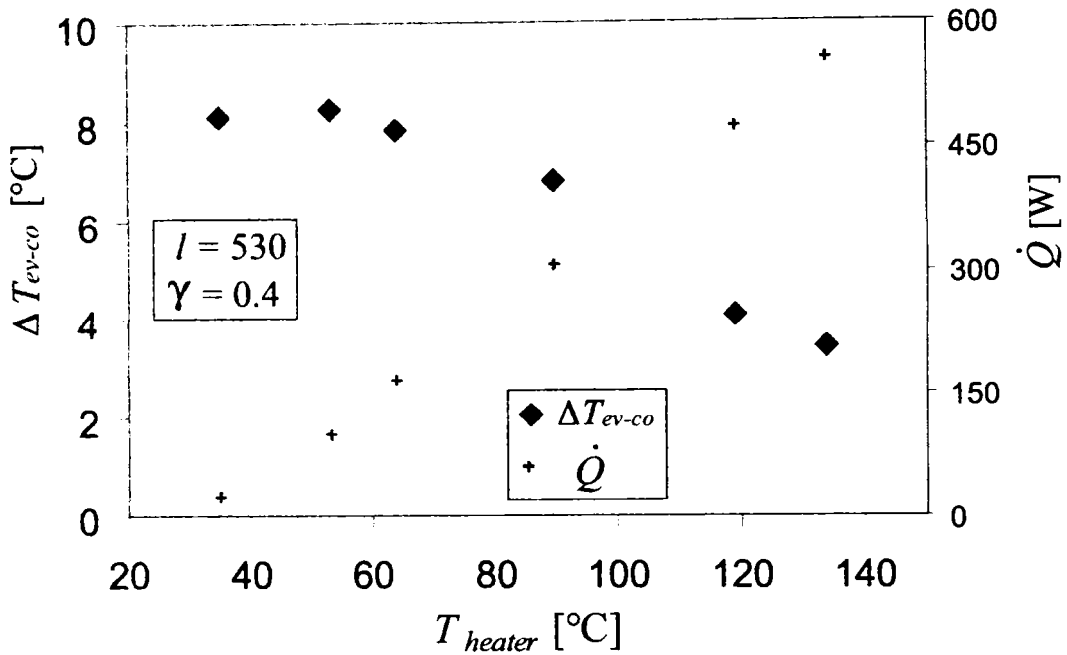


Fig.2.16 ΔT_{ev-co} and \dot{Q} plotted against T_{heater}

2.3.5 Effect of working fluid filling ratio

The amount of charged working fluid was considered to be another important parameter which may affect the performance of the present device. To determine its influence, experiments were performed for five different filling ratios (0.26, 0.37, 0.40, 0.42, 0.70) in the case of 215mm long tubes and three filling ratio (0.2, 0.4, 0.6) for the optimum length of 530 mm.

(a) For the case of 215mm length of the tubes

Fig. 2.17 shows the heat transport rate \dot{Q} versus evaporator temperature, T_{ev} , with the charging ratio of working fluid, γ , as a parameter for the vertical orientation of the device. Here, γ is defined as the ratio of the volume of the charged working fluid (pure water) in liquid state and the entire volume of the test section. One can observe from the figure that \dot{Q} increases with an increase in T_{ev} irrespective of the charging ratio. No significant difference can be observed in the trend of \dot{Q} for the five different filling ratios.

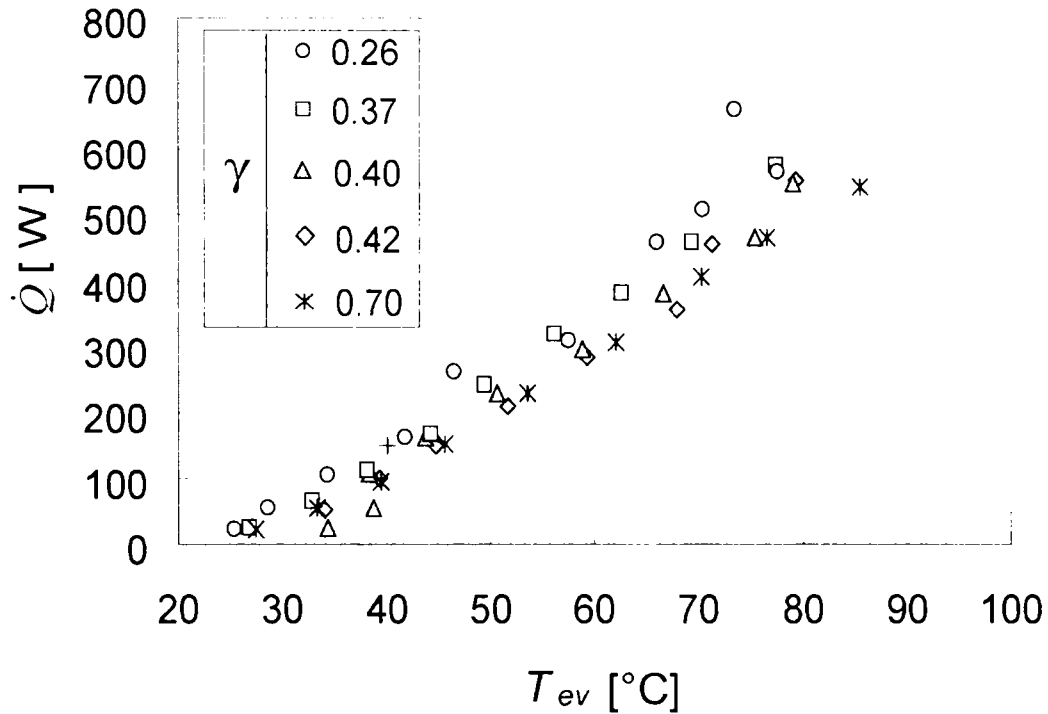


Fig. 2.17 Effective thermal conductivity k_{eff} vs. evaporator temperature T_{ev} with charging ratio, γ as a parameter.

Fig. 2.18 shows the variation of condenser temperatures T_{co} , and $\Delta T (=T_{ev} - T_{co})$ versus evaporator temperature T_{ev} for different charging ratio, γ . One can observe from the figure that with an increase in T_{ev} , T_{co} increases but ΔT decreases except for the case of $\gamma=0.70$. This fact, that an increase in \dot{Q} causes a decrease in ΔT is one of the most characteristic features of the present heat transport device. This is illustrated further in Fig. 2.19 where the effective thermal conductivity, k_{eff} , is plotted against T_{ev} . It is seen from the figure that k_{eff} reaches the highest value for $\gamma=0.26$, being 5000 times higher than the thermal conductivity of copper ($k_{copper} \sim 400\text{W/mK}$) while k_{eff} was at the lowest for $\gamma=0.70$. In the cases of $\gamma=0.37$, 0.40 and 0.42, the values of k_{eff} reduce to almost half as compared to the values for $\gamma=0.26$ but they are still much higher than those for $\gamma=0.70$.

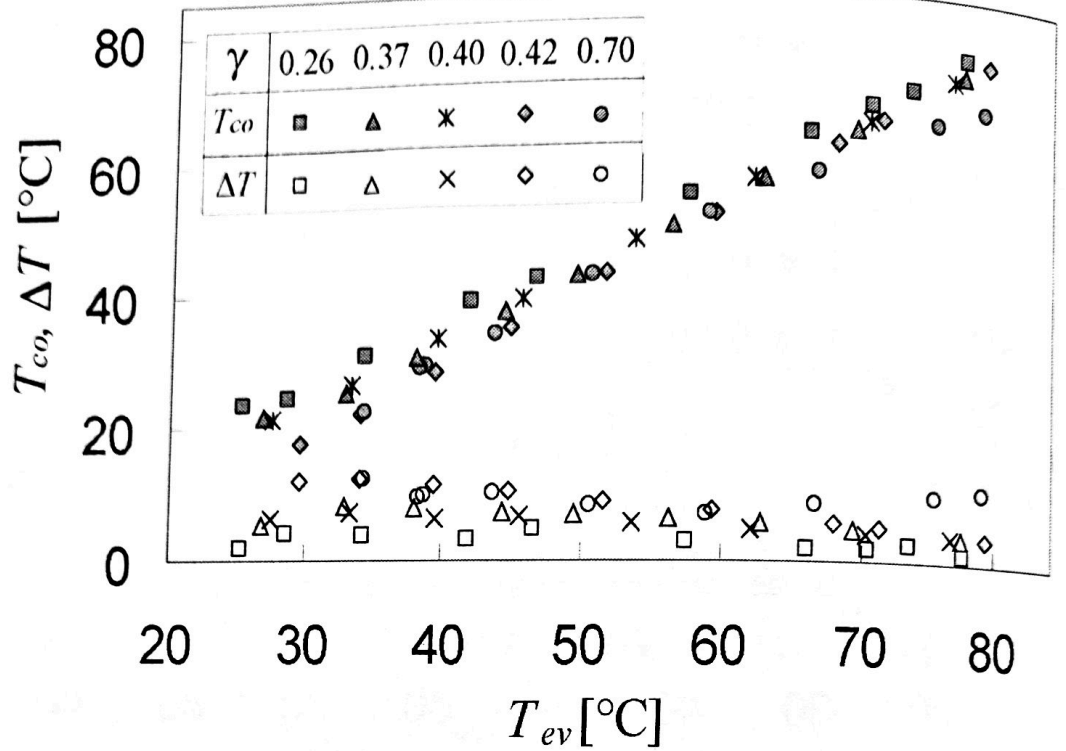


Fig. 2.18. Variation of condenser temperatures with evaporator temperature for different charging ratio, γ .

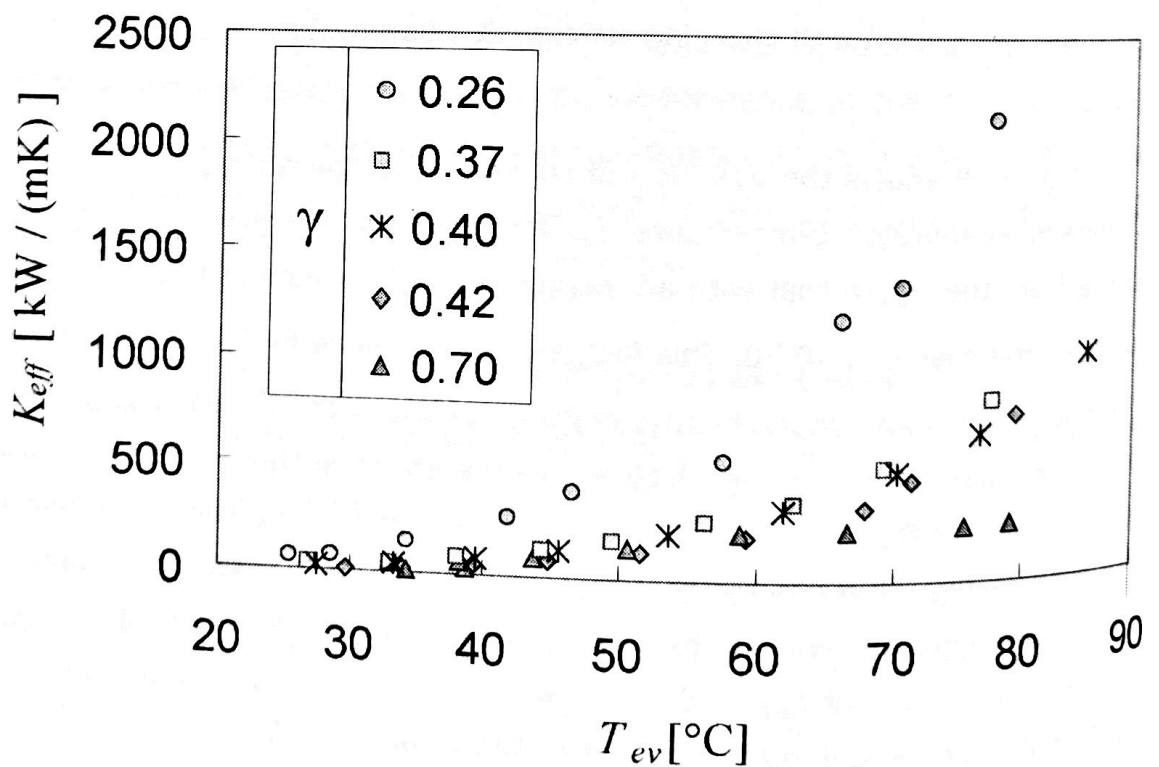


Fig. 2.19 Effective thermal conductivity k_{eff} vs. evaporator temperature T_{ev} with charging ratio, γ as a parameter.

One can observe in Fig. 2.20 the results for overall thermal resistance, R_{total} , plotted against T_{ev} with the charging ratio, γ as parameter. R_{total} is the thermal resistance over the heater surface in the evaporator and the cooling water in the condenser. Fig. 5. shows that :

(1) R_{total} decreases rapidly with an increase in T_{ev} ;
 (2) for T_{ev} larger than 50°C, the values of the thermal resistances become as low as 0.2 [°C/W].

(3) The first observation above means that the more heat load is imposed, the less becomes the thermal resistance of the system. This is a very unique feature of this kind of heat transport system. In contrast with the conventional heat pipes where the thermal resistance is increasing with an increase of working temperature, the present device has a lower thermal resistance especially for higher evaporator temperatures and this can be one of the explanations for its higher performance [15].

The lowest values of the thermal resistance were obtained for a charging ratio of $\gamma=0.26$. This is also reflected in the highest value of effective thermal conductivity which was obtained for $\gamma=0.26$.

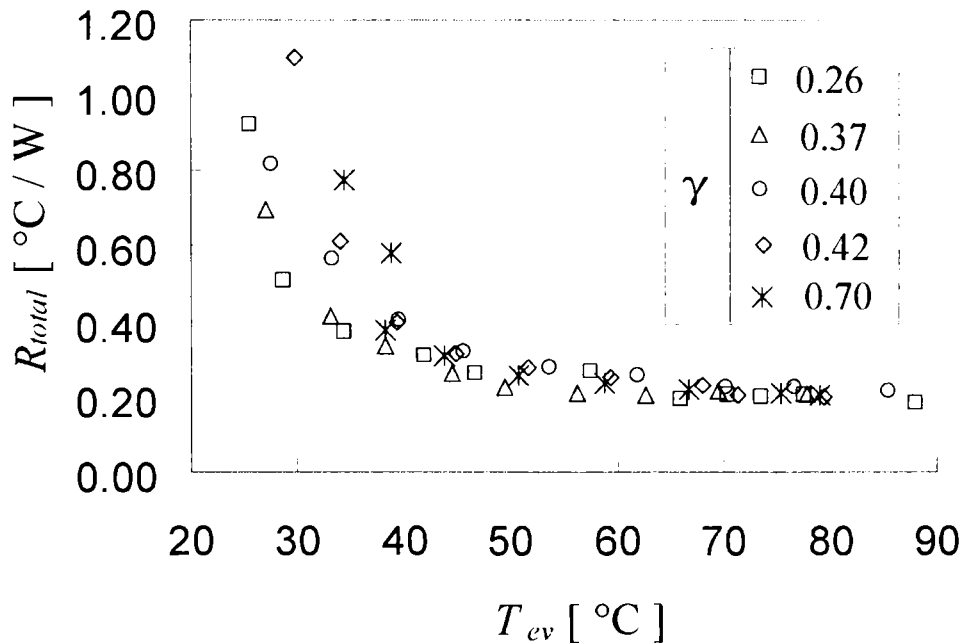


Fig. 2.20 Overall thermal resistance, R_{total} vs. evaporator temperature T_{ev} with charging ratio, γ as a parameter.

(b) For the case of 530mm length of the tubes

The contact area between the liquid working fluid and the heating surface in the evaporator, and that between the vapour and the cooling surface in the condenser, changes with the charging ratio. This may play a significant role on the characteristic of the heat transport phenomenon and influence the performance of the device.

Fig. 2.21 shows the relationship between heater temperature, T_{heater} , and Q , with γ as a parameter. From the figure one can observe that:

- (1) Irrespective of γ , T_{heater} increases with an increase in Q .
- (2) In the case of $\gamma=0.2$, T_{heater} goes up abruptly when Q increases.
- (3) There exists an optimum γ that gives highest Q for a given T_{heater} . In the present case it is $\gamma = 0.4$.

The phenomena (2) and (3) described above may be attributed to: (a) when γ is small, the boiling heat transfer surface may be partially dried up in evaporator for higher T_{heater} , resulting in lower heat transport performance; and (b) on the other hand, when γ is high, the condensing heat transfer surface may be submerged with liquid causing again a poor performance. The above explanation is reflected as well in the variation of thermal resistance with \dot{Q} for the three filling ratios.

The variation of the thermal resistance with Q for three different filling ratios can be observed in Fig. 2.22. As one can see from the figure, the lowest thermal resistance is given for $\gamma = 0.4$. The thermal resistance is decreasing with an increase in Q , reaching a value of 0.16 [$^{\circ}\text{C}/\text{W}$]. A similar trend follows in case $\gamma = 0.6$, while in case of 0.2 filling ratio, above 200W, a sharp increase of thermal resistance can be observed.

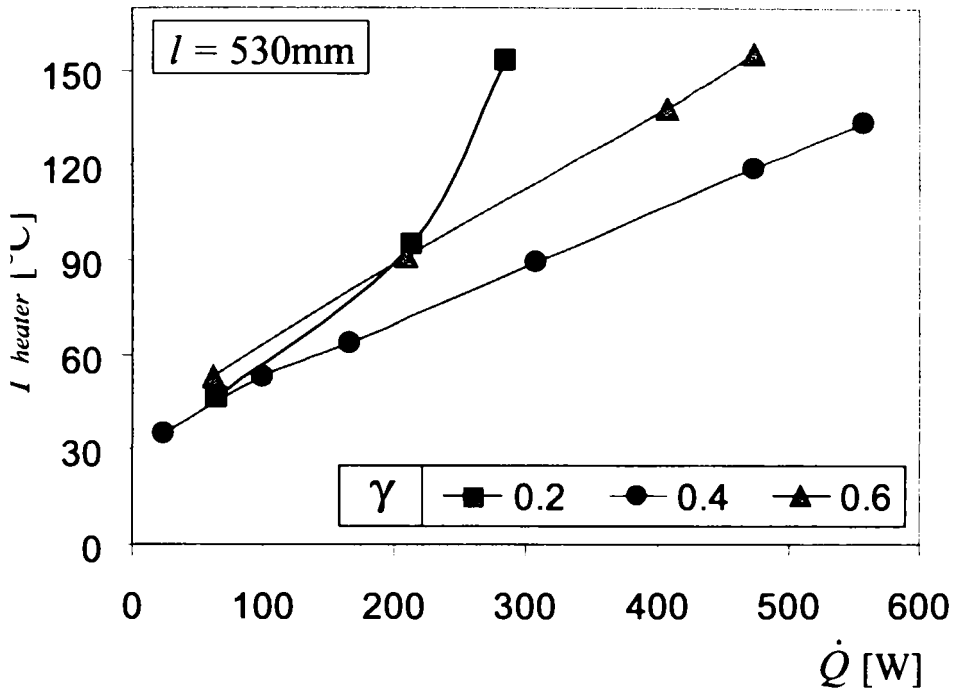


Fig. 2.21 Variation of T_{heater} versus Q with γ as a parameter

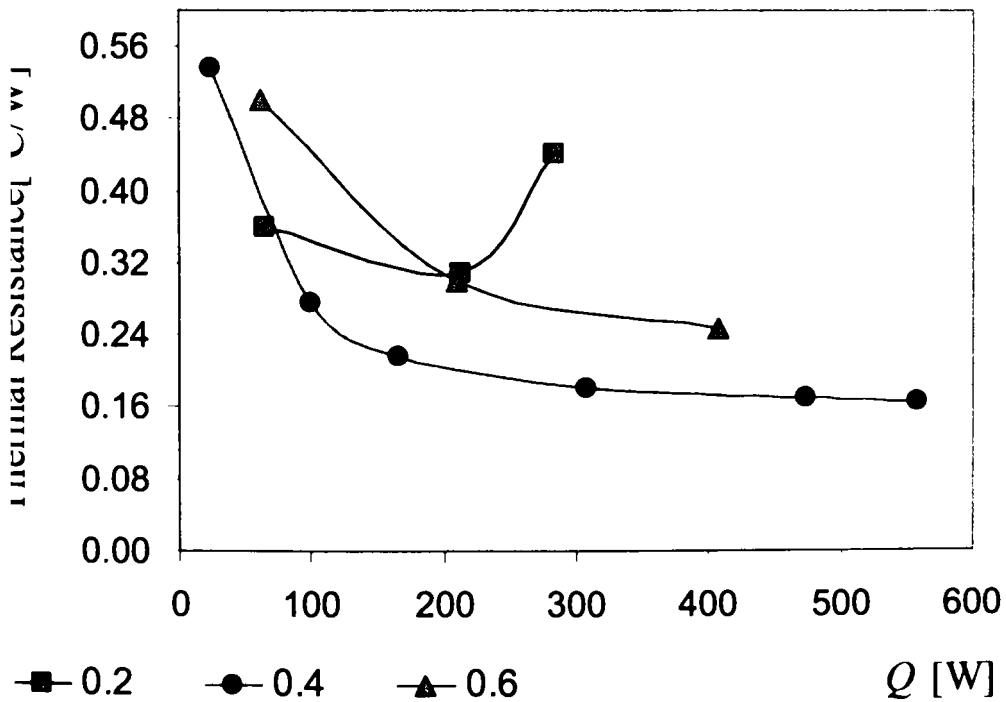


Fig. 2.22 Thermal resistance versus Q with γ as a parameter

2.4 Flow visualisation analysis

With the purpose of developing suitable descriptors of the inner flow behaviour in a two-phase heat transport device that could be related to its heat transport performance, a program was made using LabView NI Vision software. The information used to estimate the flow velocity, were extracted from flow visualization records.

2.4.1 Flow velocity estimation method

The flow velocity estimation was based on the evaluation of phase shift of two consecutive frames in the frequency domain. The algorithm, often used in PIV, is outlined in Figure 2.23.

Prior to the fast Fourier transformations (FFT) of the frames, the background, obtained as the averaged field of at least 100 frames, was removed by evaluating the absolute difference between the analyzed frames and the background. After FFT, the complex conjugate of the second frame was obtained. By multiplication of the FFT of the first frame and the complex conjugate of the FFT of the second frame, the relative phase shift of the Fourier components was obtained. After inverse FFT of the result, a peak indicated the dominant phase shift between the two frames in the space domain. The exact position of the peak was identified from quadratic interpolation near the maximum, in order to obtain sub-pixel accuracy. Alternatively, various morphological transforms were applied prior to the FFT in order to test the sensitivity of the method on the remaining noise after background removal.

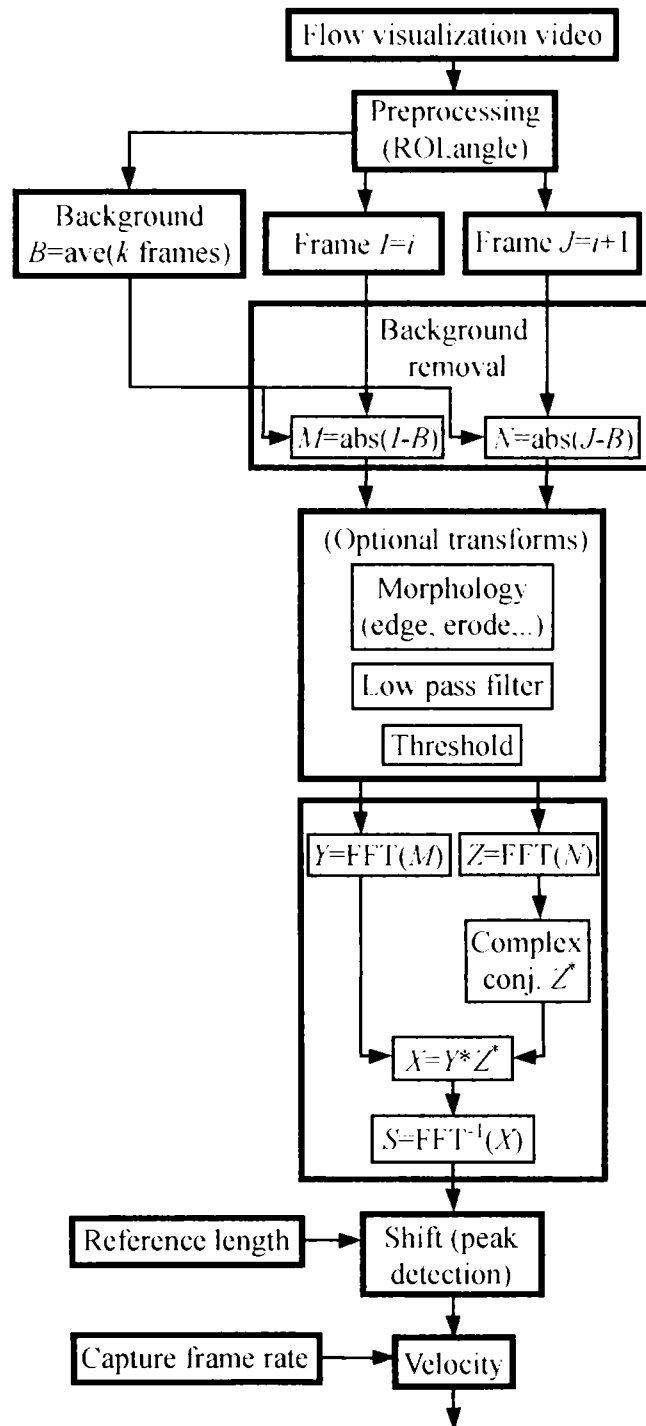


Fig. 2.23 Velocity measurement algorithm

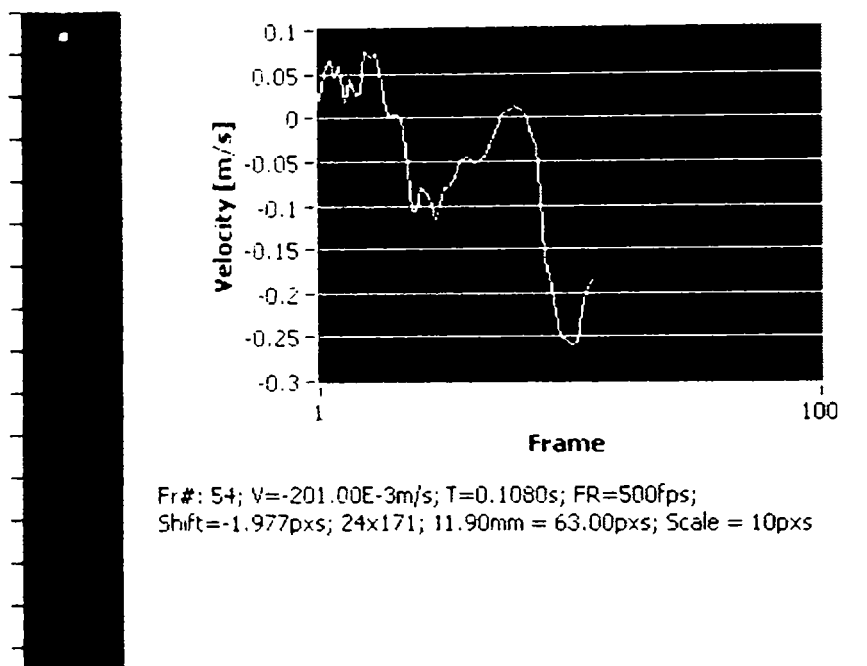


Fig. 2.24 Presentation of velocity measurement results.

The results were verified by visual comparison of the measured shift and the shift observed between frames. For this purpose, the results could be saved in the form shown in Figure 2.24, which combined the video of the analyzed area, velocity chart, and other data for each frame. For simple comparison, lines to the left from the video were distributed by 10 pixels and allowed direct comparison of the observed and computed shift between the frames. Although rigorous prove of accuracy of the method is difficult to obtain, the results were found very reasonable, with little dependence on the selected region of interest and noise. However, problems could appear during periods of very high velocity of the flow for which the capture speed was not sufficient, during entrance of large bubbles into the region of interest, and, naturally, during periods in which no distinguishable features were present in the analyzed region. These problems are the subject of future improvements.

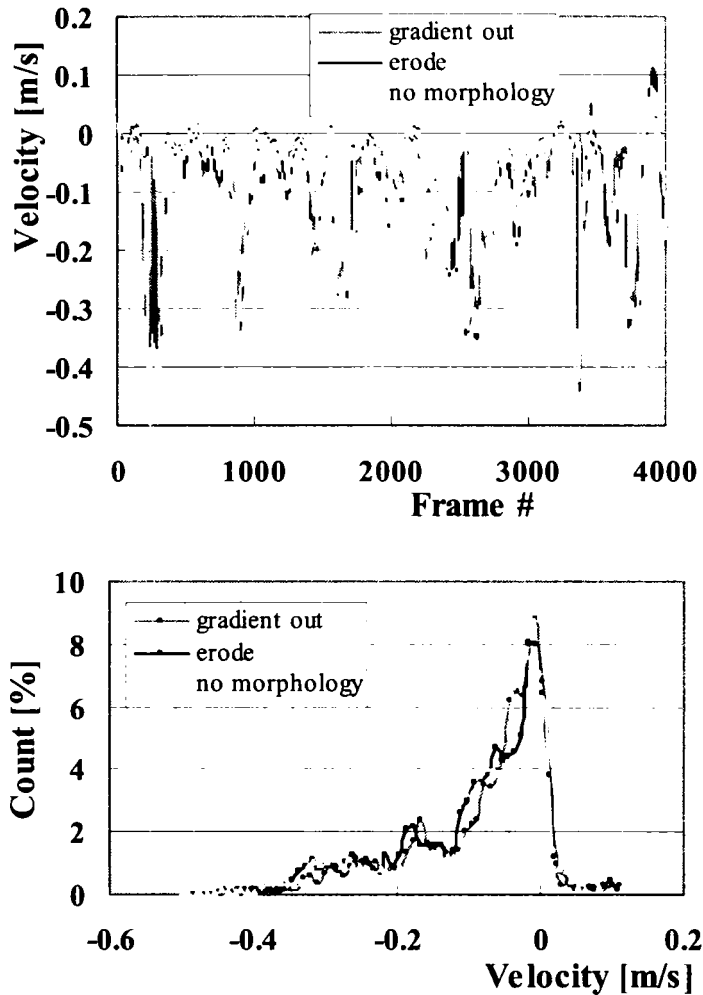


Fig. 2.25 Velocity measurement results in the thin tube of test core with different tube diameters with comparison of different morphology transforms.

Top graph: Velocity trend. Bottom graph: Velocity histogram.

An example of the resulting velocity profile and the corresponding velocity histogram is shown in Figure 2.25. This Figure corresponds to the record obtained from smaller tube of the test section shown in Figure 2A-4 (c). For comparison, the velocity profiles are shown for processing without any morphological transform as well as with erode transform and gradient transform applied prior to FFT. The very close agreement between the three methods shows small effect of the remaining background and noise.

2.4.2 Flow visualization analysis

From the video recordings of fluid flow inside the tubes, it was clearly observed that one-way recirculation with vapour up-ward flow through the larger diameter tube and condensate return through the smaller diameter tube was maintain to occur. In Fig.2.26, a capture of fluid flow for $\dot{Q} \sim 25W$ and an average temperature of the system of $34^\circ C$ can be seen. Fig. 2.26 (a) ~ (d) represents four consecutive frames from the video recordings. One can observe from the figures the up-ward flow in the larger diameter tube (left-side tube) and the down shift of the column liquid in the smaller diameter tube (right-side tube).

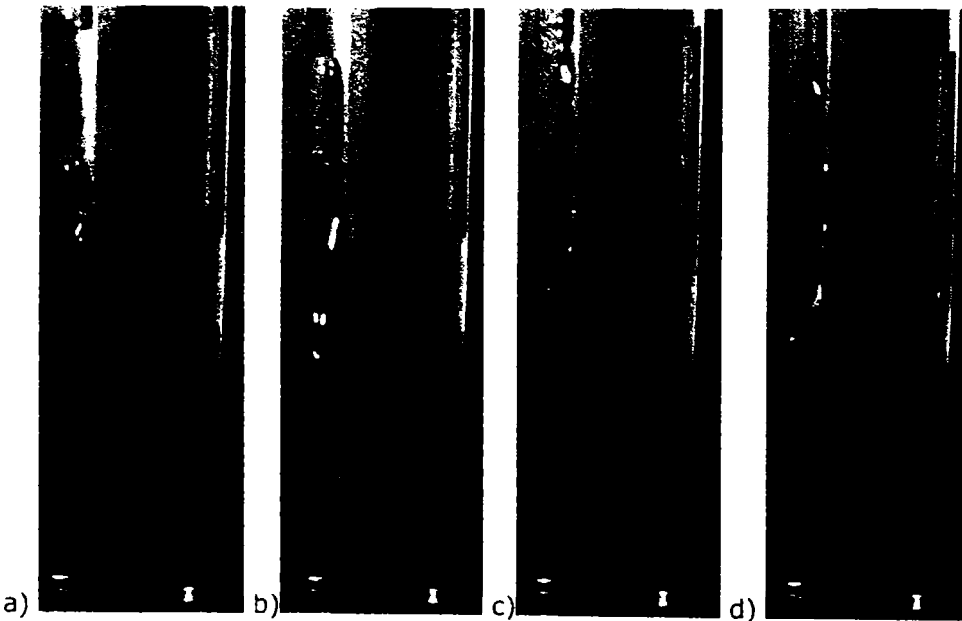


Fig. 2.26 Capture of fluid flow at $Q \sim 25W$

Fig.2.27 and Fig.2.28 are showing consecutive frames from the fluid flow video recordings at $\dot{Q} \sim 150W$ and $\dot{Q} \sim 450W$, respectively. At higher temperature range, the flow is more intermittent, larger amount of vapour is flowing through the thicker tube and consequently, the volume of condensate return is also increased. Less bubbles (and of smaller size) are observed in the thinner tube while a column of liquid is covering most of the volume of the thin tube. The up-flow at low temperature can be considered to be churn flow while at higher temperature, as annular flow. The

down flow instead, initially, at low temperature, had the characteristics of slug flow, and later, at higher temperature, it became bubble flow [13].

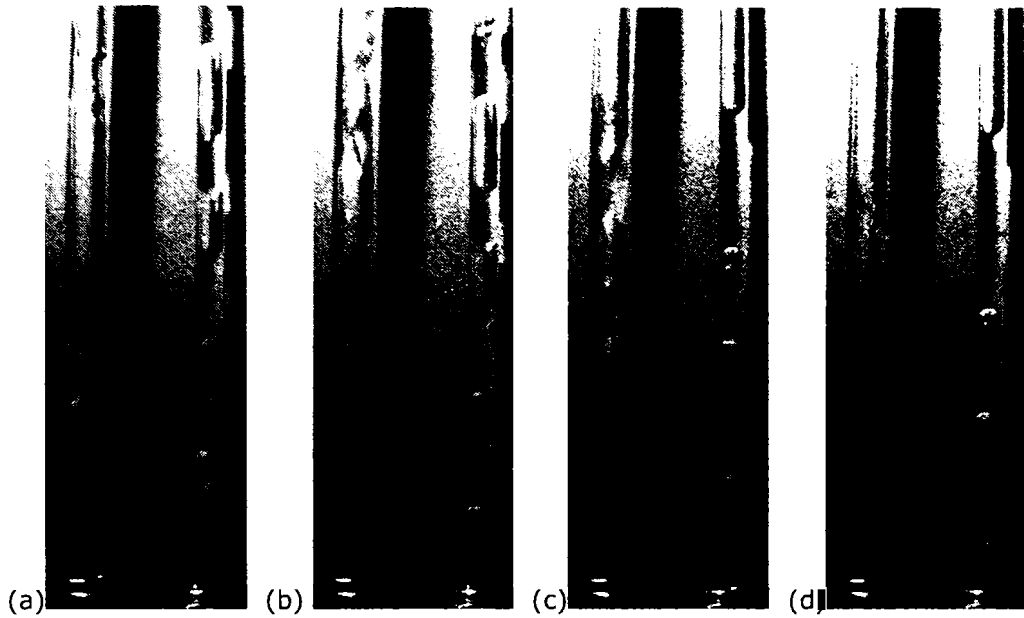


Fig. 2.28 Capture of fluid flow at $Q \sim 150W$

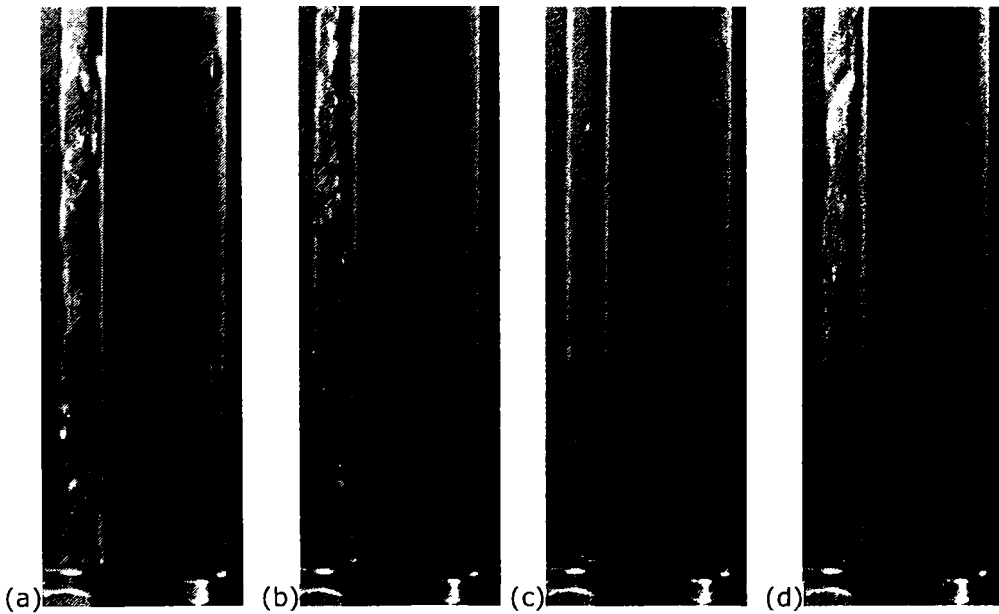
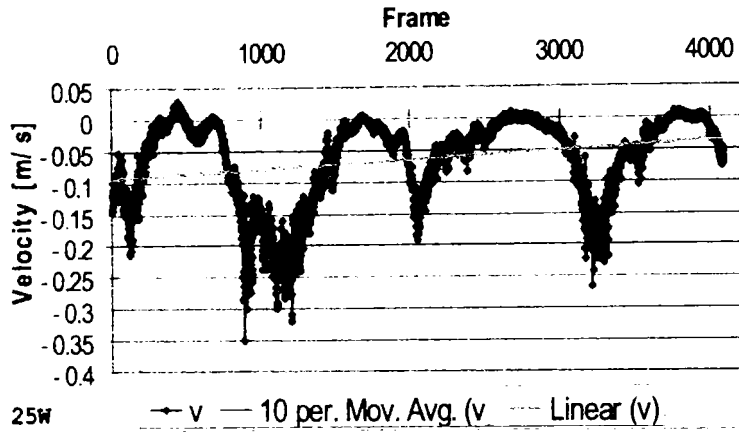
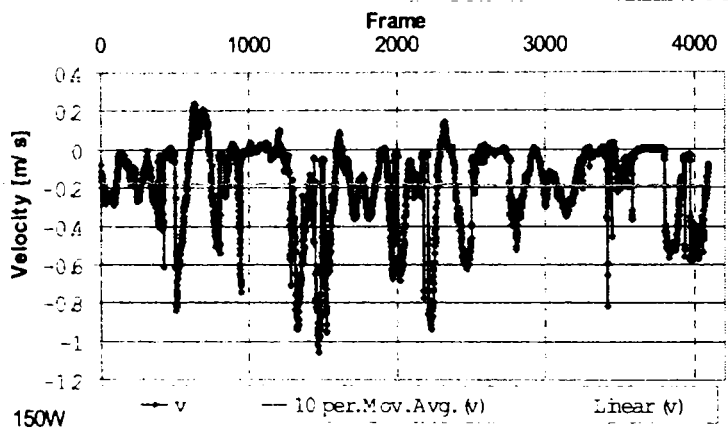


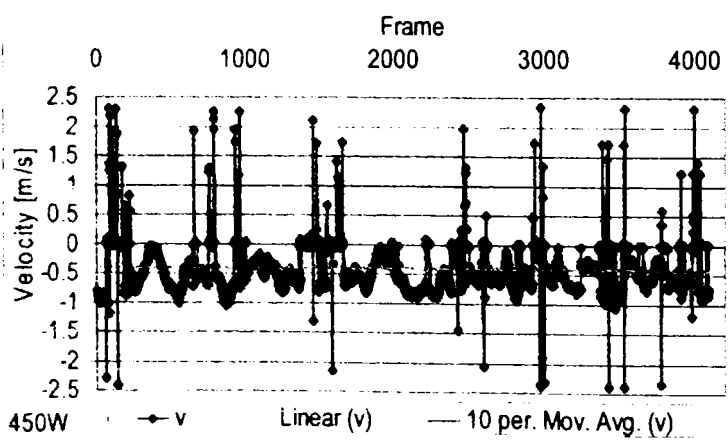
Fig. 2.29 Capture of fluid flow at $Q \sim 450W$



(a) Estimated velocity of condensate return for $Q \sim 25W$



(b) Estimated velocity of condensate return for $Q \sim 150W$



(c) Estimated velocity of condensate return for $Q \sim 450W$

Fig. 2.27 Velocity estimation

From the video recordings of flow inside the tubes, the velocity of the down-flow (condensate return) was estimated using the method described above (2.4.1). In case of up-flow the velocity couldn't be estimated using the phase-shift method, due to the irregular pattern of vapour and liquid mixture.

It was observed that the flow patterns change with temperature and the velocity of condensate return is increasing with a rise of temperature. Applying the phase-shift method the estimated velocity for $\dot{Q} \sim 25\text{W}$, 150W and 450W can be seen in Fig. 2.29 (a), (b), and (c) respectively. Although the method of estimating the flow velocity, in general it proved to be reliable (through direct comparison with the scale phase-shift), problems could appear during periods of very high velocity of the flow for which the capture speed was not sufficient, during entrance of large bubbles into the region of interest, and, naturally, during periods in which no distinguishable features were present in the analyzed region. The 0 velocity in Fig. 2.29 corresponds to the situations mentioned before or to the stagnation of flow between the cycles. The minus sign in the graphs of velocity indicates the down-flow.

Fluid flow is intermittent and the frequency of vapour up-flow and condensate return is increasing with an increase of \dot{Q} . As it can be seen from Fig. 2.29, the velocity of condensate return is increasing with an increase of heat input. At an average temperature (between evaporator and condenser) of 34°C , the average down flow velocity was around 0.1m/s (Fig. 2.27 (a)). At 48°C , the velocity was around 0.2m/s and for 82°C , it reached around 0.5m/s or even more.

2.5 Conclusions

In this chapter, a new heat transport device (HTD) was introduced and the experimental investigations results of the effect of various parameters on its performance were presented. The followings can be concluded from the above study:

- (1) the present HTD can transport more than 800W for a temperature of evaporator below 100°C;
- (2) in the higher temperature range, the present HTD shows three to four times higher performance than a conventional heat pipe of similar size and same working fluid (water);
- (3) the high performance is attributed to the unique mechanism of fluid flow. One way recirculation was maintained to occur with vapor flowing through the larger diameter tube to condenser and the condensate return to evaporator through the smaller diameter tube. Due to the separation of the two streams in opposite directions, the entrainment limit is avoided as this represents an advantage over the conventional heat pipes;
- (4) the gravitation plays an important role in the recirculation of the fluid and this results in the performance of the device; the highest performance was achieved for the vertical orientation with the evaporator placed below condenser;
- (5) although the device can transport heat efficiently over a large range of tube length, there exists an optimum length at 530mm;
- (6) the filling ratio has also appreciable effect on the performance of device and the optimum was found to be 40% from the total inner volume.

APPENDIX – 2

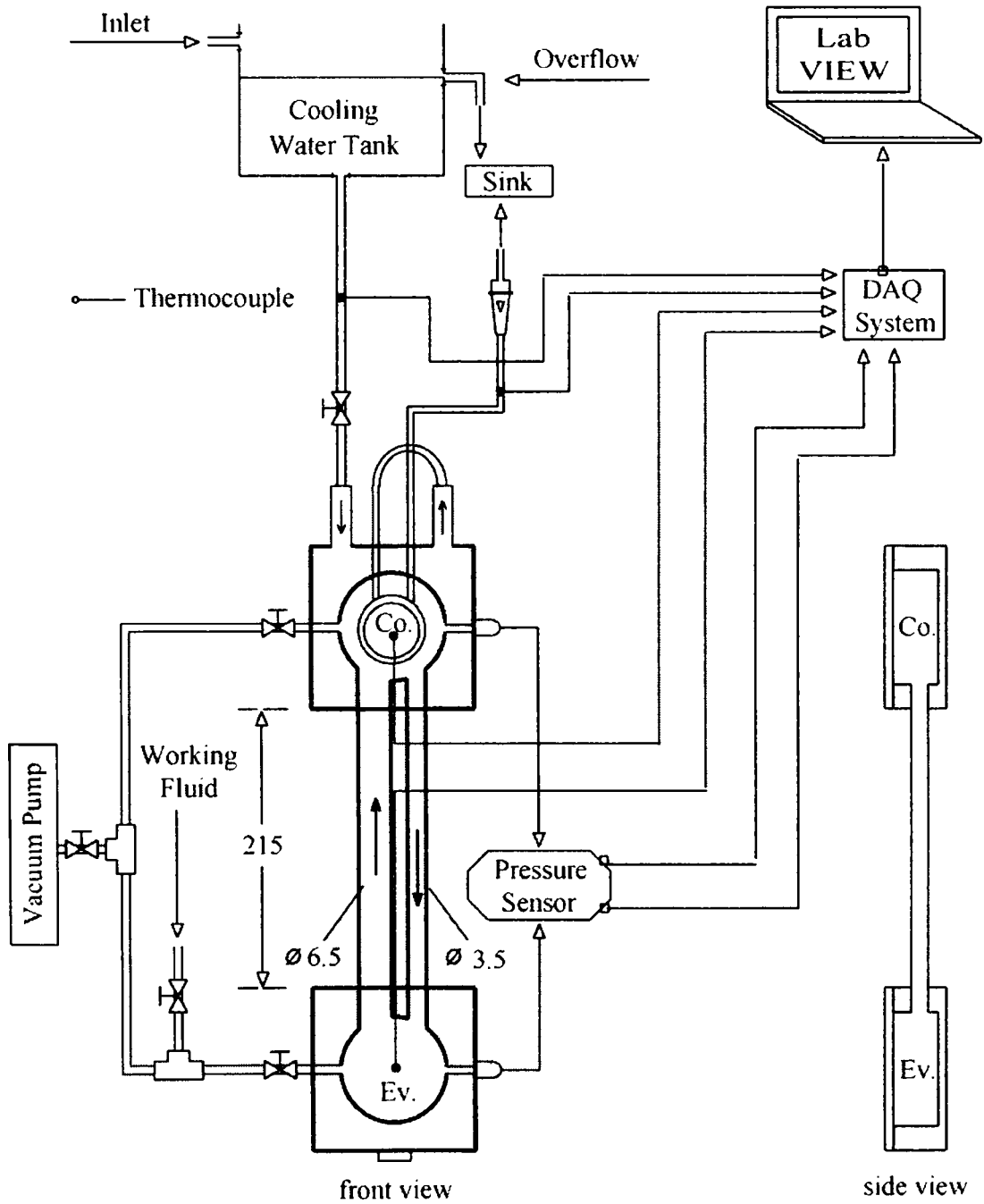


Fig. 2A-1 Schematic of experimental set up with 2 tubes of different diameters

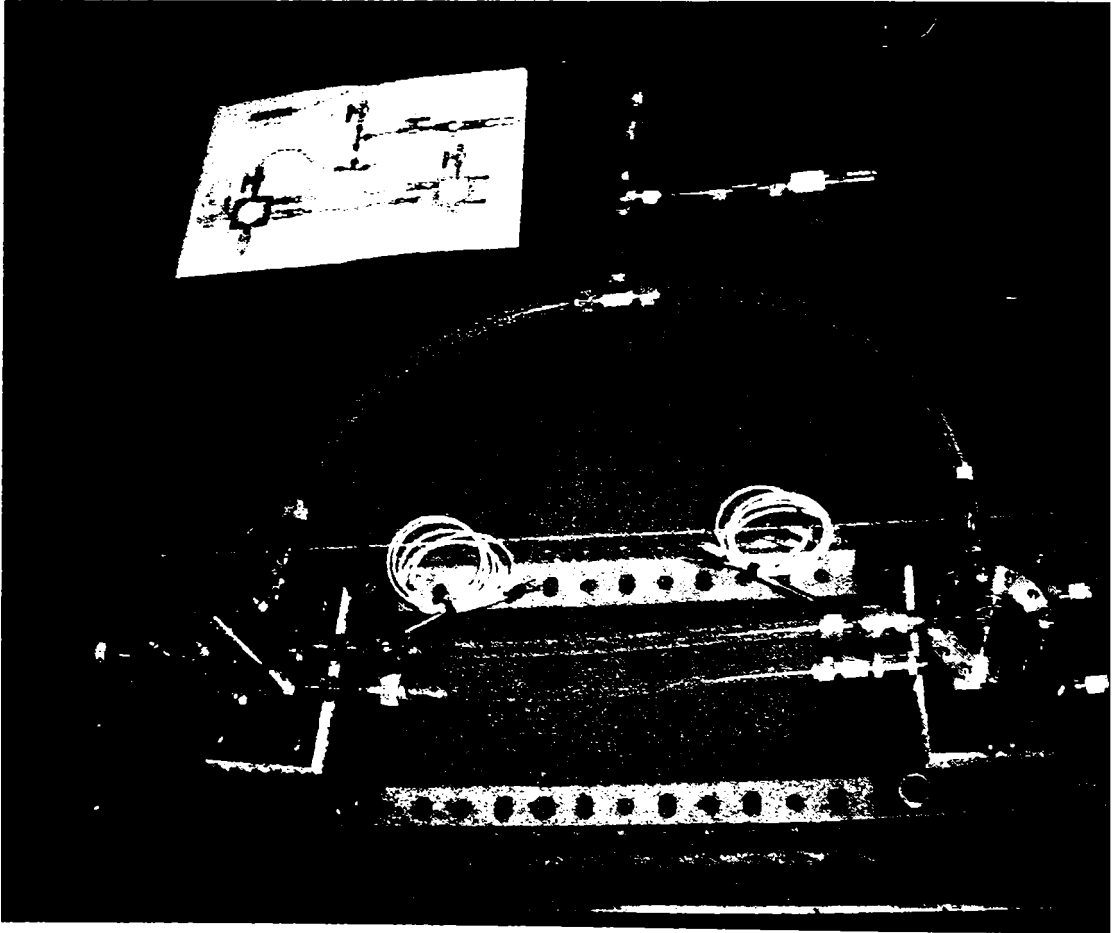


Fig. 2A-2. View of test section during first assembling

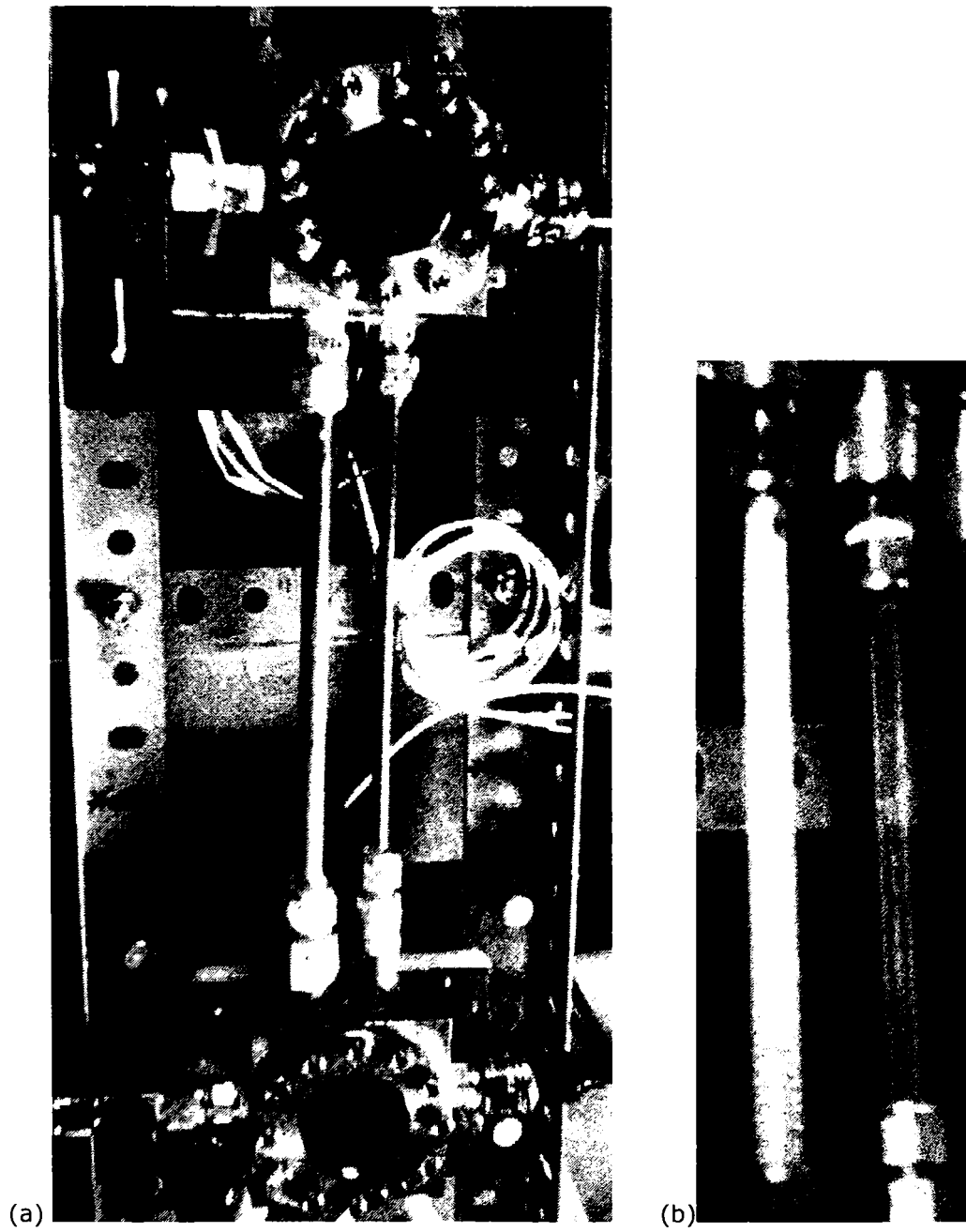


Fig. 2A-3. Test core with copper tubes (a) and Teflon tubes (b)

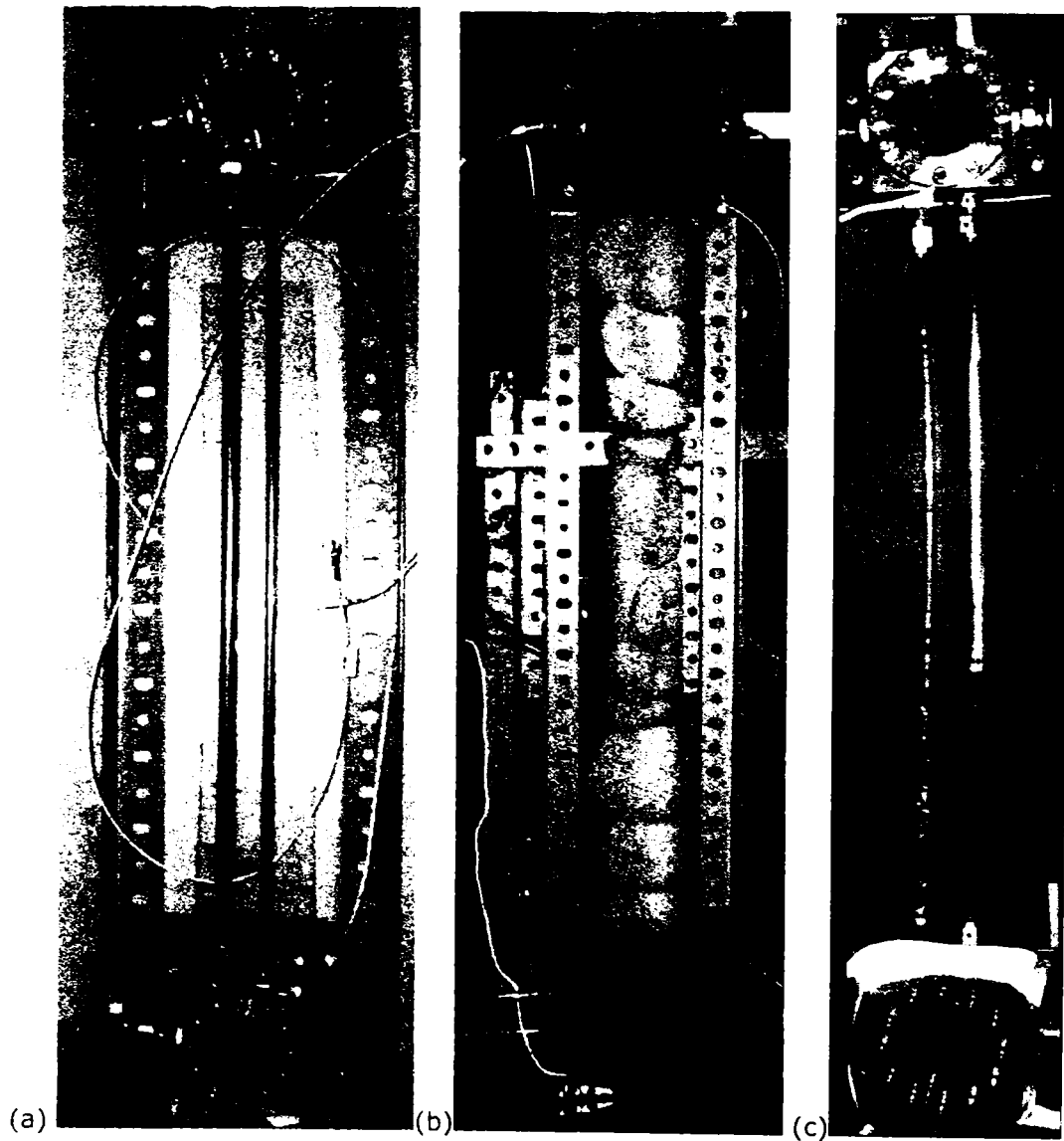


Fig. 2A-4 Test core (a) with copper tubes without insulation, (b) insulated, (c) with Teflon tubes.

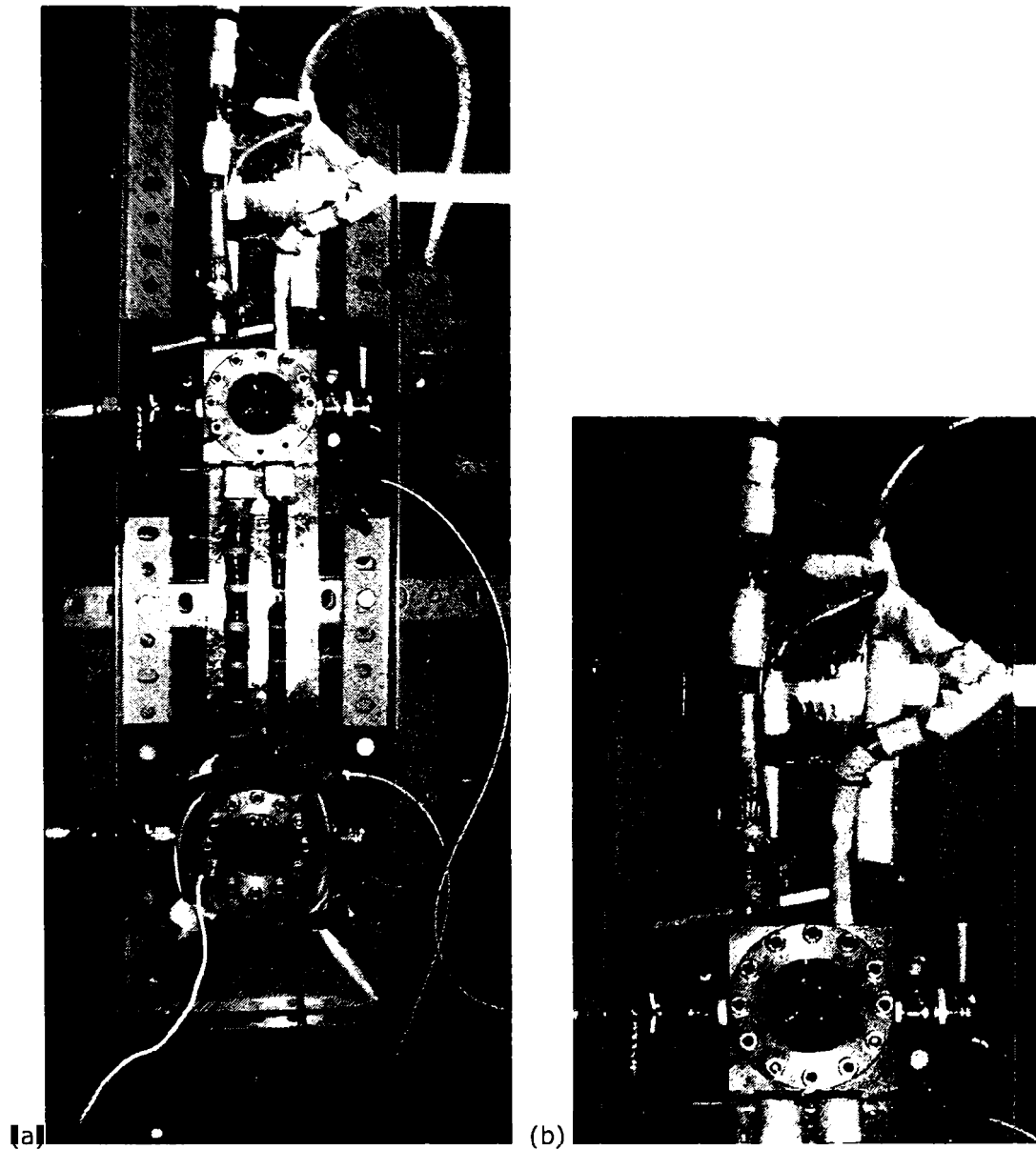


Fig. 2A-5 (a) View of initial Test Core; (b) cooling water branching

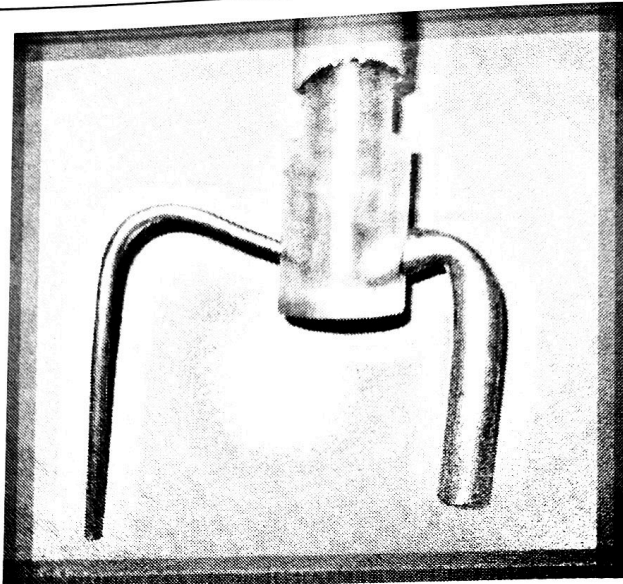


Fig. 2A-6 Mixing chamber for the cooling water outlet.

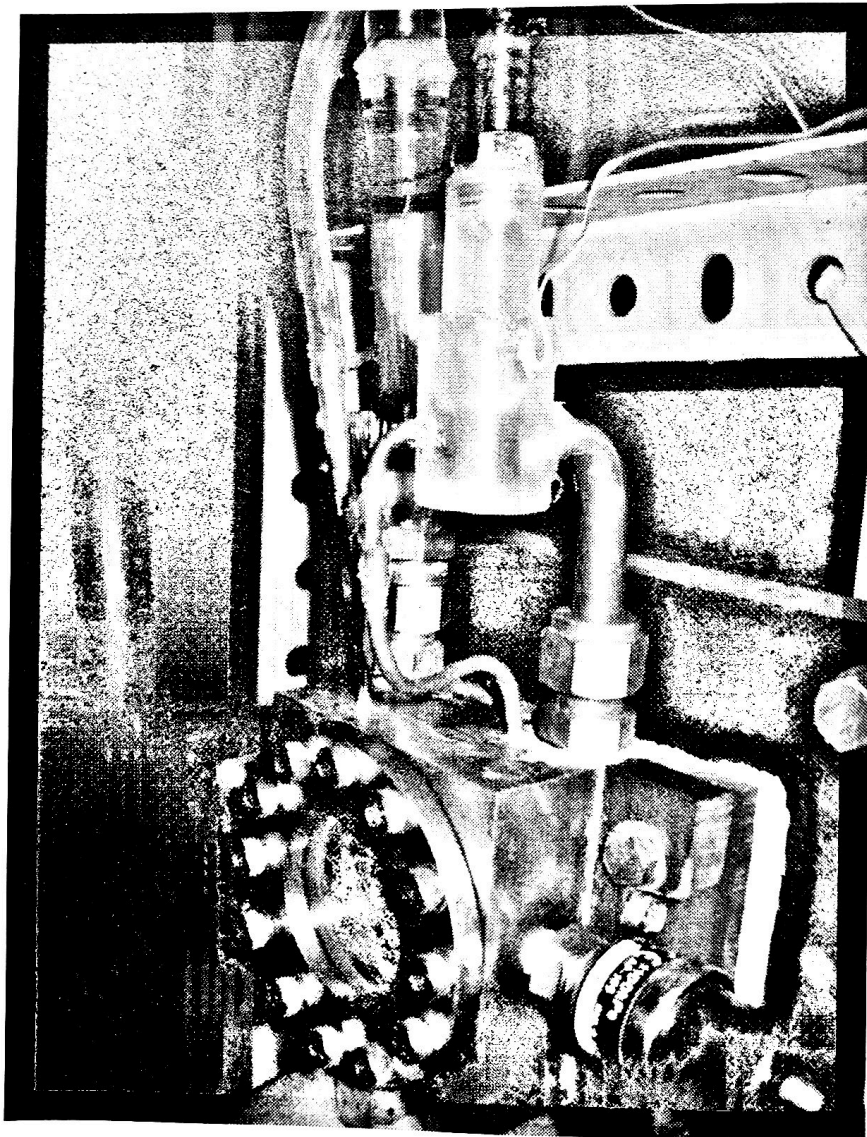


Fig. 2A-7 Mixing chamber attached to condenser.

3. PT-HTD with five parallel tubes

3.1 Experimental set up and procedure

For further improvements of HTDs a new test section was design, manufactured and tested under certain experimental conditions. The schematic of the new test core is shown in Fig. 3.1. It consists of five parallel copper tubes (200 mm in length and 2.8mm and 4 mm inner and outer diameter, respectively), which connect an electrically heated evaporator and water cooled condenser. A ceramic heater (50x50) was placed on the backside of evaporator and connected to a regulated power supply. The backside wall of condenser was water cooled. To provide a constant flow rate with certain head level a reservoir for water was placed above the test section. The flow rate of cooling water was measured using a stop watch and a mass cylinder.

Both evaporator and condenser chambers have a quartz-glass window to enable the visualization of inner flow. A high-speed video camera was used to record the flow behaviour inside the evaporator and condenser. Before charging the working fluid (water), the test section was evacuated to around 4 kPa. Pressure sensors were attached to both evaporator and condenser chambers. The amount of charged fluid was around 45% of the test section total inner volume. Thermocouples were placed for measuring temperatures of (1) inlet and outlet cooling water at condenser $T_{w,in}$, $T_{w,out}$, (2) working fluid inside evaporator and condenser, $T_{f,ev}$, $T_{f,co}$ (3) heater and condenser wall, $T_{w,ev}$, $T_{w,co}$ and (4) tube wall at three positions along the axis of each tube, (T_e , close to evaporator, T_m , middle and T_c , close to condenser, see Fig. 3.1). In case of copper tubes (not transparent), for estimating the fluid phase inside the tubes, the temperature of tubes wall were measured. The method predicts that, high wall temperature indicates that vapor is flowing through the tube, while lower temperatures will correspond to the condensate return. The method proved to be reliable by comparing the results of tube wall temperature measurements with the flow behavior recorded inside condenser chamber. The estimation done by temperature measurements agreed very well with the flow visualization results.

The pressure and temperature measurements were fed to a data acquisition card (DAQ) and were analyzed using LabView software. The heat transport rate was obtained from the temperature rise (averaged values during the steady state) and the mass flow rate of cooling water flowing through the condenser.

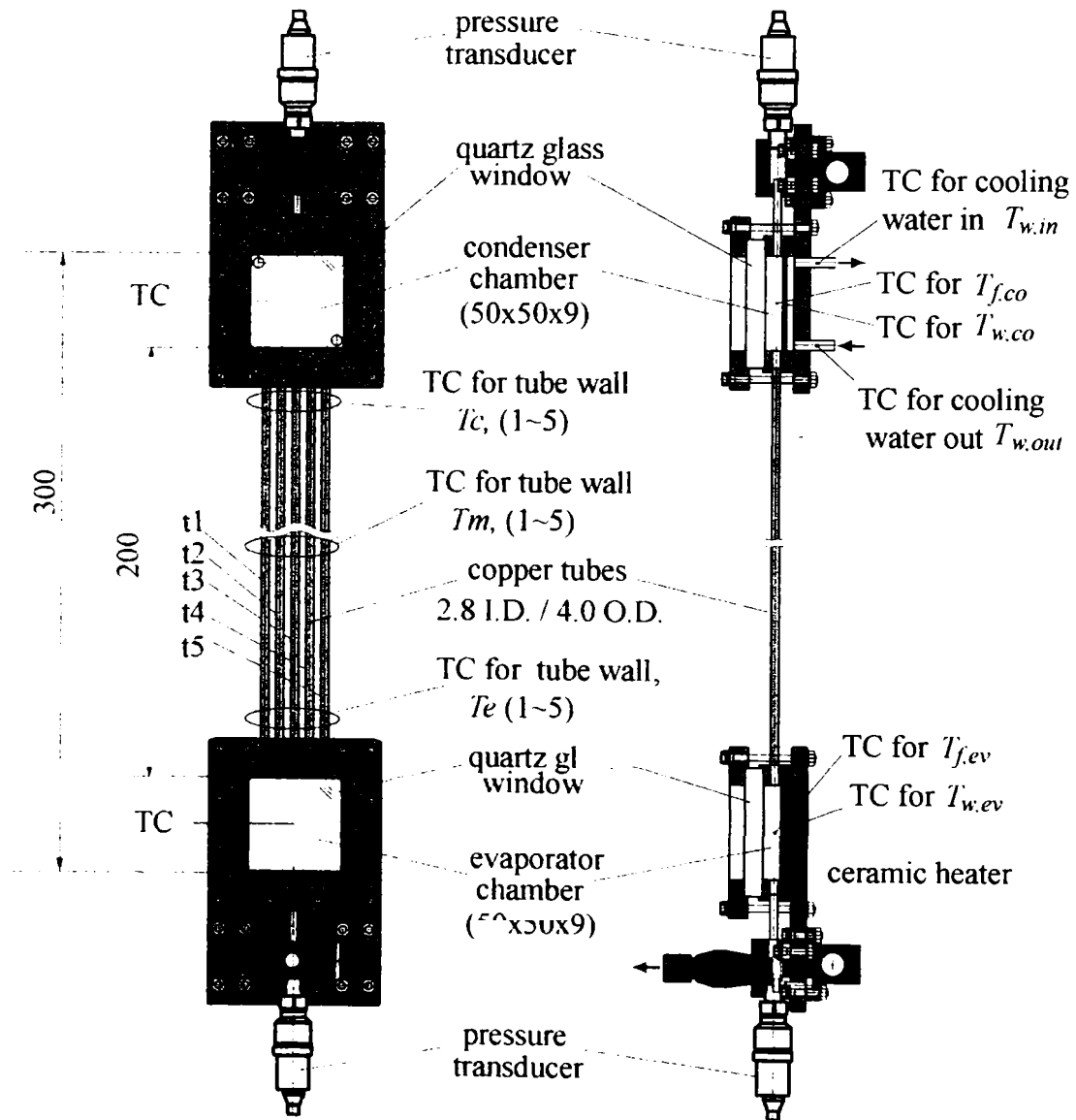


Fig. 3.1 Schematic of test section with 5 parallel tubes

Note: TC stands for thermocouple

The experiments were conducted under following experimental setups:

- (I) vertical orientation of device, with the evaporator placed at the bottom, as it can be seen in the below illustration (Fig. 3.2)
- (II) horizontal orientation of device;
- (III) bent tubes, with the evaporator placed on horizontal position (Fig. 3.3)

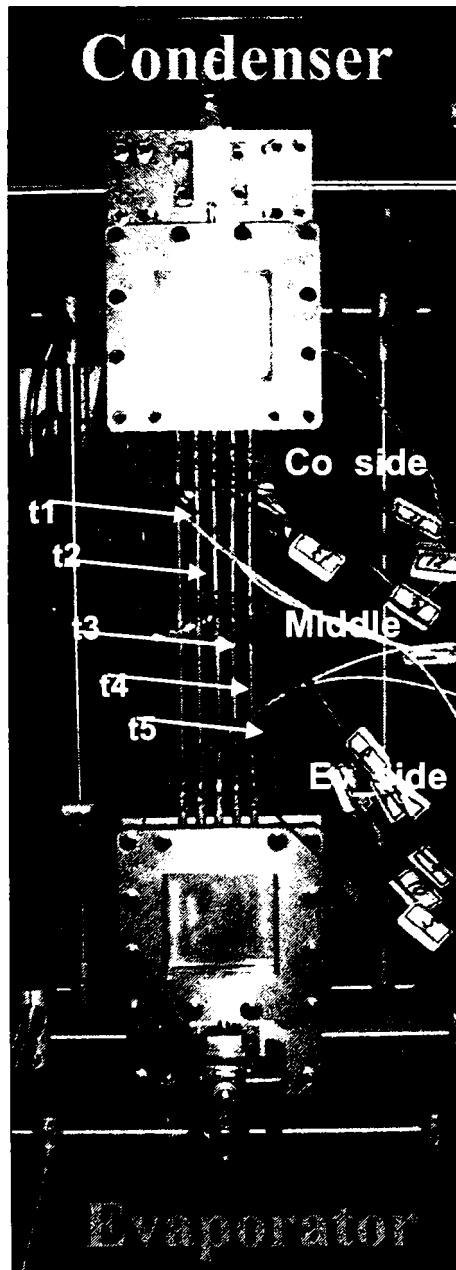
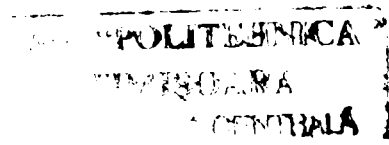


Fig. 3.2 Illustration of the 5-PT-HTD in vertical orientation



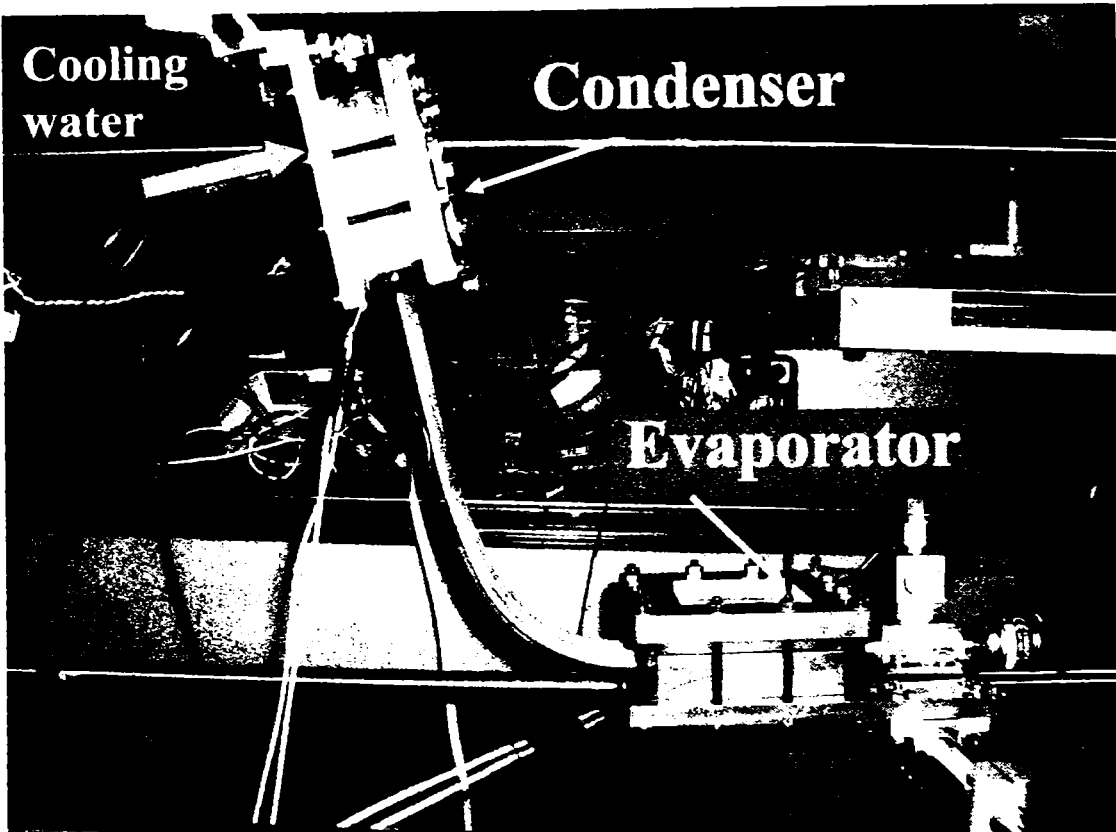


Fig. 3.3 Representation of the 5-PT-HTD with the evaporator placed on horizontal

As one can observe from Fig.3.3, the evaporator in this case was placed on horizontal position with the purpose of maximizing the contact between the hot surface and the working fluid inside the chamber. The angle of tubes bending was avoided to be sharp for not creating a resistance of inner flow. The condenser orientation is debatable. For the first run of experiments, based on results of previous work, the almost vertical orientation was considered. In previous chapter, it was shown that, for certain inclinations of test core, the submersion of condenser into the liquid, causes a reduced heat transport performance due to the lower heat transfer coefficient (of film condensation as compared to that of drop wise condensation). The other dimensions were kept same as for the vertical orientation case (tube length, 200mm, inner and outer diameter 2.8mm and 4mm respectively, amount of working fluid, 45%) .

3.2 Data Reduction

The heat transport rate was obtained from the temperature rise and mass flow rate of cooling water flowing through the condenser. It was calculated by:

$$\dot{Q} = \rho c_p \dot{V} (T_{w,out} - T_{w,in}) \quad (1)$$

where $T_{w,in}$, $T_{w,out}$ and \dot{V} are the condenser inlet, outlet temperatures and the volume flow rate of the cooling water, respectively.

In the present study, an effective thermal conductivity, k_{eff} , was introduced as a measure of the heat transport performance of the device. It was defined by the following equation:

$$k_{eff} = \frac{\dot{Q}l}{A_t(T_{w,ev} - T_{w,co})} \quad (2)$$

where l is the tube length (distance between the evaporator and condenser) and A_t is the total of the inner cross sectional areas of the two tubes; $T_{w,ev}$ and $T_{w,co}$ are the wall temperature of evaporator and condenser chamber.

The overall thermal resistance, R_{total} , between the heater and the cooling water was calculated using the following relationship:

$$R_{total} = \left[T_{heater} - (T_{w,in} + T_{w,out})/2 \right] / \dot{Q} \quad (3)$$

3.3 Results and Discussions

3.3.1 Vertical Orientation

3.3.1.1 Performance of the new test section

Fig. 3.4 shows the performance of the present device for the vertical orientation with the evaporator places at the bottom. It can be seen from the figure that Q increases with a rise of heater temperature and that the present device can transport up to 600W.

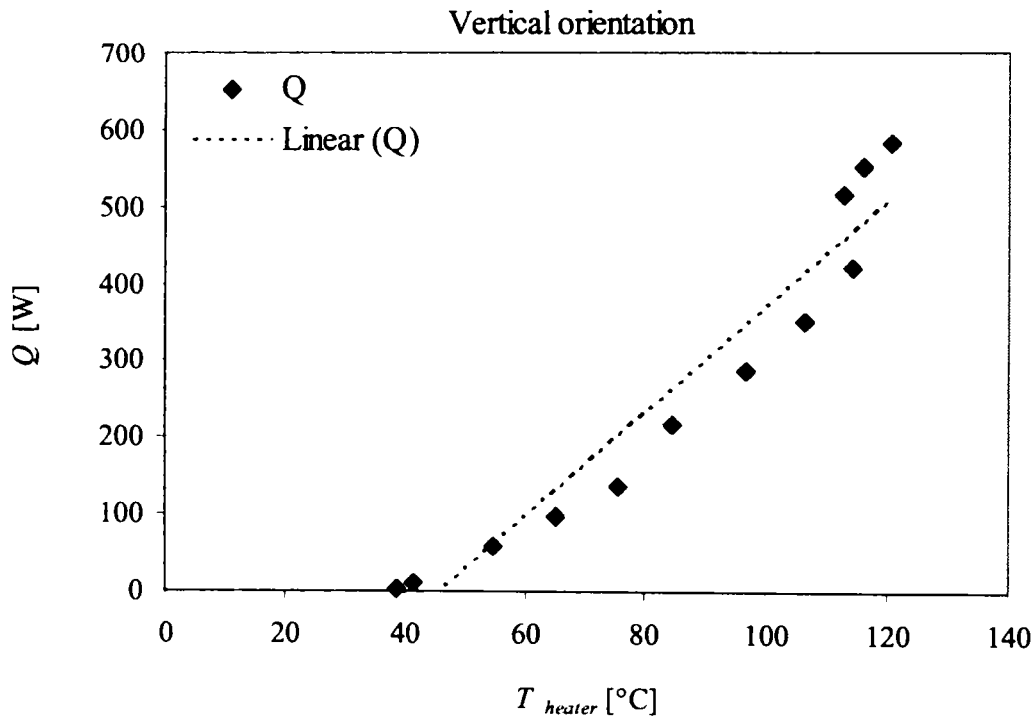


Fig. 3.4 Heat transport performance of 5-PT-HTD

Above this point, sharp pick of heater temperature was observed, indicating the beginning of evaporator dry out. Fig 3.5 shows the abrupt rise of heater temperature in time. At this particular moment, vapor was flowing through all 5 tubes and for a short period of time there was no condensate return back to evaporator. Although the picks appear periodical, the high value of heater temperature (180°C) may damage some components of the test core and therefore the experiments were stopped at this point.

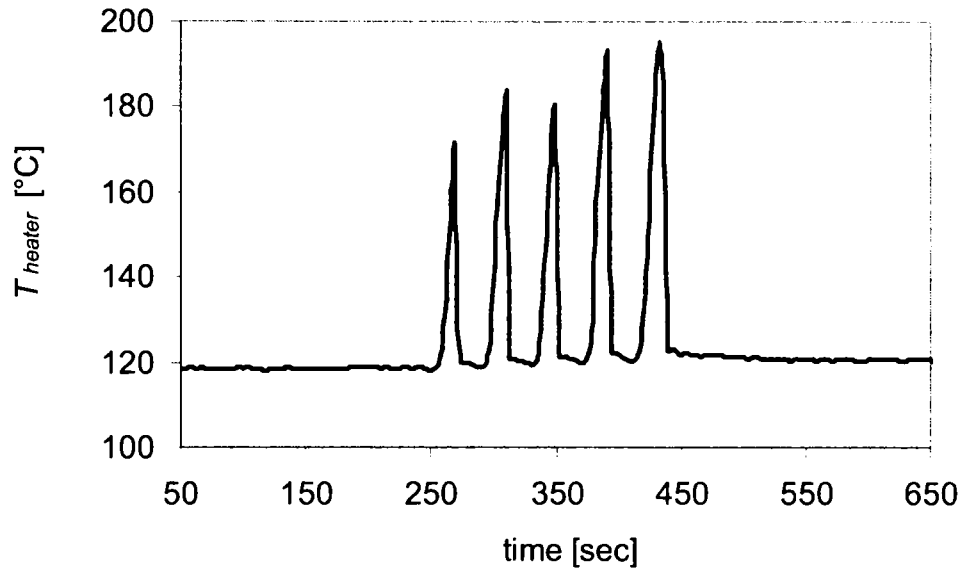


Fig. 3.5 Variation of heater temperature in time for $Q \sim 600\text{W}$

One can see in Fig. 3.6 the effective thermal conductivity of present HTD compared to those of three typical conventional heat pipes (HP) with similar sizes (see Fig.3.7 and Table 1) and same working fluid (water). As it can be observed from Fig. 3.6, at lower heat transport rate, $Q < 100\text{W}$, the conventional HP1 [36] and HP2 [29] show higher performance. For $Q = 300\text{W}$, a large size heat pipe (15.9mm in diameter and 370mm long), HP3 [34], shows lower performance than the present HTD. It is clearly seen that the present HTD can carry much larger Q which conventional HPs cannot achieve. The highest Q of the present setup of HTD was up to 600W with k_{eff} being 200 times more than the thermal conductivity of copper.

Table 1. Dimensions of HPs compared with the present HTD

	HTD	HP 1	HP 2	HP 3
$\varnothing \times \text{No. [mm]}$	2.8 x 5	4 x 1	6.35 x 1	15.9 x 1
$A_t \text{ [mm]}$	30.8	12.6	31.7	198
$L_{ad} \text{ [mm]}$	200	55	200	98
$L_t \text{ [mm]}$	300	160	276	370

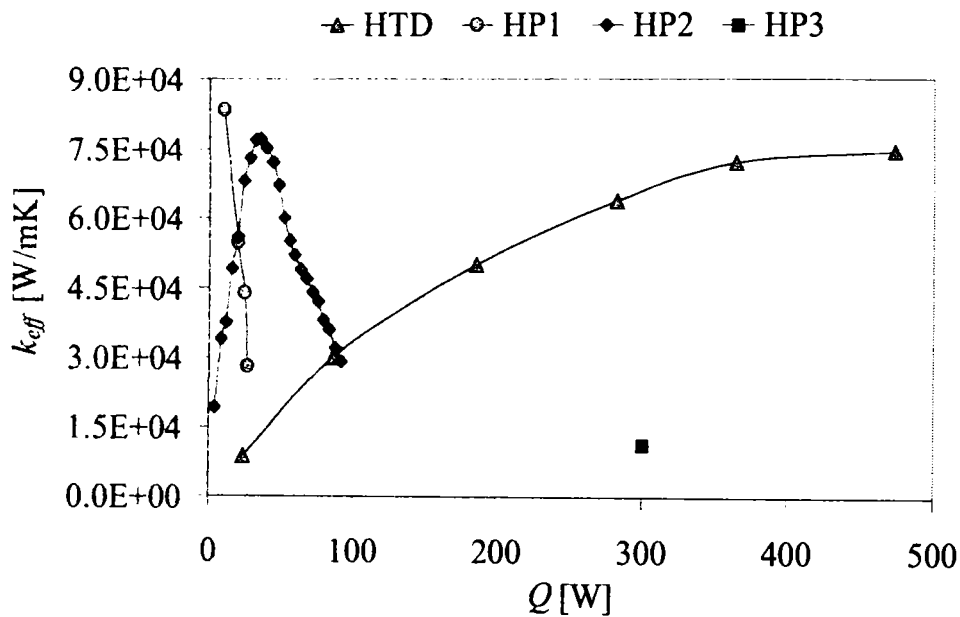


Fig.3.6 Effective thermal conductivity vs. Q

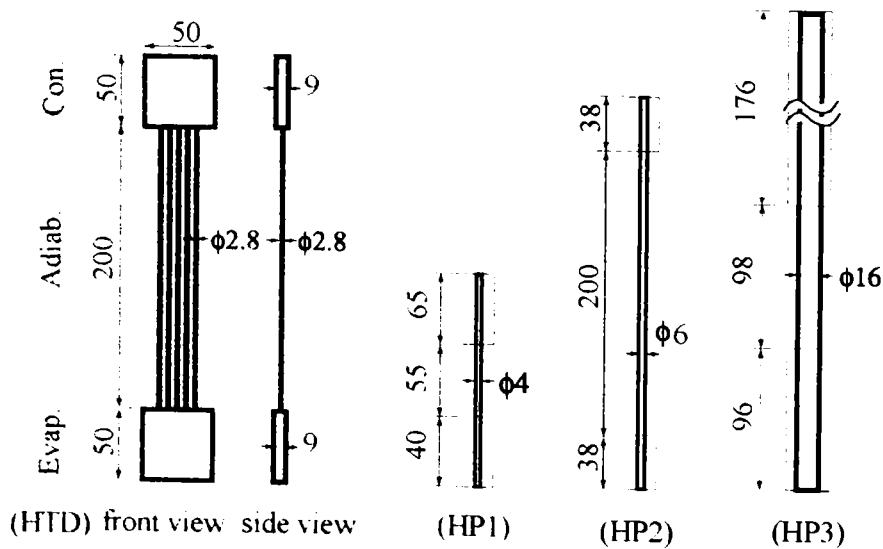


Fig 3.7 Geometry of HPs compared with the present HTD

3.3.1.2 Relationship between tube wall temperature measurements and the fluid phase inside the tube

By measuring the wall temperature of tubes, the flow inside the tube can be deduced through the assumption that, high temperature corresponds to vapour flow inside the tube, while low temperature indicates the presence of condensate in the tube. Fig. 3.8 represents wall temperatures at three axial positions (T_e , T_m and T_c) for each of the five tubes (t1 to t5, see Fig. 3.1) for the case of low Q , 20W. It can be seen from the figure that all 5 tubes have almost the same axial temperature distribution. This indicates that all tubes were functioning in the same way carrying vapour and condensate. In this low Q case, the presence of an oscillatory flow in every tube was confirmed through high-speed video records of the flow in the condenser chamber.

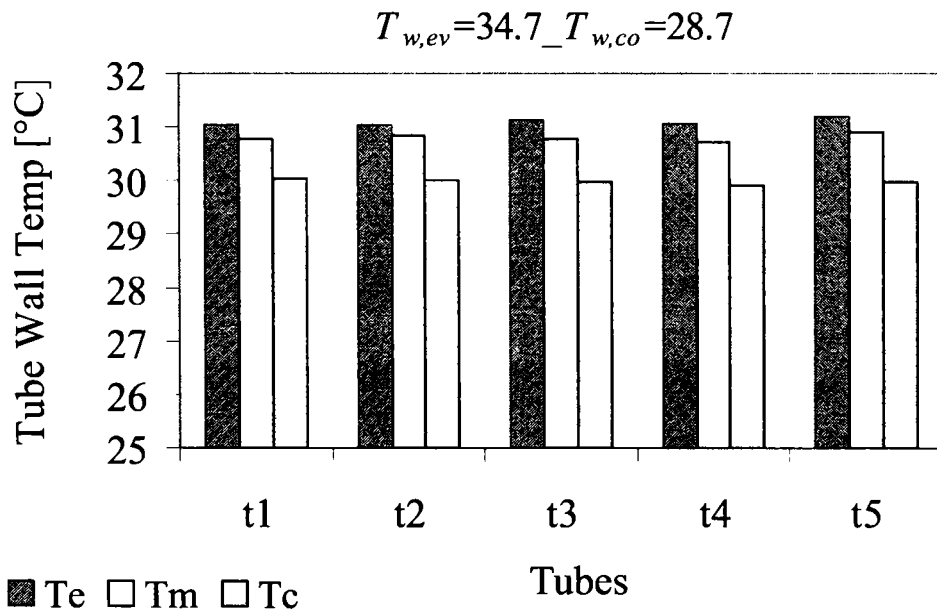


Fig. 3.8 Wall temperatures of tubes at low Q (=20W)

For high Q case, (500W, for example), a stable re-circulating flow was observed, with four tubes working to carry vapour from evaporator to condenser and one tube for condensate return, as can be seen in Fig. 3.9 where the lower temperature of tube number one (t1) indicates that this tube is working for

condensate return (Case A). This is due to the depth of water accumulated in the colder region in the condenser (close to the inlet of cooling water), which adds to the gravity head and drives the condensate back to evaporator. By changing the position of cooling water inlet and outlet, a switching of the condensate return tube was observed (Case B). One can see from Fig. 3.10 that, in contrast with Case A, t5 is working as the condensate return tube while the other four tubes are for vapour flow.

Flow visualization (movie) records were in good agreement with the conclusions obtained from the tube wall temperature measurements. Fig. 3.11 is a capture of an instantaneous existence of a liquid of vast bulk formed on the colder region (above t5) inside the condenser in Case B.

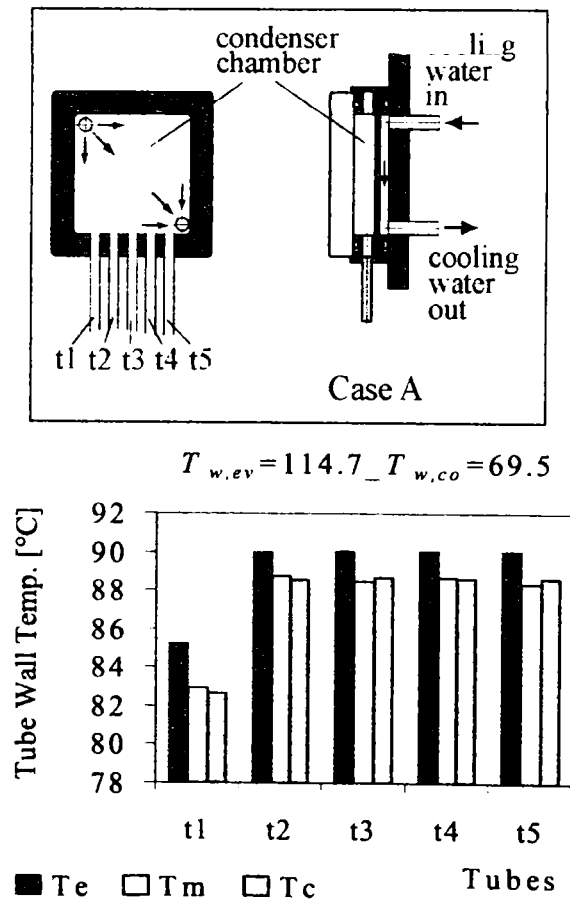


Fig. 3.9 Wall temperatures of tubes at high Q (=500W) for Case A

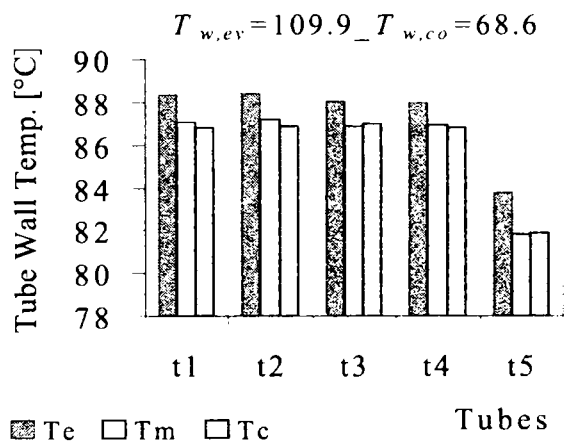
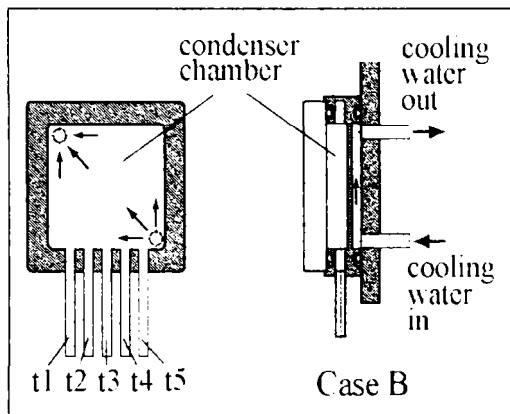


Fig.3.10 Wall temperatures of tubes at high Q for Case B

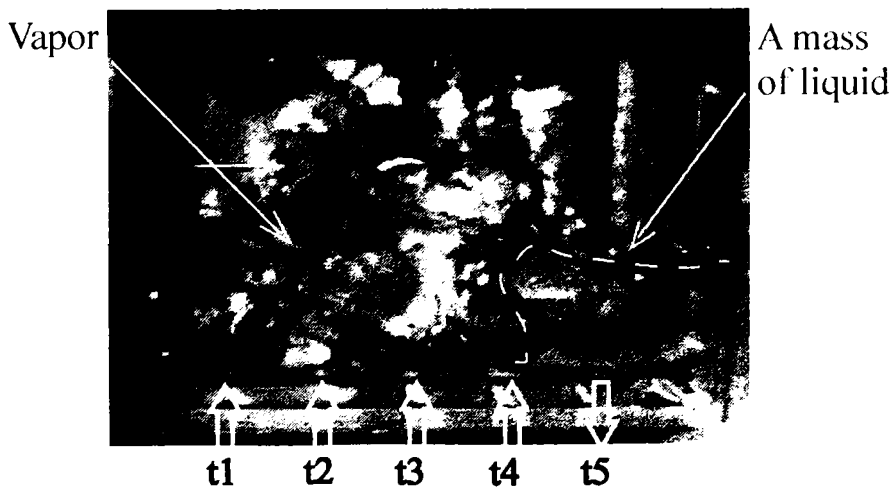


Fig.3.11 Flow visualization in condenser chamber (case B)

3.3.2 Horizontal orientation of device

In case of horizontal orientation, the present device was able to transport heat up to 40W for a heater temperature around 60°C. The variation of Q with T_{heater} for the horizontal case, is shown in Fig. 3.12. Although initially there is an abrupt increase of Q with a rise of T_{heater} , after 40°C, the heat transport rates have the tendency to saturate. The working fluid is accumulating in condenser chamber and gradually the evaporator tends to dry out. By looking at the effective thermal conductivity variation with T_{heater} , one can see in Fig. 3.13 that a sudden drop is occurring after 40°C. The performance is decreasing with further increase of heater temperature. Due to the absence of pressure head between evaporator and condenser, the liquid accumulated in condensed can not easy flow back to evaporator. The amount of transported heat is much less as compared to the vertical orientation, yet, the horizontal case can be used in a range of low Q .

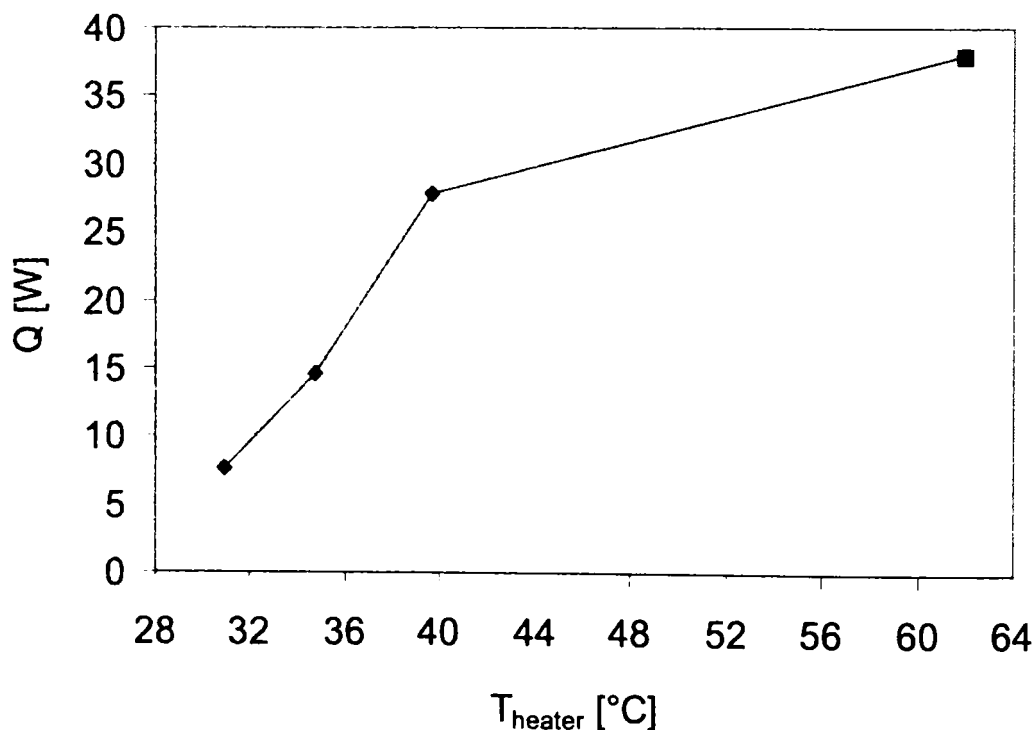


Fig. 3.12 Heat transport rate vs. heater temperature for the horizontal orientation

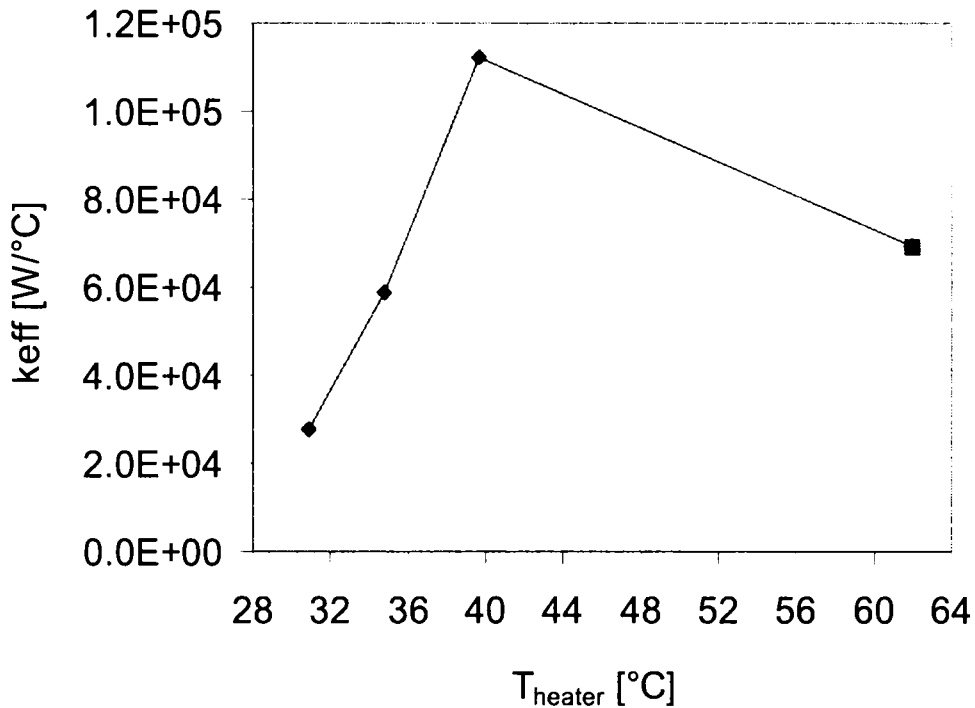


Fig. 3.13 Effective thermal conductivity in case of horizontal orientation

3.3.3 Bent tubes – horizontal position of evaporator

3.3.3.1 Performance of the 5-PT-HTD for the bent tubes case

As it can be seen from the above Fig. 3.14, for the experimental setup with the evaporator placed on horizontal position, the performance of the present device is up to 700W. Compare with the vertical orientation, in the present case, the experiments were stopped at this point due to the limitation of auxiliary devices used for experiments. The slide regulator (connected to the 200V panel) used to control the heat input, was 240V, which is close to the maximum point, and the current was 2.5A. The Keytley multimeter used to measure the electrical current, can not exceed 3A. To avoid any possible damage of devices, the experimental conditions were kept within the safety range. The above description indicates that, the maximum heat transport of present device was not determinate and that actually it can exceed 700W.

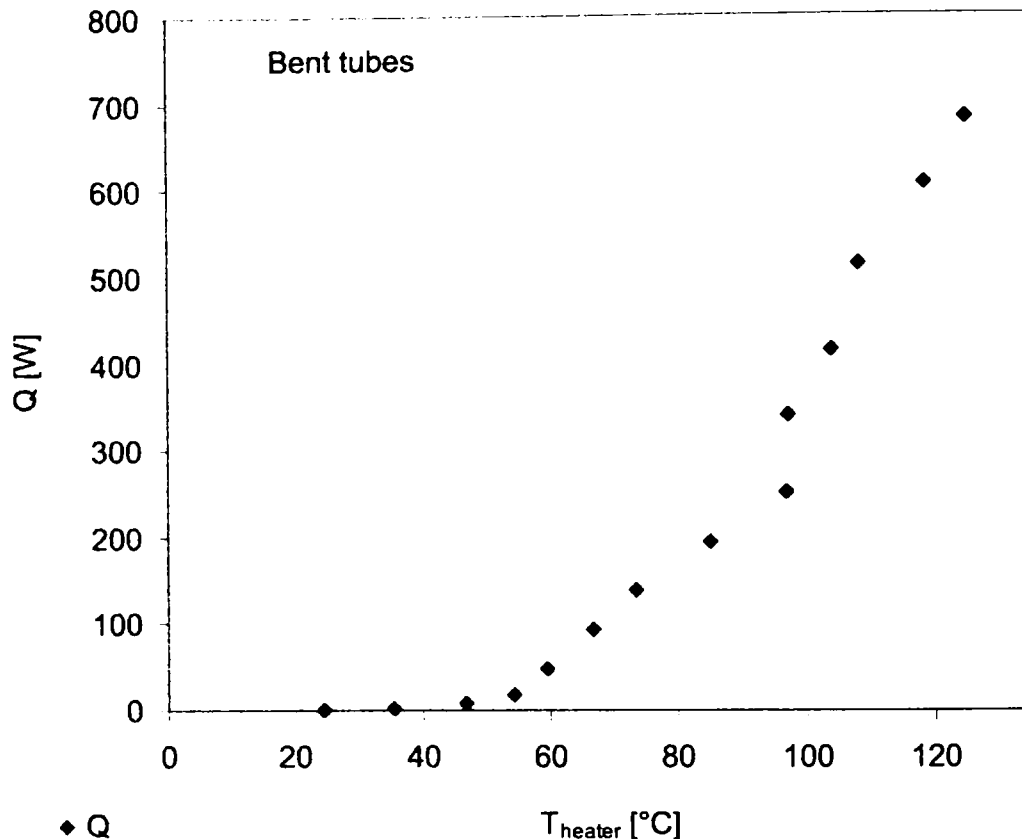


Fig. 3.14 Heat transport rate variation with heater temperature

3.3.3.2 Inner flow behavior analysis

Through flow visualization (movies), at low heat input, a periodical condensate return was observed. First, the liquid is accumulating in condenser up to a certain level, (almost 2/3 of condenser chamber was filled with liquid) as seen in Fig. 3.15. When the column of liquid reaches the indicated level, the condensate starts to return to evaporator through 4 of the tubes, while in the same time, vapor is flowing through one of the tubes. At same heat input, this behavior of inner flow was not observed for the experiments performed under the vertical orientation.

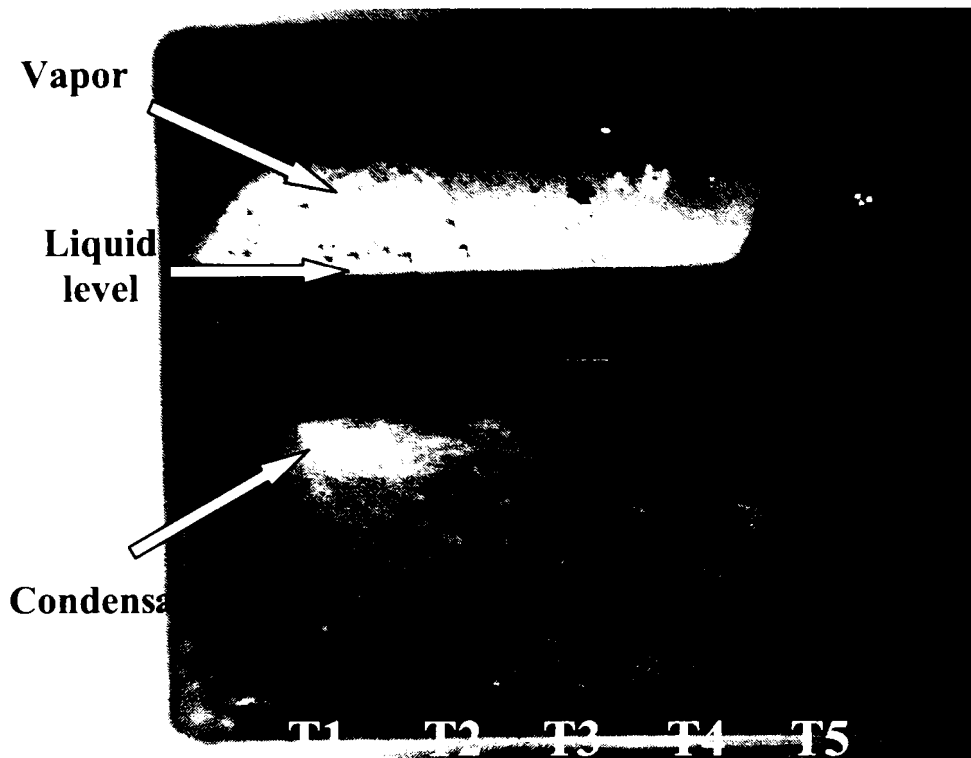


Fig. 3.15 Snap shot of fluid in condenser chamber at $Q \sim 25W$

Looking at the heater temperature variations in time (Fig.3.16), a periodical rise and drop can be observed. The averaged value is though kept constant at around $54^{\circ}C$ for $Q \sim 25W$. The pick of the T_{heater} corresponds to the level of liquid accumulated in condenser. When the condensate returns, the heater temperature decreases and the cycles of fluid movement correspond to the variations of heater temperature. For an interval of 10 minutes, 12 cycles can be observed which indicates a low frequency.

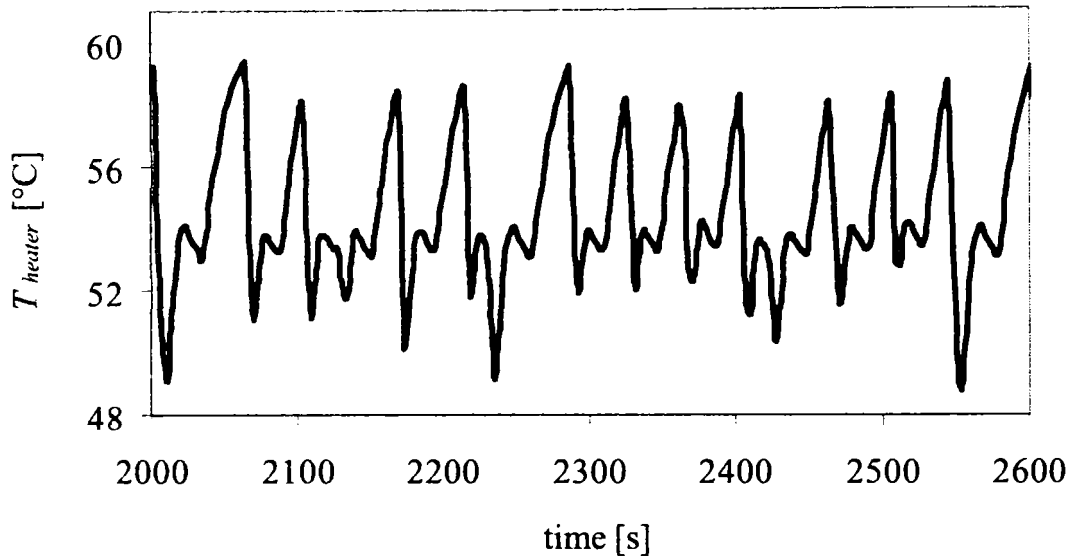


Fig. 3.16 Heater temperature variation in time for $Q \sim 25\text{W}$

Increasing the heat input, different flow behaviour was observed. At 100W for example, a stable recirculation of the flow can be seen in Fig. 3.17, with two tubes carrying vapour and three for condensate return.

A method to estimate the fluid phase inside the copper tubes was developed by measuring the tube wall temperatures at three locations close to evaporator, middle of the tubes, and close to condenser. It was considered that high temperature indicates that vapour is flowing through the tubes while low temperature value would correspond to the presence of condensate in the tubes.

Fig. 3.18 shows the tube wall measurement at 100W. One can see from the figure that, two of the tubes have higher temperature compared with the other three. This means that vapour is flowing through tube number 1 and 2, while condensate is returning through tube 3, 4 and 5.

By comparing the flow visualization results (Fig. 3.17) and the tube wall temperature measurements (Fig. 3.18) a good agreement can clearly be seen.



Fig. 3.17 Flow visualization in condenser for $Q \sim 100W$

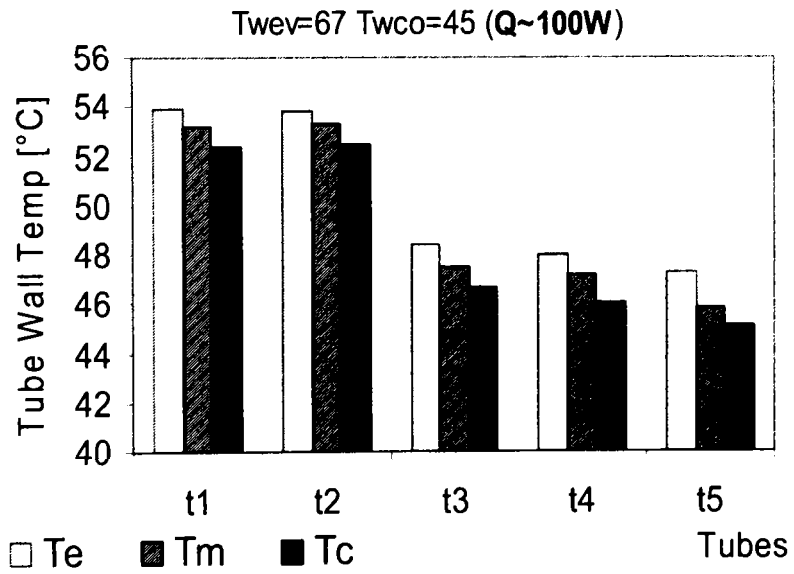


Fig. 3.18 Averaged tube wall temperature for $Q \sim 100W$

Furthermore, for $Q \sim 200W$, four tubes were observed to carry vapor and one tube number 5 was set for condensate return (Fig. 3.19). The tube wall temperature measurements are in good agreement with the flow visualization. As it can be seen in Fig. 3.20, tube 1, 2, 3 and 4 are showing high temperature, which means vapor is flowing through them; while tube's 5 low temperature corresponds to the condensate return.



Fig . 3.19 Flow visualization in condenser for $Q \sim 200W$

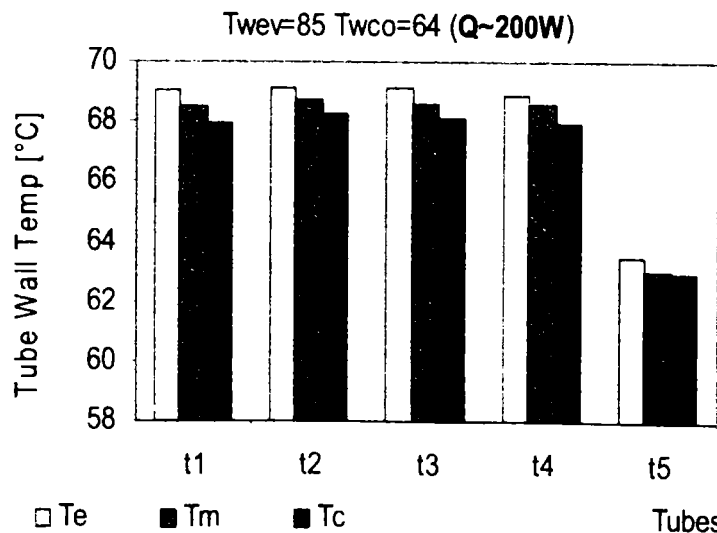


Fig. 3. 20 Averaged tube wall temperature for $Q \sim 100W$

3.4 Conclusions:

The main conclusions of the present study are as follows:

- (1) For the vertical orientation, the present device can transport heat efficiently up to 600W;
- (2) Compared with similar size HPs, the present HTD can cover a wider range of Q , with an effective thermal conductivity up to 200 times more than that of Copper;
- (3) Two flow patterns were observed: an oscillatory flow in each tube at lower Q range, and a stable re-circulating flow in the higher Q range;
- (4) Gravity seems to play an important role for the fluid recirculation, which results in heat transport performance of present HTD;
- (5) For horizontal orientation of evaporator and vertical of condenser (bent tubes case), dry out of evaporator was not observed and the performance was up to 700W.
- (6) Through flow visualization, the method of estimating the fluid phase inside the copper tubes by measuring the tube wall temperature was proved to be reliable.

APPENDIX -3

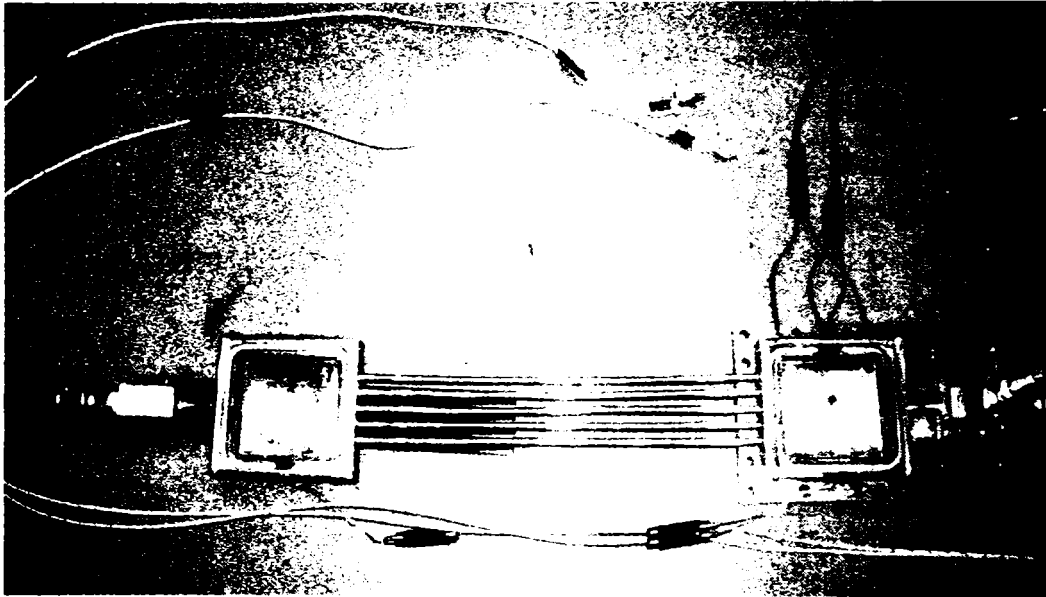


Fig. 3A-1 Assembling view of the 5-PT-HTD

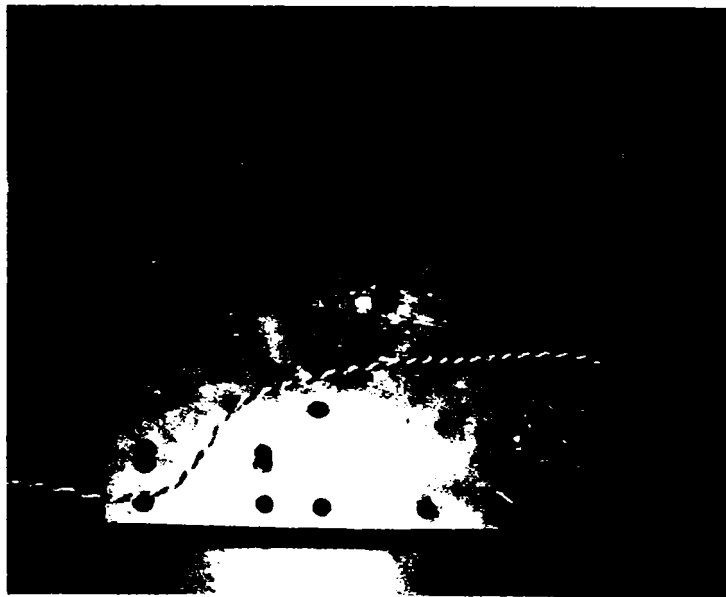


Fig. 3A-2 Cooling water inlet/outlet connections on the backside plate of condenser

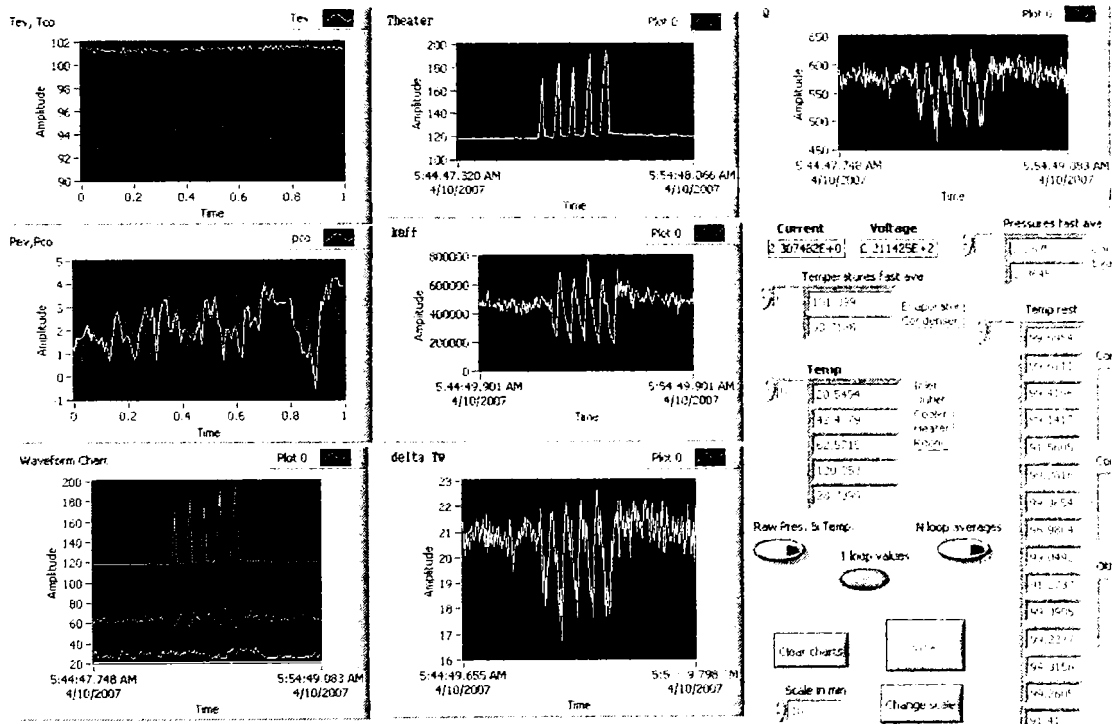


Fig. 3A-3 LabView Interface – monitoring of measurements

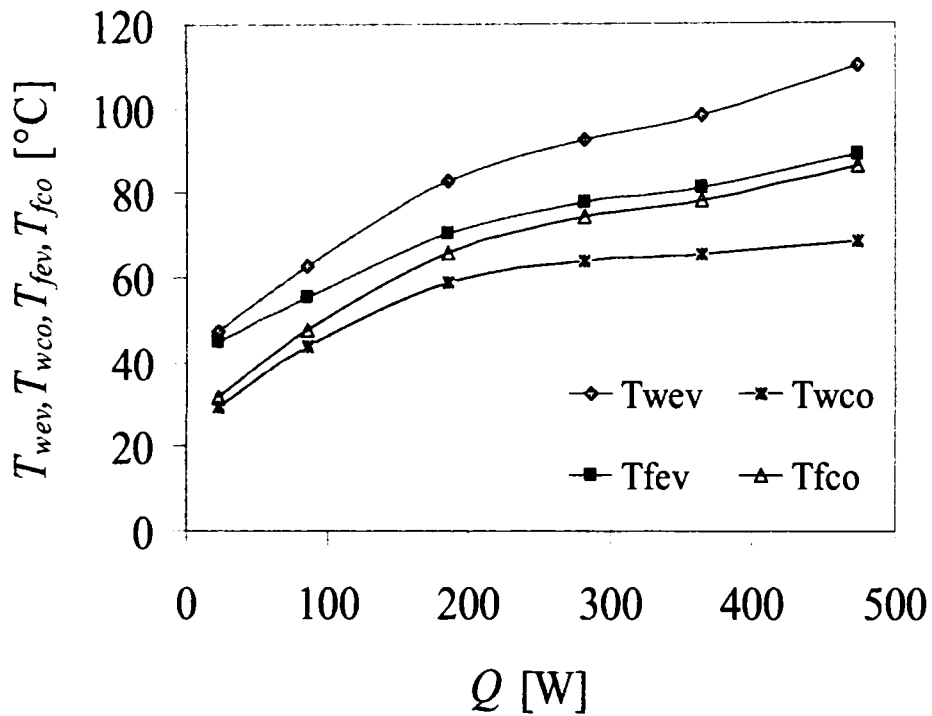
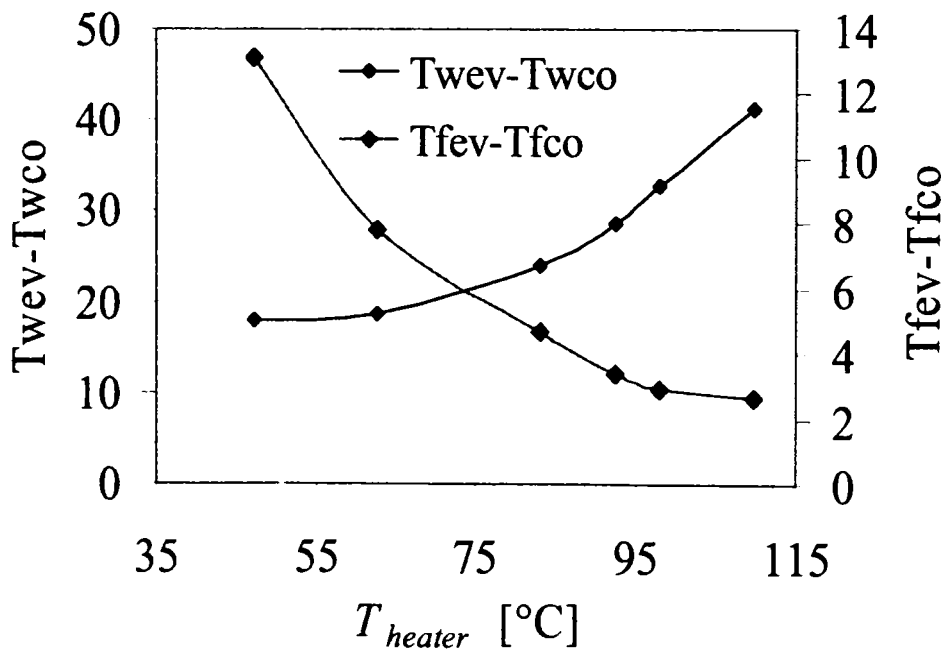
Fig. 3A-4 Fluid and wall temperatures inside evaporator and condenser vs. Q 

Fig. 3A-5 Temperature difference variation vs. heater temperature

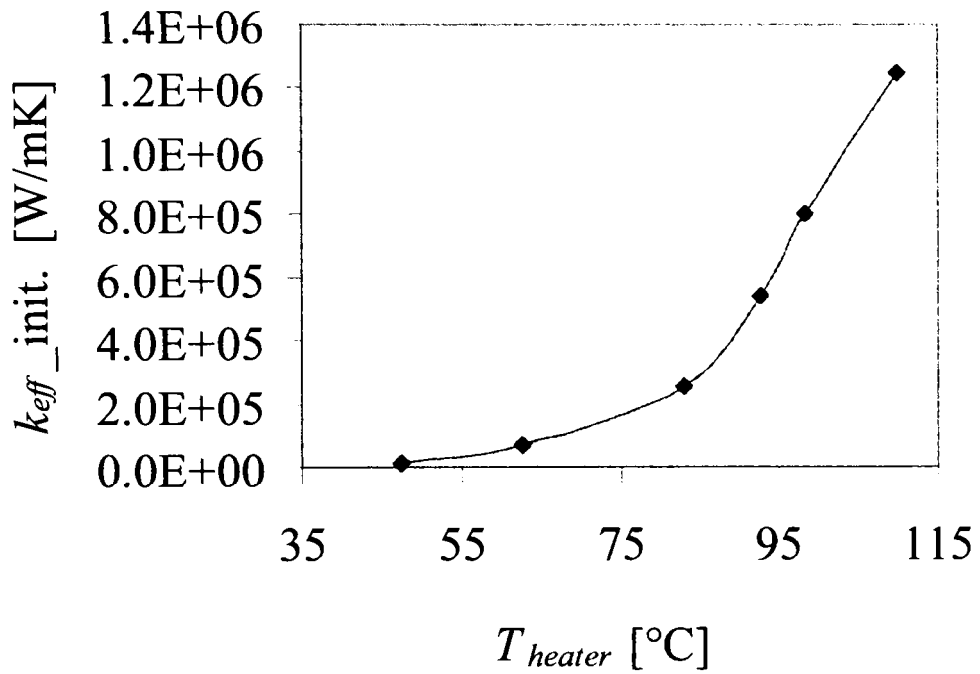


Fig. 3A-6 k_{eff} as function of fluid temperature difference, vs. heater temperature

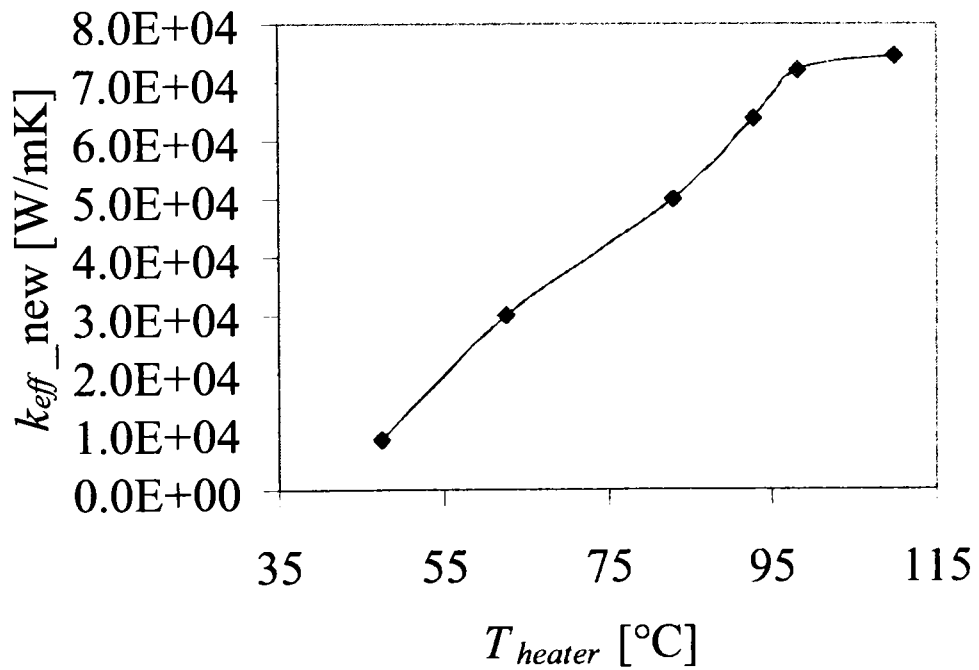
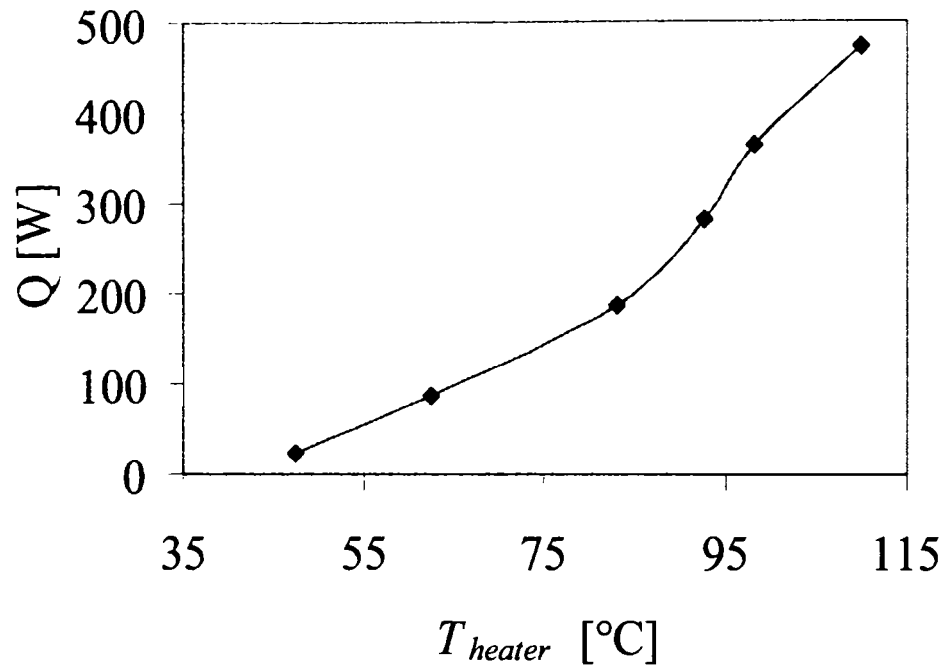
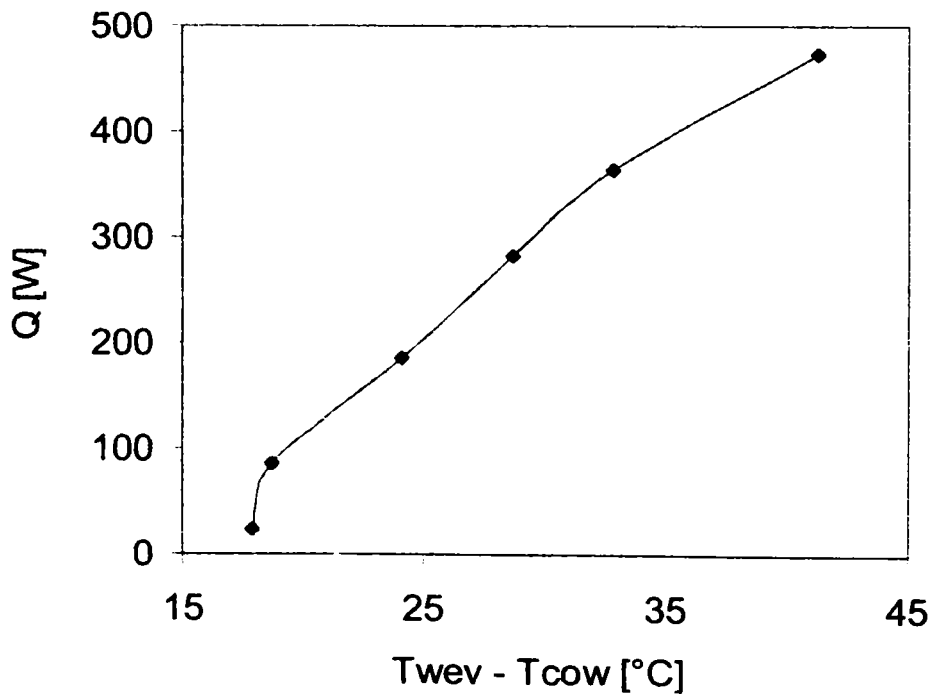


Fig. 3A-6 k_{eff} as function of wall temperature difference, vs. heater temperature

Fig. 3A-8 Variation of Q with heater temperature for vertical caseFig. 3A-9 Variation of Q with temperature difference between evaporator and condenser wall (for the vertical orientation of test section)

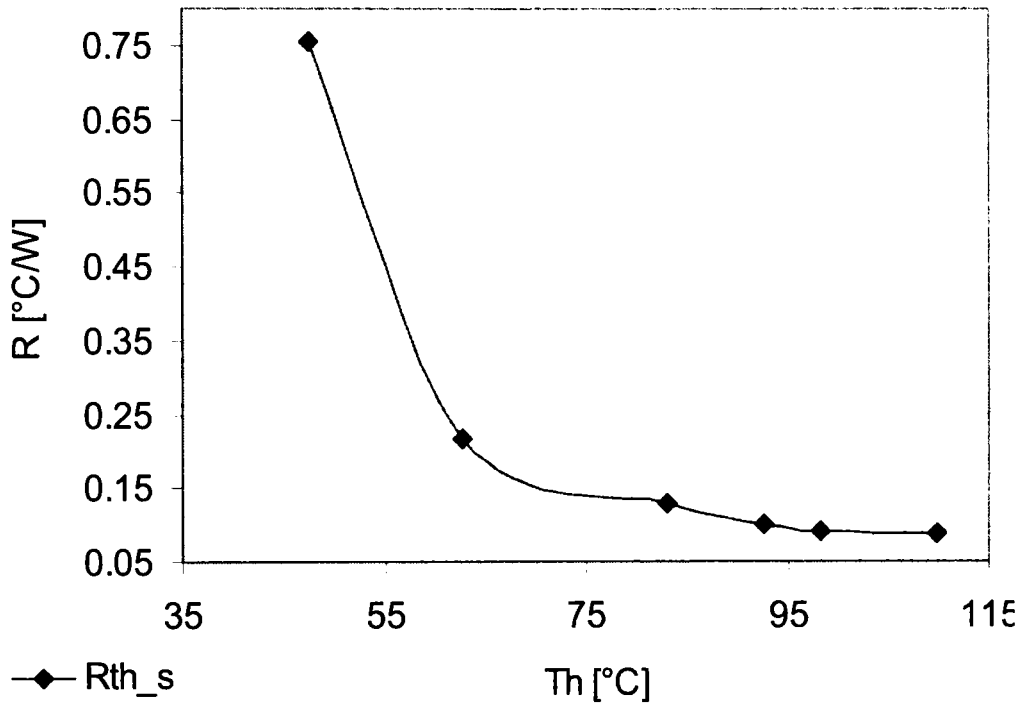


Fig. 3A-10 Thermal resistance vs. heater temperature

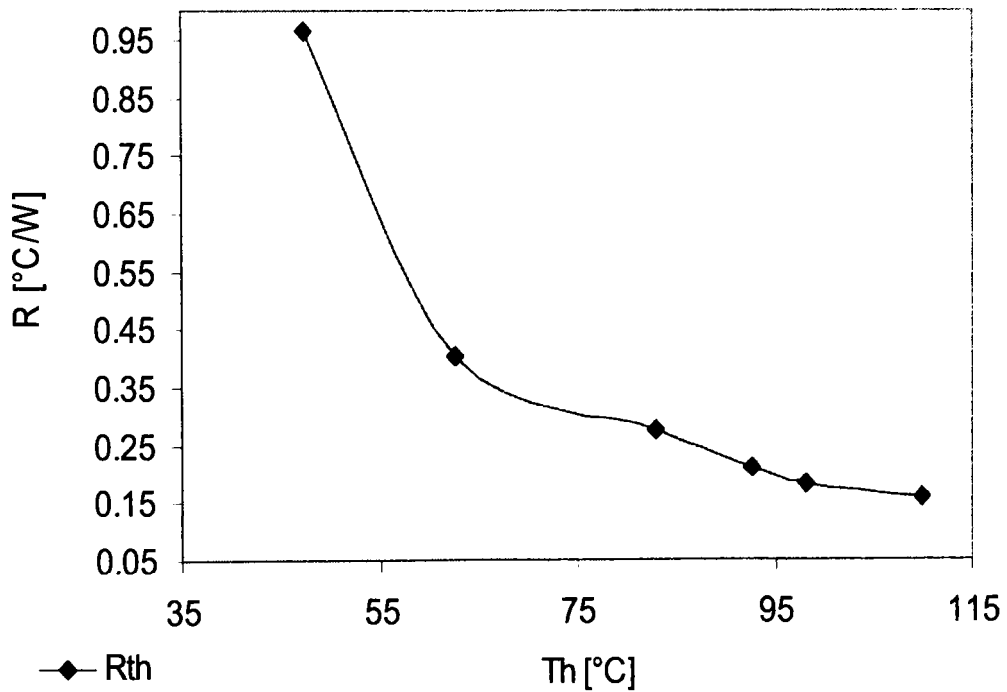


Fig. 3A-11 Thermal resistance vs. heater temperature

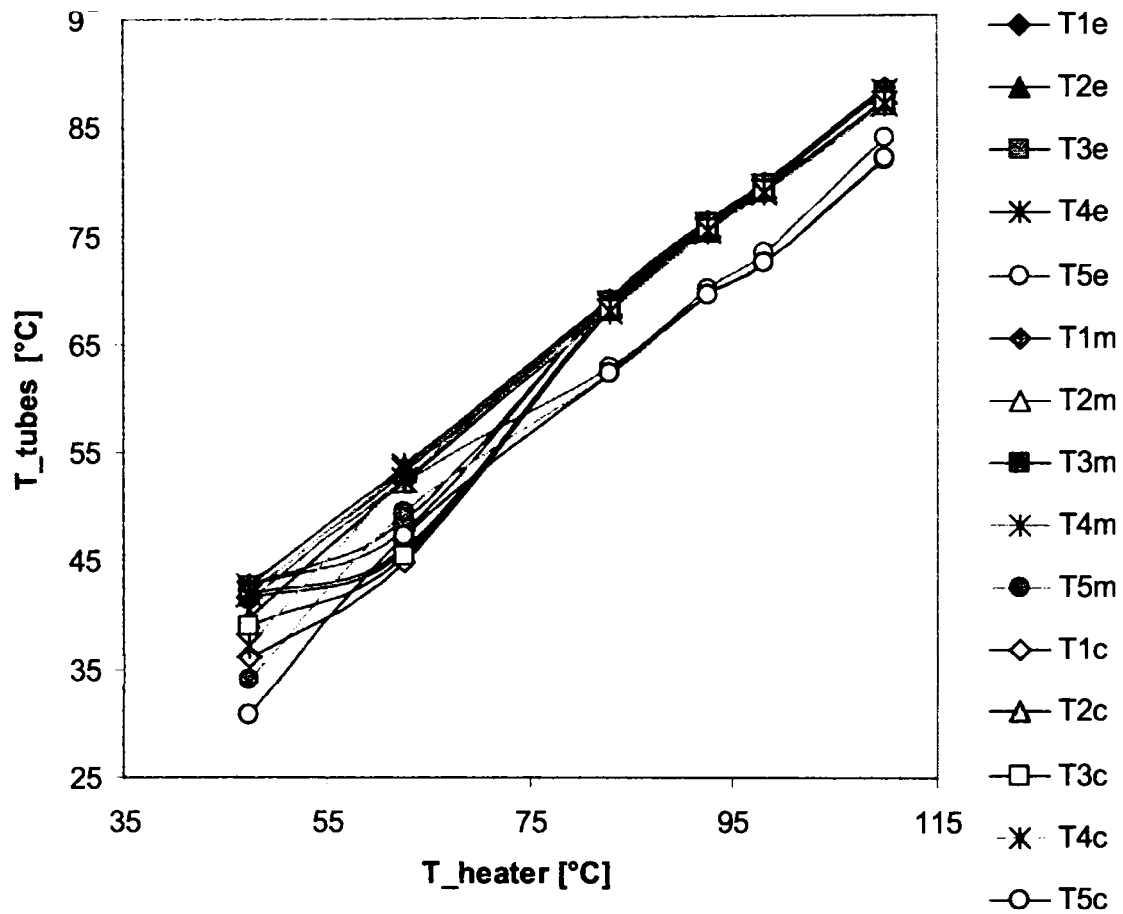


Fig. 3A-12 Tube wall temperatures at 3 locations, close to evaporator, T_e , at middle of the tubes, T_m , and close to condenser, T_c , versus heater temperature

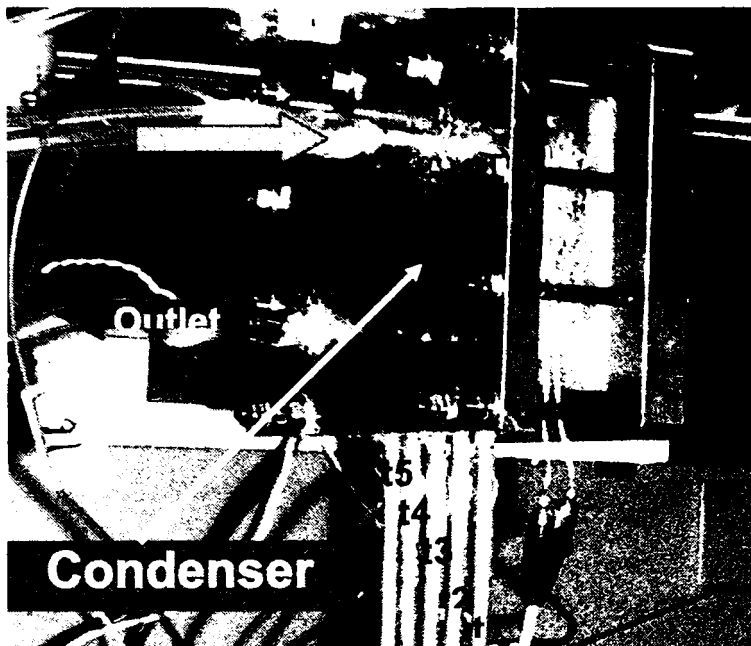


Fig. 3A-13 Backside of condenser, case A for cooling water inlet/outlet

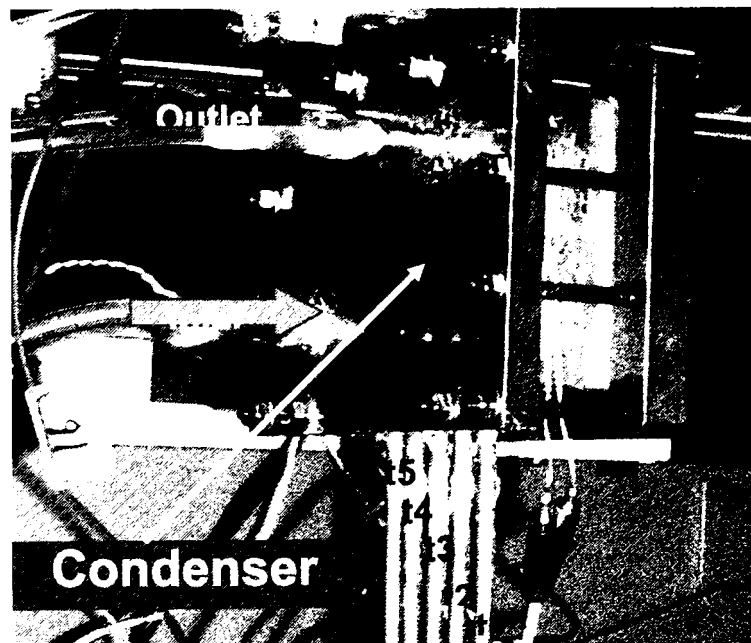


Fig. 3A-13 Backside of condenser, case B for cooling water inlet/outlet

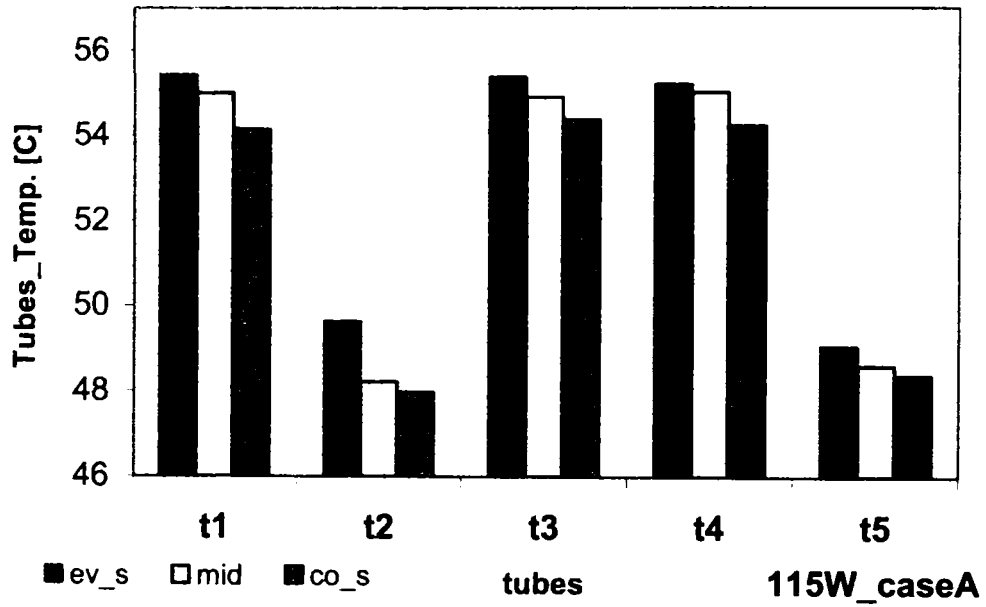


Fig.3A-15 Tube wall temperatures for case A at 115W

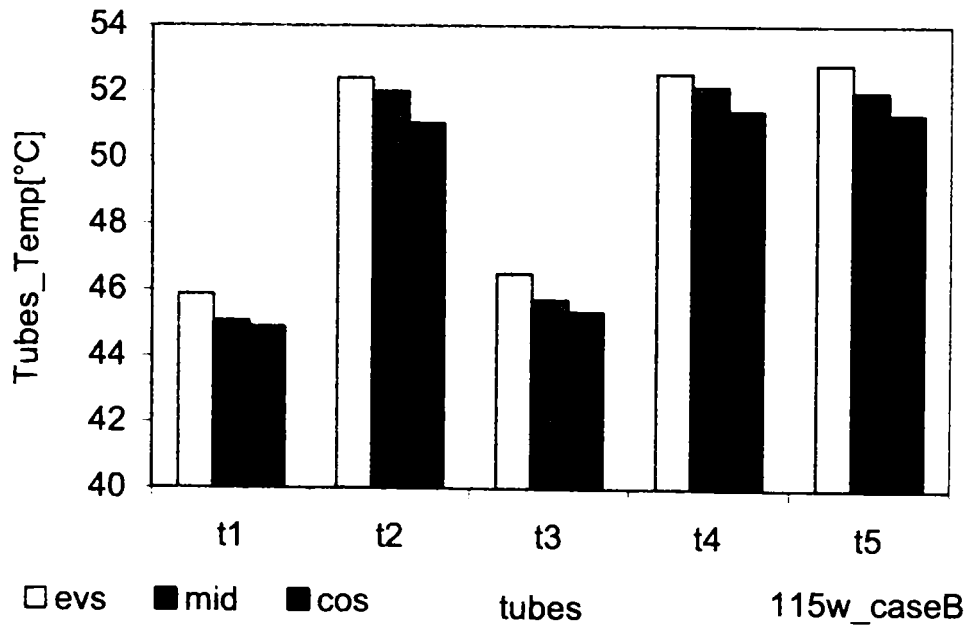


Fig.3A-16 Tube wall temperatures for case B at 115W

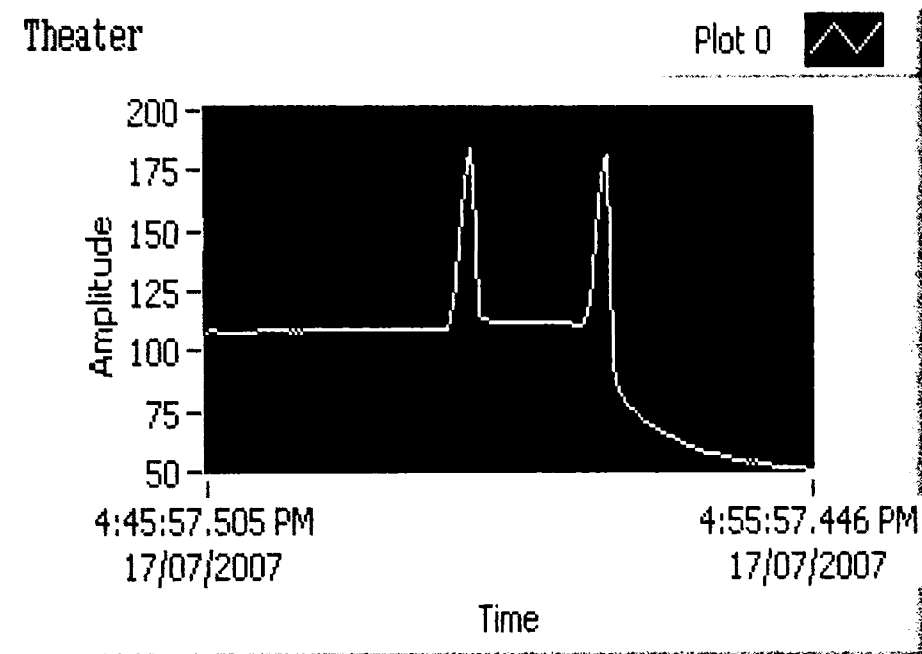


Fig.3A-17 Abrupt variation of heater temperature in time seen on the monitoring screen

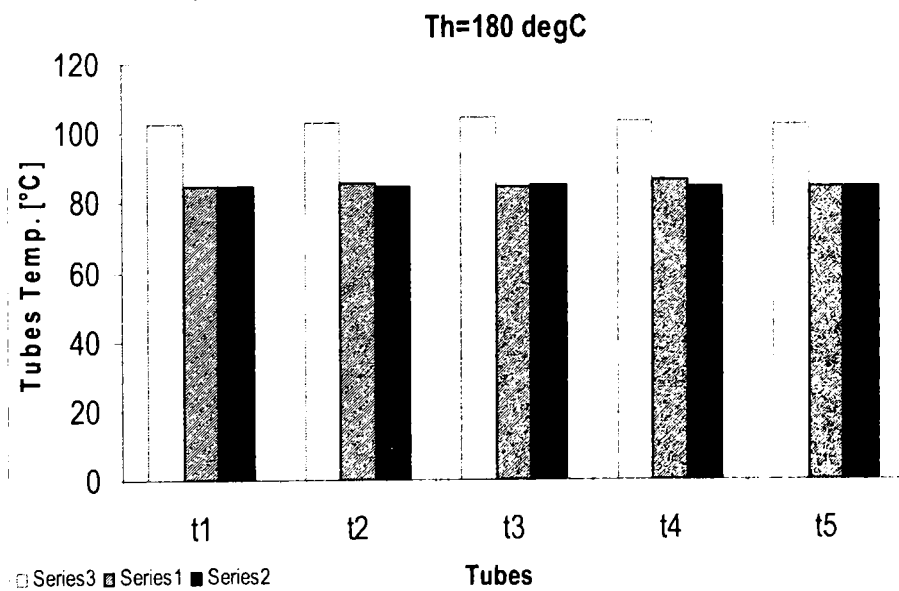


Fig.3A-18 Tube wall temperatures corresponding to the pick of heater temperature, observed in the previous figure (3A-17)

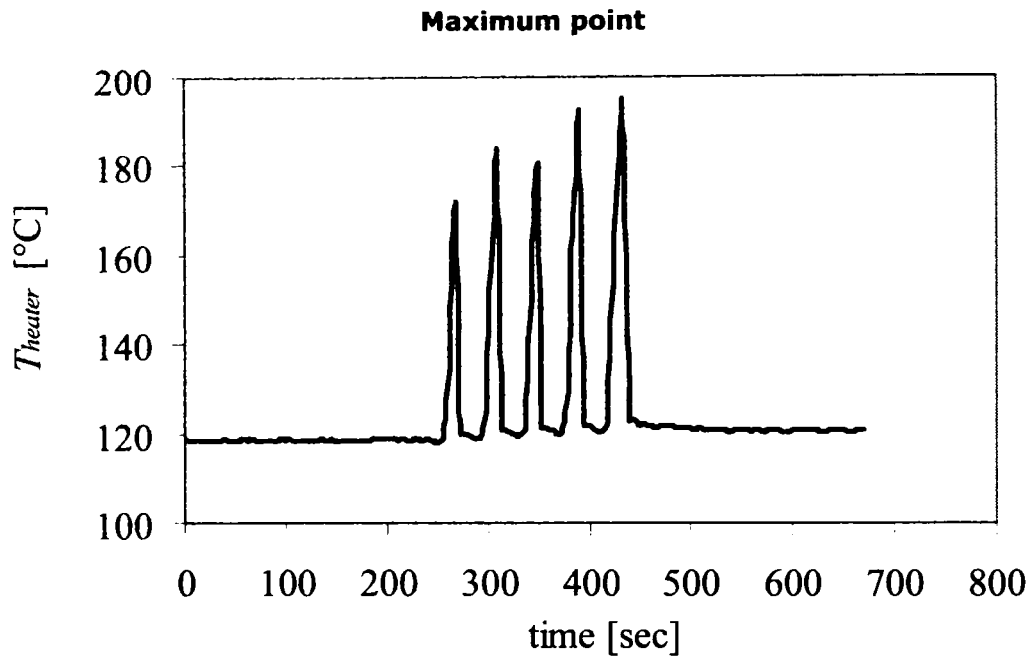


Fig. 3A-19 Variation of heater temperature at $Q \sim 600\text{W}$, for the vertical orientation case

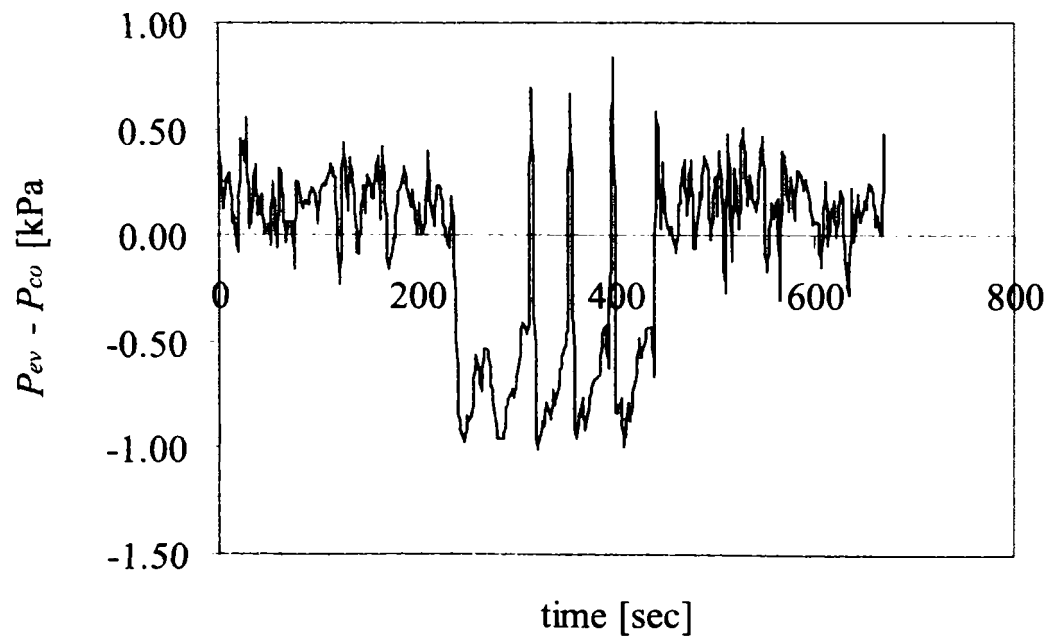


Fig. 3A-20 Variation of pressures in time at $Q \sim 600\text{W}$, for the vertical orientation case

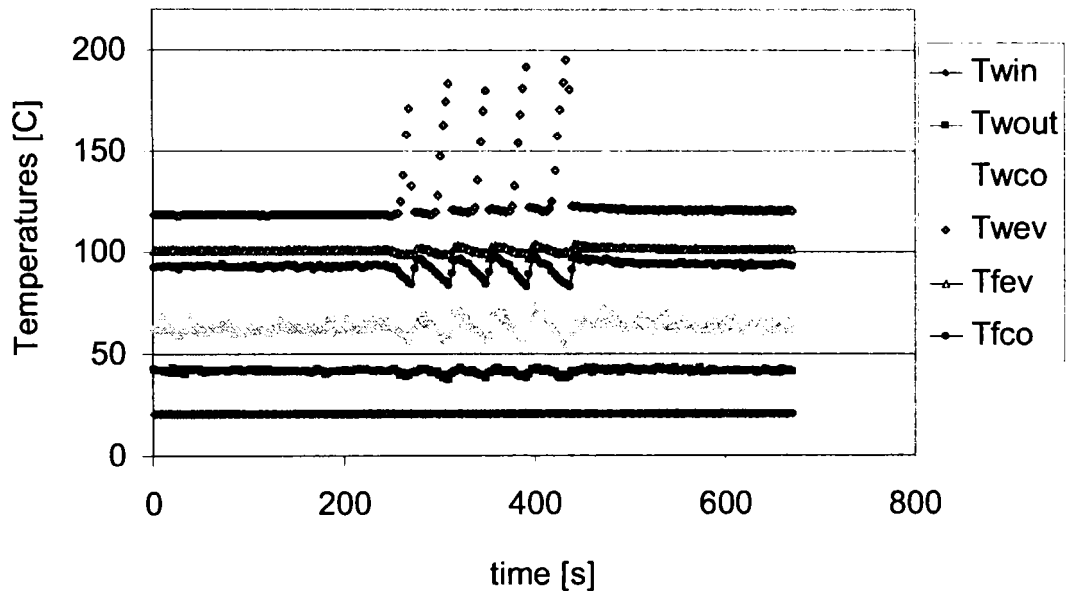


Fig. 3A-21 Variation of temperatures in time at $Q \sim 600W$, for the vertical orientation

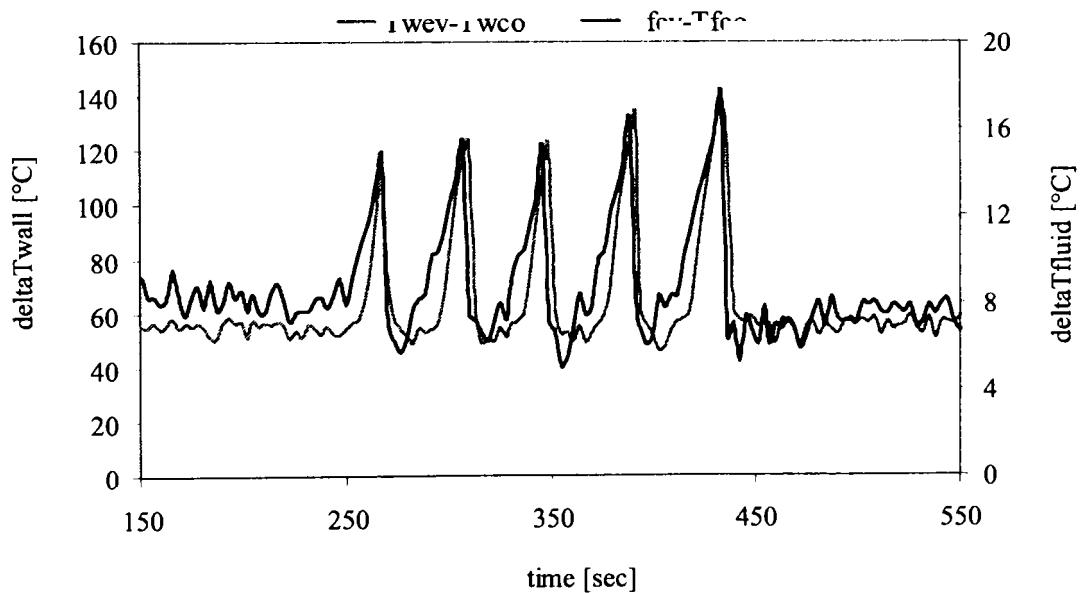


Fig. 3A-22 Variation of temperature difference $Q \sim 600W$, for the vertical orientation

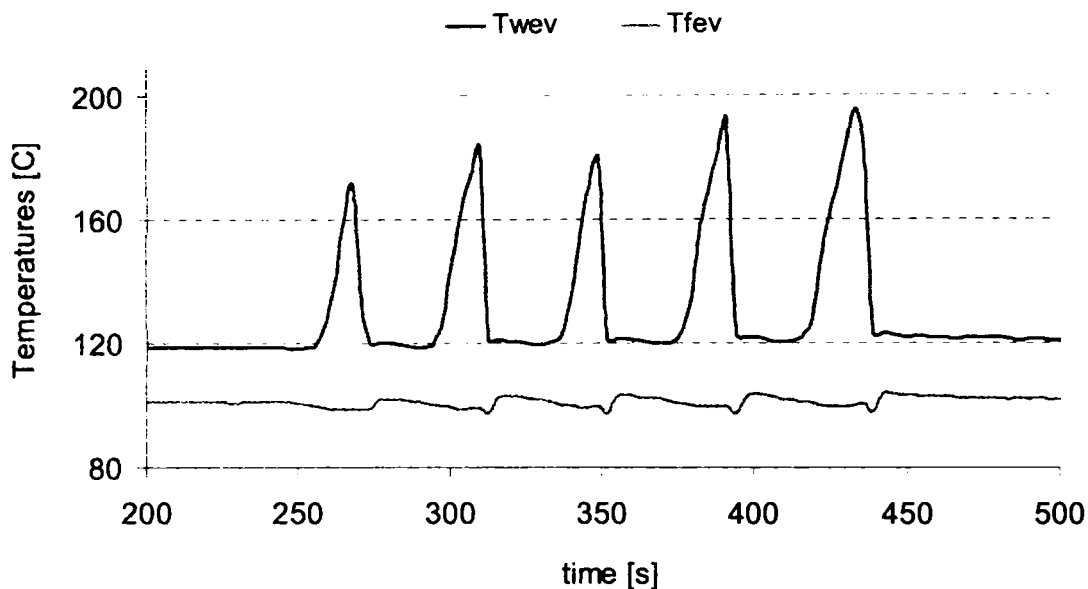


Fig. 3A-23 Temperature of evaporator wall and temperature of fluid in evaporator, vs. time at $Q \sim 600W$, for the vertical orientation case

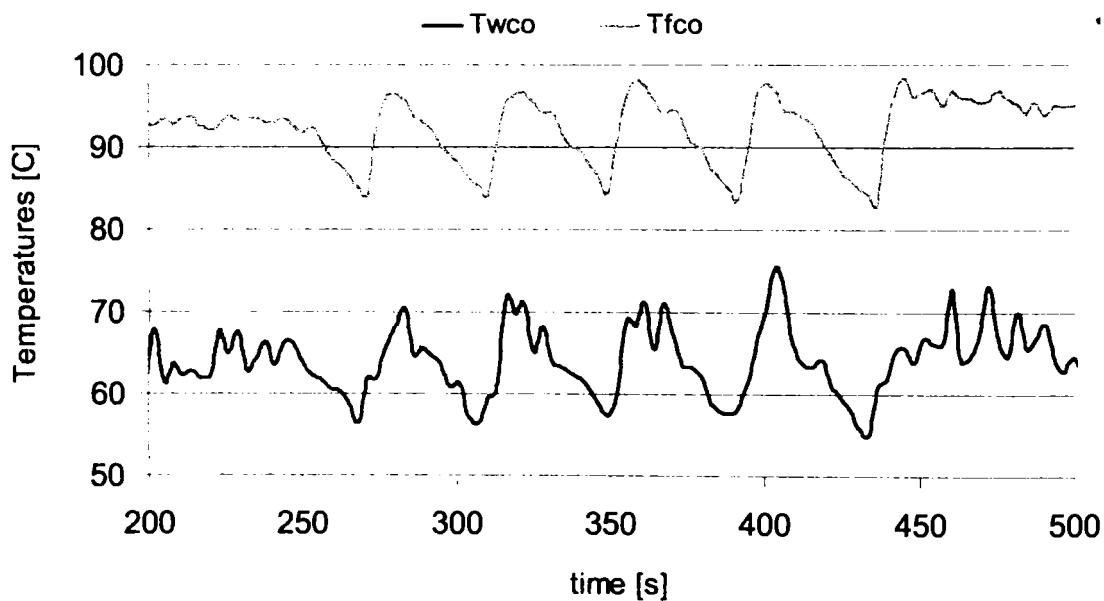


Fig. 3A-24 Temperature of condenser wall and temperature of fluid in condenser, vs. time at $Q \sim 600W$, for the vertical orientation case

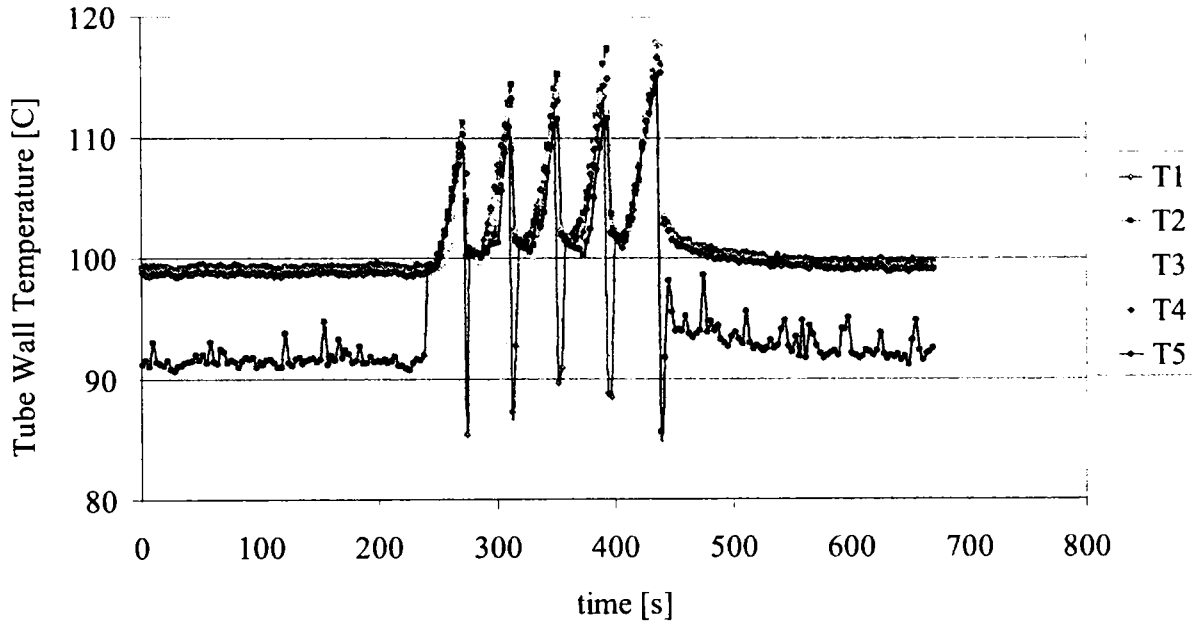


Fig. 3A-25 Tube wall temperature close to evaporator, T_e , vs. time at $Q \sim 600W$, for the vertical orientation case

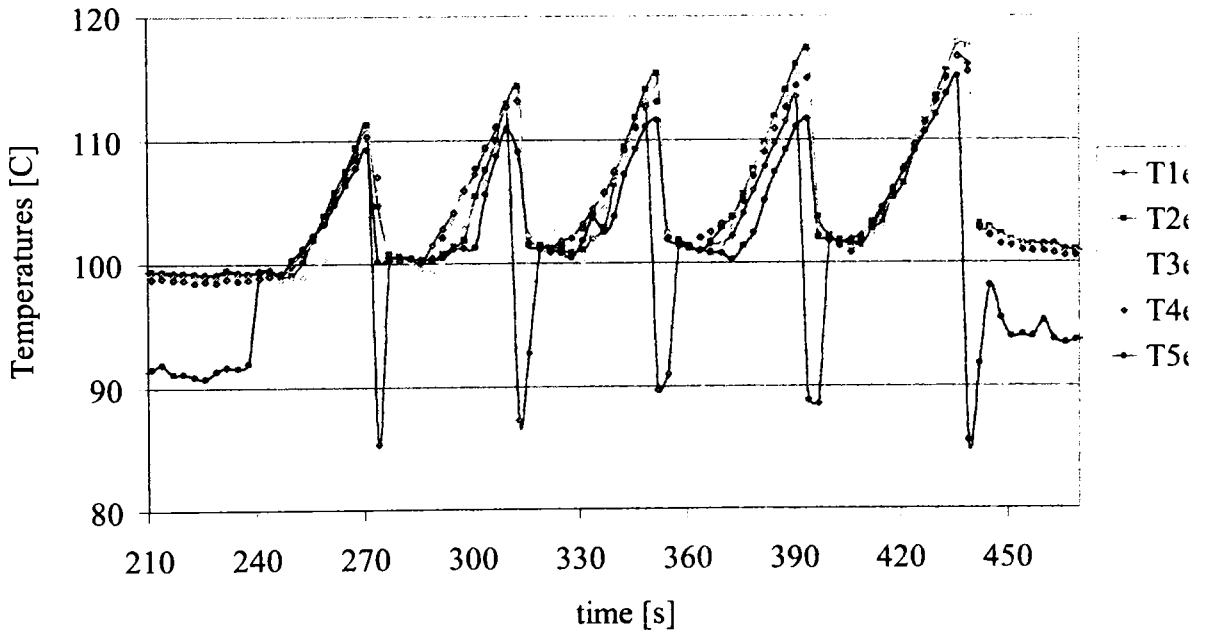


Fig. 3A-25 (II) Detail

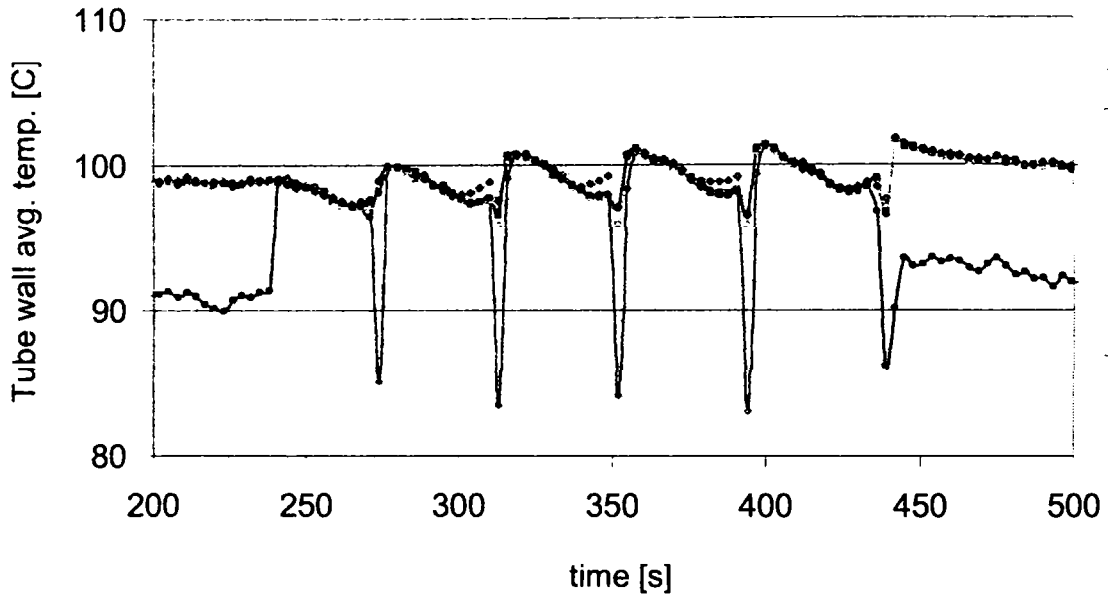


Fig. 3A-26 Tube wall temperature at middle of the tube, T_m , vs. time at $Q \sim 600W$, for the vertical orientation case

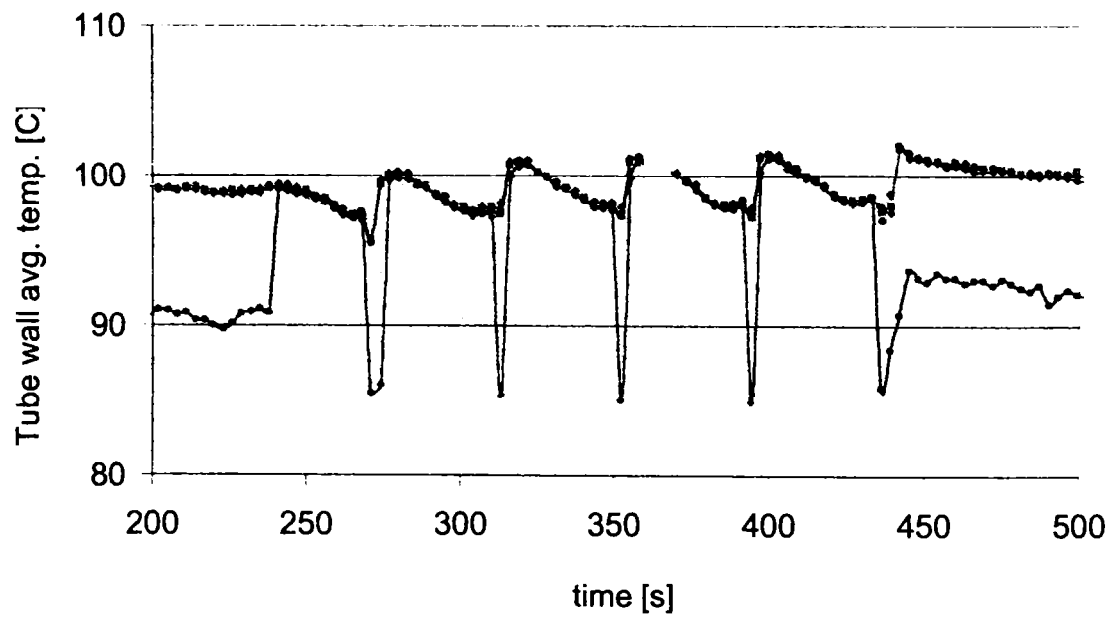


Fig. 3A-27 Tube wall temperature close to condenser, T_c , vs. time at $Q \sim 600W$, for the vertical orientation case

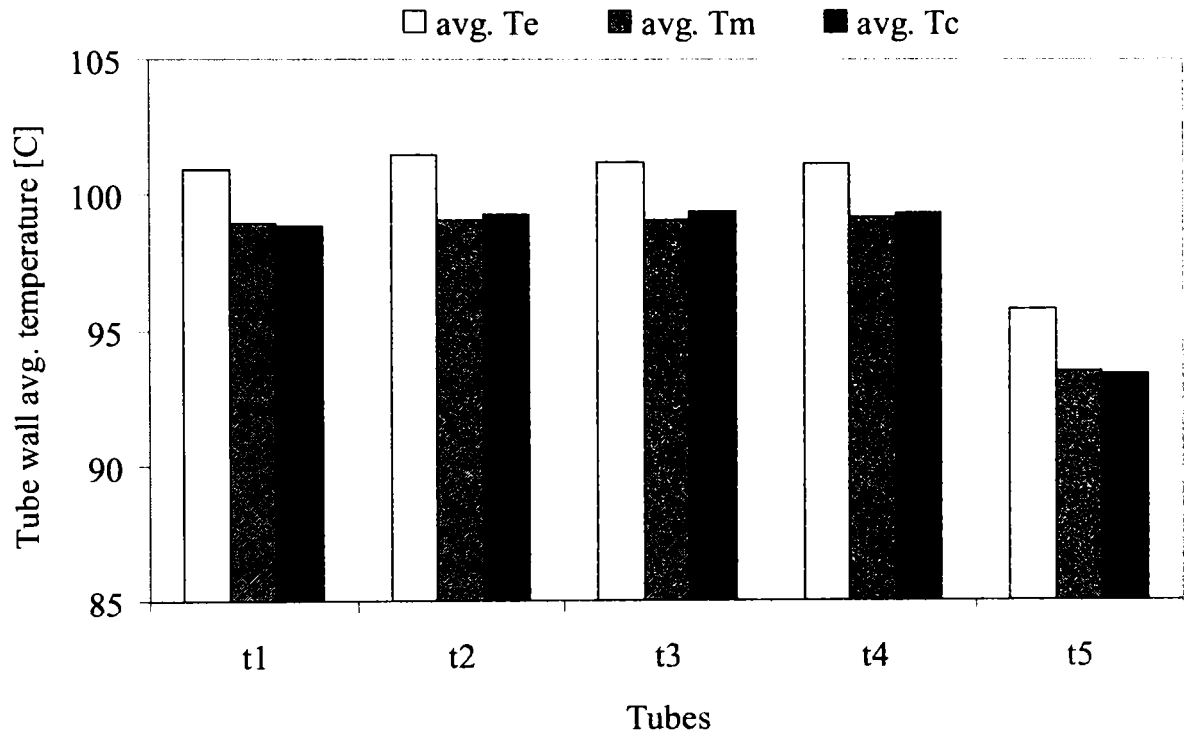


Fig.3A-28 Averaged temperature of tube wall at the three locations, Te, Tm, Tc

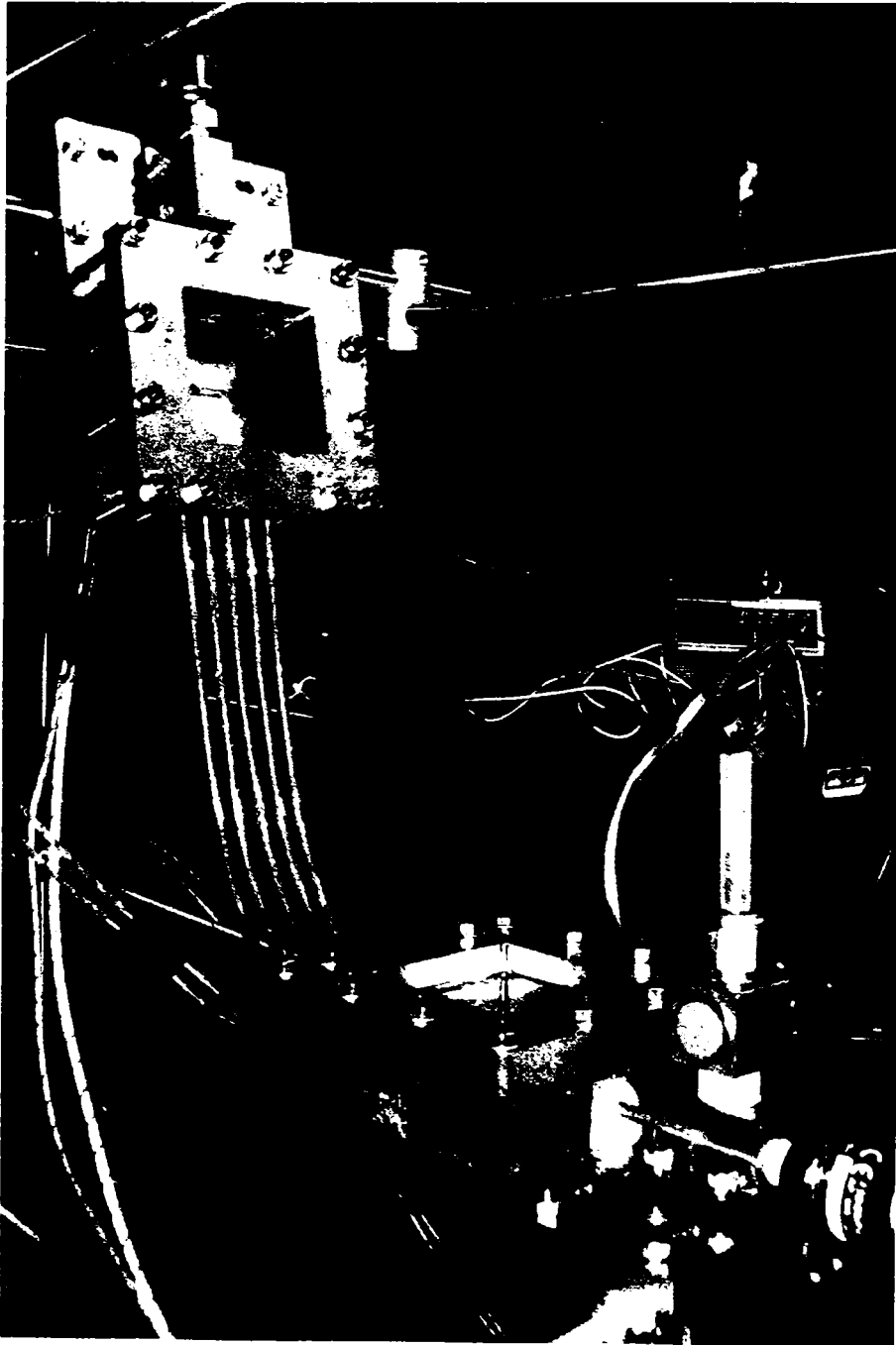


Fig. 3A-29 Bent tubes case – evaporator on horizontal position

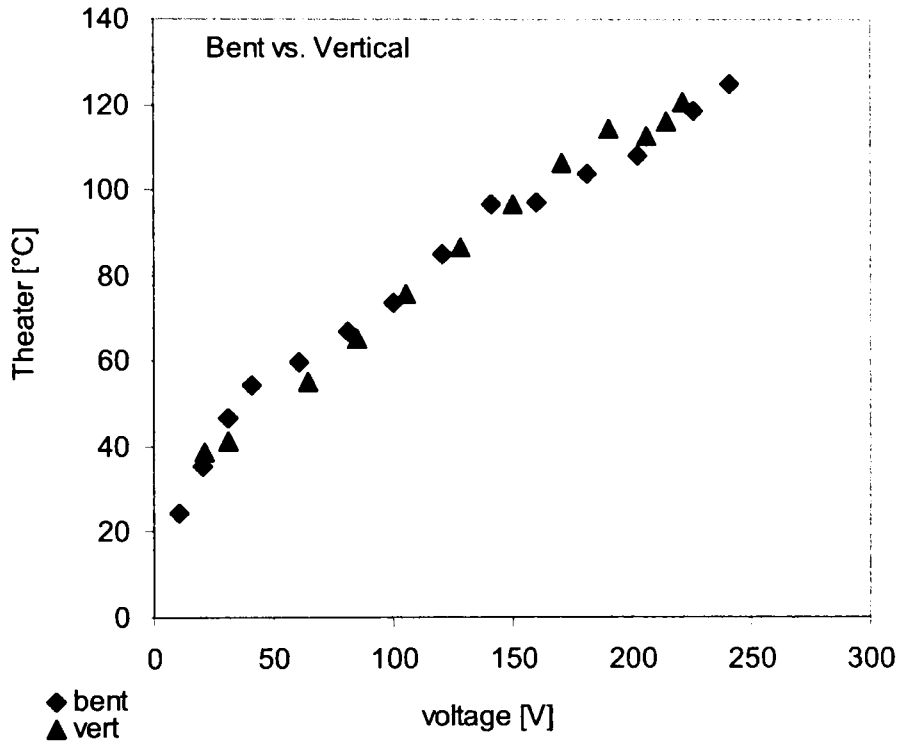


Fig. 3A-30 Heater temperature variation with voltage increase for the two cases (vertical orientation and bent tubes case)

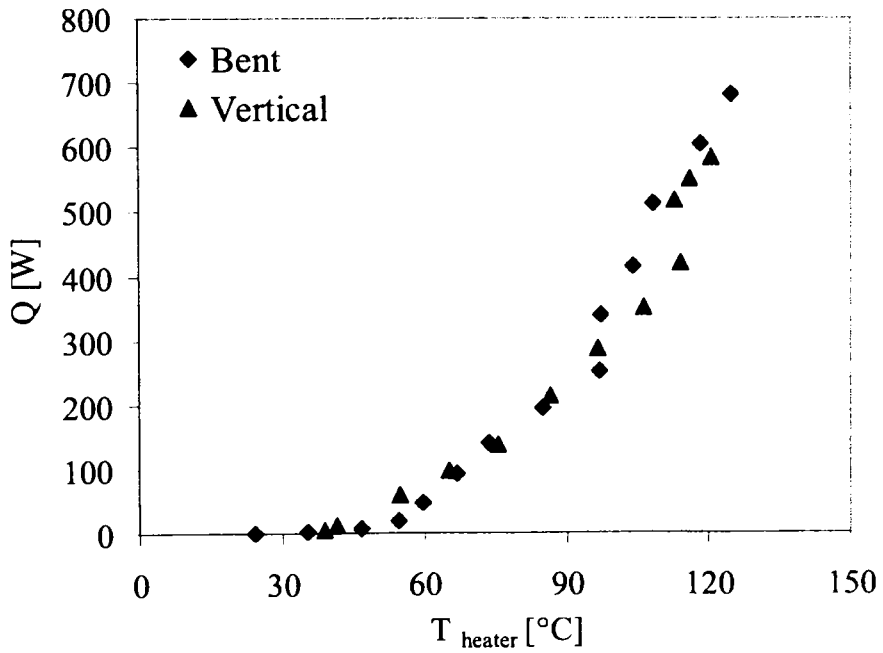


Fig. 3A-31 Q vs. heater temperature for the two cases

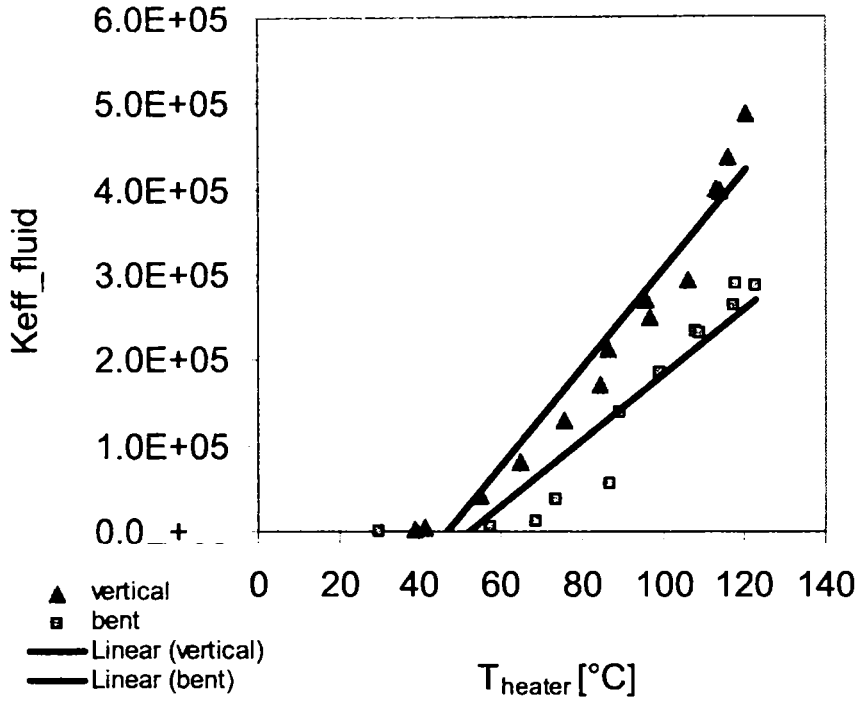


Fig. 3A-32 Q vs. heater temperature for the two cases

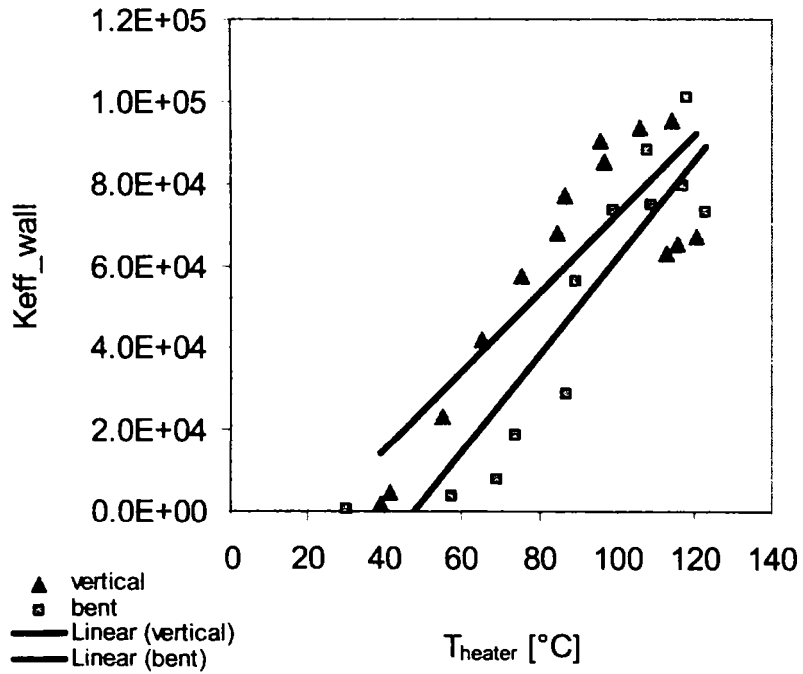


Fig. 3A-33 Q vs. heater temperature for the two cases

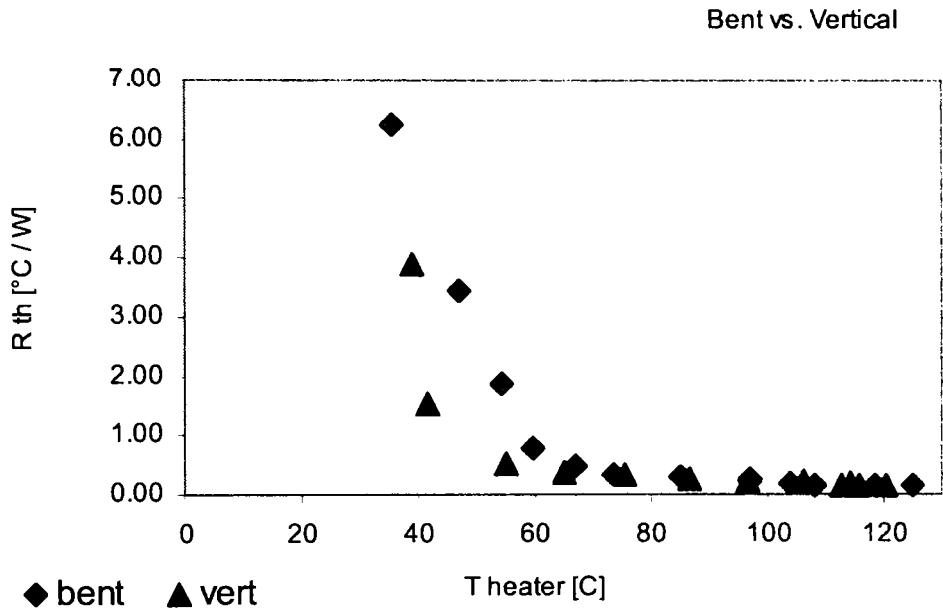
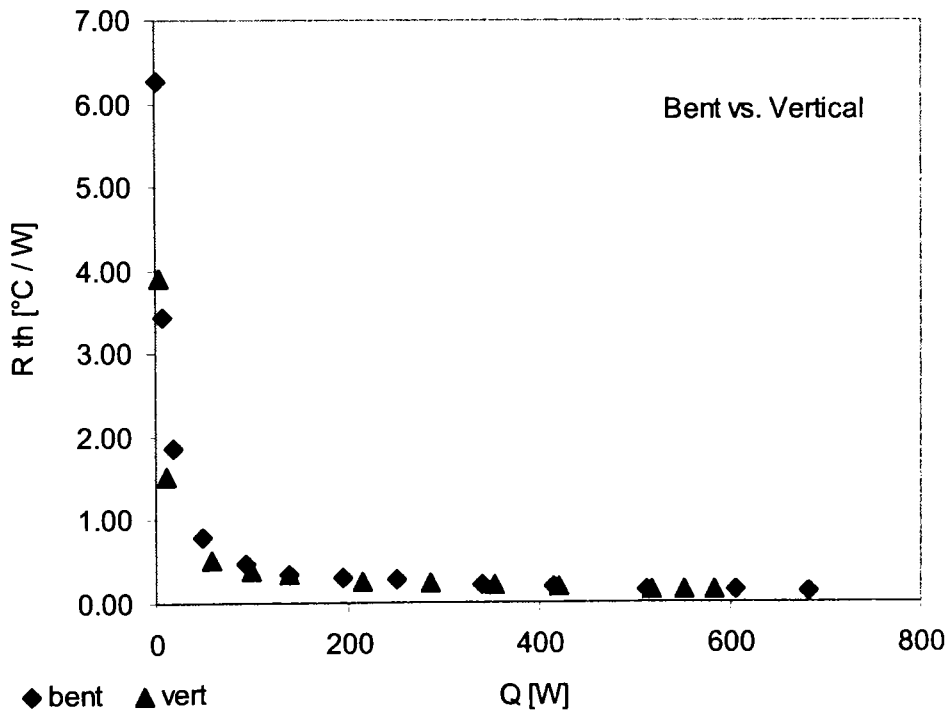


Fig. 3A-34 Thermal resistance vs. heater temperature for the two cases

Fig. 3A-35 Thermal resistance vs. Q for the two cases

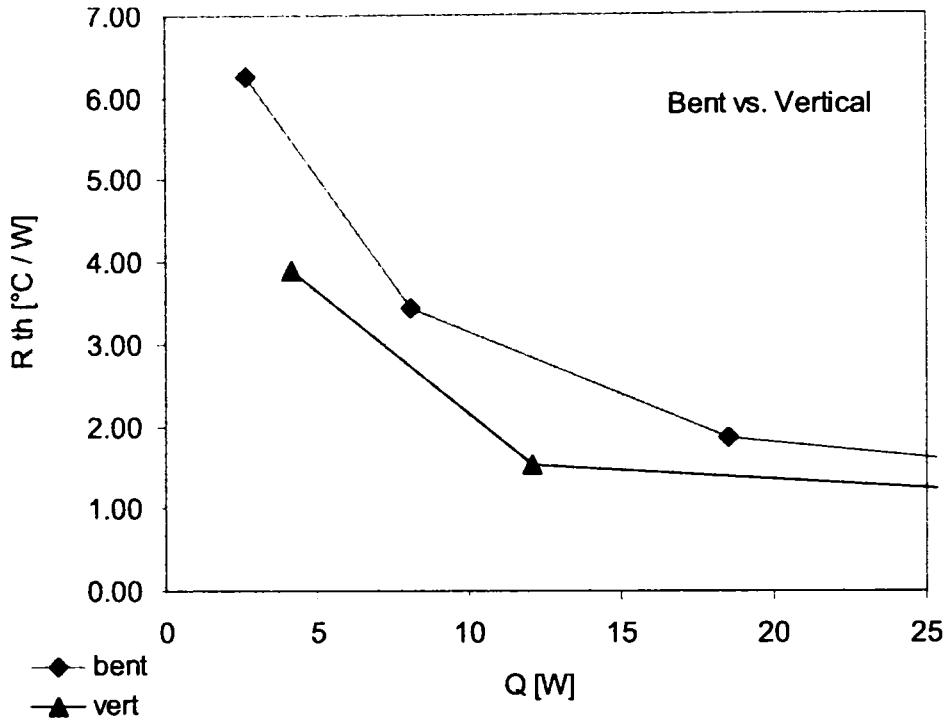


Fig. 3A-36 Thermal resistance at low Q for the two cases

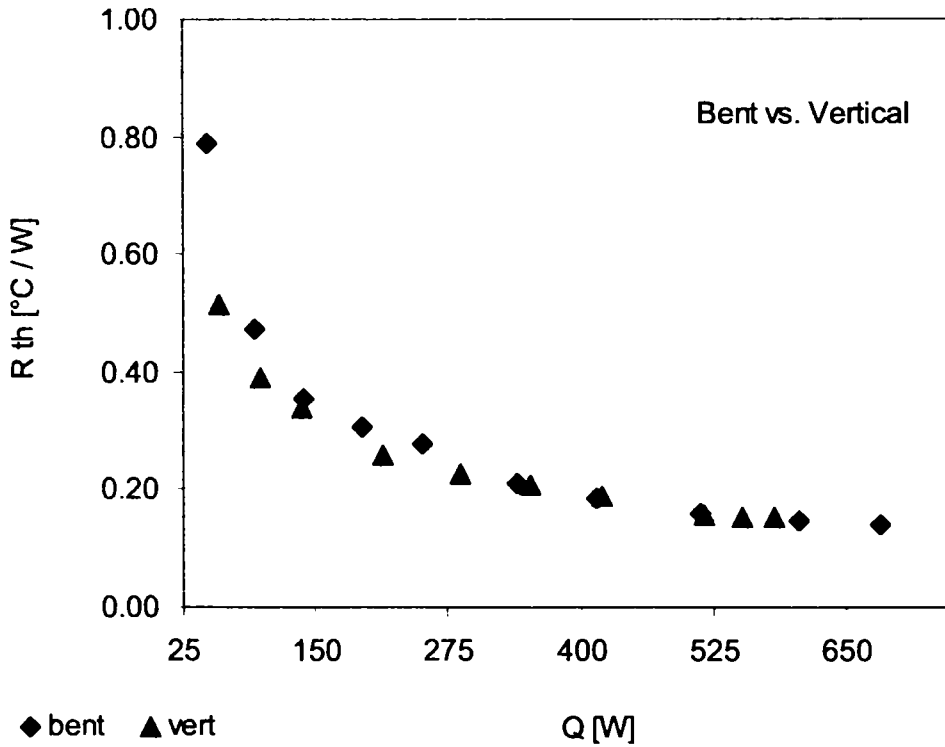


Fig. 3A-37 Thermal resistance at high Q for the two cases

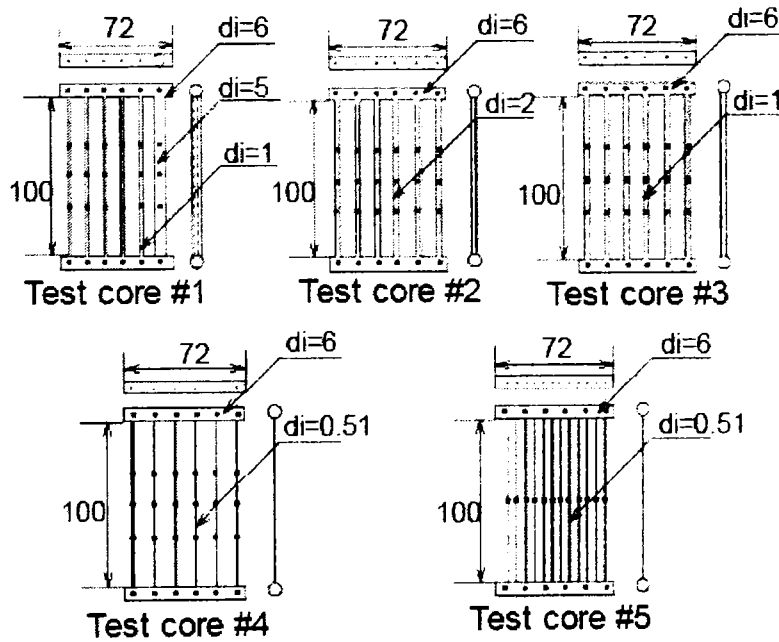
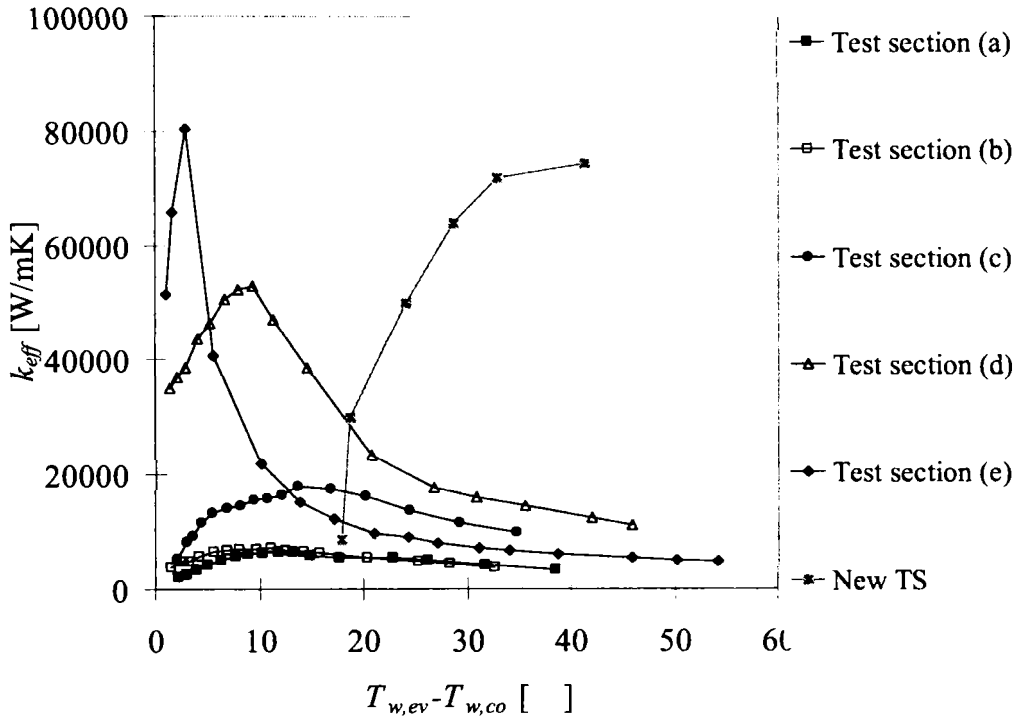


Fig. 3A-39 (II) Geometry of the Test Sections a~e

Note: Data for TS a~e are from the MS thesis of Noguchi, MMLab, 2003

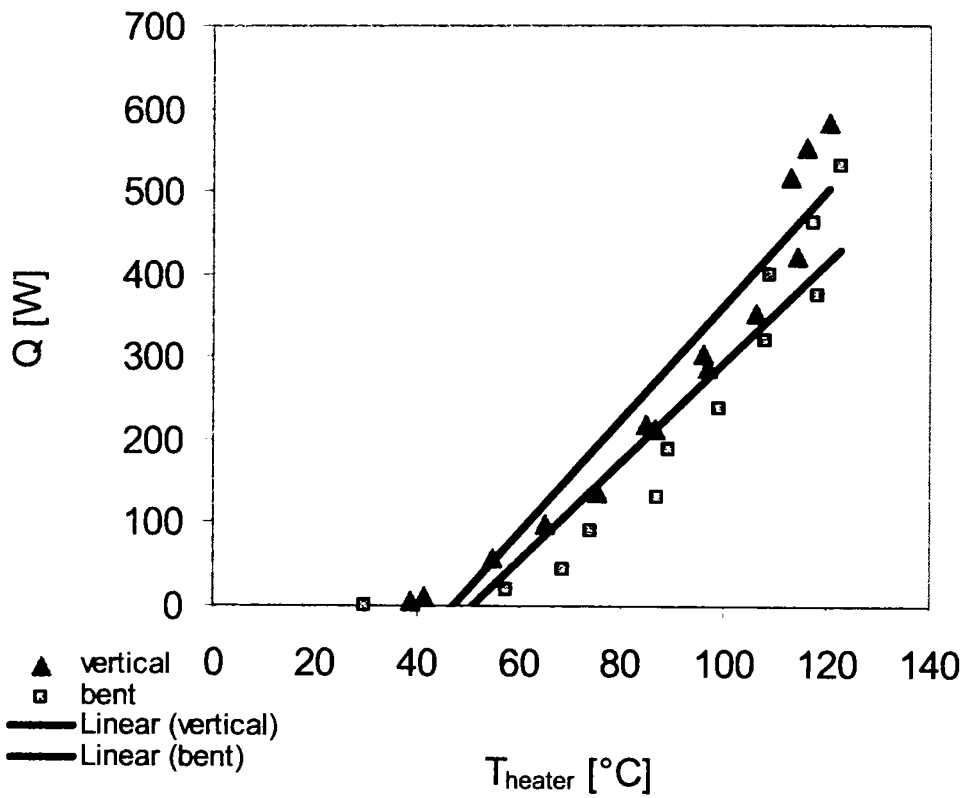


Fig. 3A-40 Heat transport rate for the vertical orientation versus bent tube case

4. Summary and General Conclusion

After an intense literature review related to the present subject it was found that, there is still a lack of knowledge regarding the complex phenomena which are occurring during the process of heat transport. Different devices have been developed in the past decades aiming an efficient heat transport and the improvement of their performance is still a task of nowadays engineers.

The need for a more compact and efficient heat transport device (HTD) led to the development of the two new devices presented in this thesis. The characteristics of the novel devices consist in their different structure as compared with the conventional HTDs. The devices consist of parallel tubes connected to an evaporator (hot header) and a condenser (cold header). The new HTDs have the advantage of the tubes being open to both headers and therefore, the resistance in the flow existing in case of a meandering closed loop (MCL) is avoided. The tubes are simple, without any internal structure (wick) and compared with conventional heat pipes (HP), the performance of the new devices is not limited by the capillary limit.

Taking into account the basic theory of thermodynamics and the information found in the literature related to the conventional HTD, two new test sections were design, constructed and experimentally investigated under different conditions. At first, the working mechanism was analyzed and later on optimized. Two methods were used to prove the results, measuring all values and in the same time recording the behavior of the inner flow. A good agreement was found between the flow visualization results and the measurements results. Reproducibility of results was obtained through a large series of performed experiments. Observing the fluid flow, allows one to get a better understanding of the mechanism, and this is the first step to improvement. The flow visualization analysis gives us an insight view of the phenomena occurring during the process of heat transport. Each new finding lead to a further step into the research and there is still more to go.

Besides the main target of the present research, there were other problems which occurred during the experiments and needed to be solved. One can learn a lot from dealing with some practical issues. There is no perfect design from the first

beginning and in time, many aspects were improved (for example, avoiding the leakage). To confirm the high value obtained for the heat transport, two systems were used to check the temperature readings. The values were proved to be accurate.

From the present study, the following main conclusions can be drawn:

1). Two new types of HTD were developed and experimentally investigated for a series of parameters (temperatures range, effect of orientation, length of tubes, and amount of charged working fluid). For both newly developed devices the optimum working conditions were found.

2) The optimum conditions for the first device was the vertical orientation with the evaporator at the bottom, the optimum filling ratio was found to be 40% of the total inner volume of the test core, and the optimum length of the tubes was 530mm.

3) The performance of both devices proved to be very high as compared to that of conventional HPs of similar dimensions:

- I. The two different diameter tubes PT-HTD can transport three to four times more heat (800W) than a conventional heat pipe of similar size, for a temperature of evaporator below 100°C.
- II. Compared with similar size HPs, the PT-HTD with five tubes can cover a wider range of Q (up to 700W), with an effective thermal conductivity up to 200 times more than that of Copper.

4) New finding consists in:

- III. The unique mechanism of fluid flow with the separation of vapour through the larger diameter tube and condensate return through the smaller diameter tube, in case of PT-HTD with 2 different diameter tubes. This is considered to be the main cause for the high efficiency of heat transport.

- IV. The two different flow patterns observed in the 5-PT-HTD; an oscillatory flow in all tubes present at low Q , and the stable re-circulating flow in case of high Q .

5) Through flow visualization, the method of estimating the fluid phase inside the tubes by measuring the tube wall temperatures was proved to be reliable.

The results of this study have been presented in many international conferences and were as well published in international journals [38, 39, 40, 41, 42, 43, 44, 45, 46]. This fact reflects that the results shown here are valuable and the research in this field is of high interest.

The new concept of HTD proved to be reliable and is promising for applications. Further study is needed to find an approach between the complex phenomena of heat transport (including boiling, condensation and two-phase flow) and the optimum design of devices.

Recommendations for future work

Based on the results presented here, further research in this field can be done. It would be interesting to investigate different combinations of tube diameters (for both test section, with two and five tubes respectively), to determine its effect on the heat transport performance, and to find the optimum. Also, designing and testing a new test core more application oriented, with a much simple structure (e.g. removing the glass windows), would be very useful. Although the phenomena (including boiling, condensation and two-phase flow) existing in the newly developed HTDs are very complex, a trial in developing a numerical model can lead to further understanding of the mechanism of present devices, which will be useful for further development of HTDs.

REFERENCES

1. Akaki, H. "Structure of a heat pipe", (1990), U.S. Patent 4,921,041.
2. Anderson, W.G., "Evaluation of Heat Pipes in the Temperature Range of 450 to 700K", (2004), NASA Center: Glenn Research Centre, Space Technology and Applications International Forum, pp.171-178.
3. Beitelman, M. H., Patel, C. D., (2002), "Two-Phase Loop: Compact Thermosyphon", Hewlett Packard Company, Pages 1-22.
4. Cai, Q., Chen, C., Asfia, J.F., "Operating Characteristic Investigations in Pulsating Heat Pipe", (2006), Journal of Heat Transfer, Transaction of ASME, vol.128, pp.1329-1334.
5. Charoensawan P., Khandekar, S., Groll, M., Terdtoon, P., (2003), "Closed loop pulsating heat pipes Part A: parametric experimental investigations", Applied Thermal Engineering, vol. 23, issue 16, pp.2009-2020.
6. Delil, A.A.M., "Pulsating and oscillating heat transfer devices in acceleration environments from microgravity to super gravity", (2001), NLR-TP-2001-001, The 31st Conference on Space Environmental Systems, Orlando, USA.
7. Eguchi, K., Mochizuki, M., Mashiko, M., Goto, K., Saito, K., Nagaki, Y., Takamiya, A., Nguyen, T., and Sauciuc, I., (1998), "Micro Heat Pipe for Cooling CPU", Fujikura Technical Review, no. 27, pp. 63-67
8. El-Genk, M.S., and Sarber, H.H., (1997), "Flooding limit in closed, two-phase flow thermosyphons", Int. J. Heat Mass Transfer, vol. 40, no.9, pp.2147-2164.
9. Furukawa, M., "Design Formulas for Oscillatory Heat Transport in Open-Ended Tubes", (2003), Journal of Heat Transfer, Transaction of ASME, vol.125, pp.1183-1186.
10. Grover, G. M., Cotter, T. P. and Erickson, G. F., (1964), "Structures of very high thermal conductance", J. Appl. Phys. vol. 35, pp. 1990-1991.
11. Hosoda, M. Nishio S. and Shirakashi, R., (1999), "Study of Meandering Closed-Loop Heat-Transport Device", JSME Int. J, Ser. B, Vol. 42, No. 4. pp. 737-744.
12. Imura, H., Koito, Y., Ichinomiya, T., and Torii, S., "Heat Transport from Higher to Lower Positions Using Slight External Power", (2004), Proceedings of the 10th APCCHE Congress, Japan.

13. Incopera F.P. and De Witt, D.P., *Fundamentals of Heat and Mass Transfer*, 3rd edition, John Wiley & Sons, NY, pp. 607-608. (1990).
14. Jana, A.K., Das, G., and Das, P.K., "Flow regime identification of two-phase liquid-liquid upflow through vertical pipe", (2006), *Chemical Engineering Science*, vol. 61, issue 5, pp.1500-1515.
15. Japan Association for Heat Pipe ed., (2001), *Heat Pipe*, Nikkan Kogyo Shinbusha, p.104 (in Japanese).
16. Kadoguchi, K., and Yamazaki, M., "Intermittent heat transport by discharging of accumulated vapours", (2004), *Applied Thermal Engineering*, vol. 24, no.17-18, pp. 2761-2775.
17. Karimi, G., and Culham, J.R., "Review and assessments of pulsating heat pipe mechanism for high heat flux electronic cooling", (2004), *IEEE, Inter Society Conference on Thermal Phenomena*, pp.52-59.
18. Khandekar S., Dollinger N., and Groll, M., (2003) "Understanding operational regimes of closed loop pulsating heat pipes: an experimental study", *Applied Thermal Engineering*, vol. 23, issue 6, pp.707-719.
19. Khandekar S., Charoensawan, P., Groll, M., Terdtoon, P., (2003), "Closed loop pulsating heat pipes Part B: visualization and semi-empirical modeling", *Applied Thermal Engineering*, vol. 23, issue 16, pp.2021-2033.
20. Khandekar, S., Groll, M., (2004), "An insight into thermo-hydrodynamic coupling in closed loop pulsating heat pipe", *Int. Journal of Thermal Sciences*, 43, pp.13-20.
21. Kline, S.J. and McClintock, F.A., "Describing uncertainties in single sample experiments", *Mech. Eng. ASME*, 75 (1953), 3-8.
22. Ma, H.B., Hanlon, M.A., and Chen, C.L., (2006), "An investigation of oscillating motions in a miniature pulsating heat pipe", *Microfluid Nanofluid*, vol.2, pp. 171-179.
23. Nakabeppu, O., Miyata, Y., and Hori, T., "Heat Transport Characteristics of Micro-Loop Heat Pipe with Capillary Pump Structure", (2005), *Thermal Science and Engineering*, vol. 13, no.1, pp.47-52.
24. Nishio, S., (1999), "Oscillatory-Flow Heat-Transport Device", *Proc. Of 11th Int. Heat Pipe Conf. Vol. 3*, pp. 39-49.

25. Nishio, S., Nagata, S., Numata, S., Shirakashi, R., (2003), "Study on Thermal Characteristics of Bubble Driven Heat - Transport Device", *Heat Transfer - Asian Research*, 32(2), pp.167-177.
26. Ogushi, T., Murakami, M., and Yamanaka, G., "Study of a Downward Heat Transport Device Utilizing Vapour Pressure as the Liquid Pumping Force (Part 1, the Analysis of the Static Characteristics)", (1988), *Heat Transfer Japanese Research / the Society of Chemical Engineers, Japan and the Heat Transfer Division of the ASME*, vol.1, no.8, pp.45-55.
27. Onishi, T., Mochizuki, S., and Murata, A., (2004), "Heat transport device consisting of capillary tubes with boiling driven heat transfer mechanism inside", *Proceedings of 1st International Symposium on Micro and Nano Technology, Hawaii*.
28. Onishi, T., Kanatsugu, T., Mochizuki, S., and Murata A., (2005), "Flow Phenomena in a Parallel Tube Heat Transport Device with Phase Change", *Proceedings of 5th Pacific Symposium on Flow Visualization and Image Processing, Australia*.
29. Odhekar, D., "Experimental Investigation of Bendable, Heat Pipe" Auburn University, MS Degree Thesis, 2005.
30. Pal, A., Joshi, Y.K., Beitelmal, M.H., Patel, C.D., and Wenger, T.M., (2002), "Design and Performance Evaluation of a Compact Thermosyphon", (2002), *Components and Packaging Technologies, IEEE Transactions*, vol. 25, issue 4, pp.601- 607.
31. Richter, R., and Gottschlich, J.M., (1994), "Thermodynamic Aspects of Heat Pipe Operation", *Journal of Thermophysics and Heat Transfer*, vol.8, no.2, pp.334-340.
32. Shafii, M., Faghri, A., Zhang, Y., (2001), "Thermal Modeling of Unlooped and Looped Pulsating Heat Pipes", *Journal of Heat Transfer, Transactions of the ASME*, vol. 123, pp. 1159-1172.
33. Stauder, F.A. and McDonald, T.W., (1986), "Experimental study of a two-phase flow thermosiphon loop heat exchanger", *ASHREA Trans.* 92, Pt.2A, pp.486-496.
34. Ueda, K. and Isobe, G., (2005), "Effects of Inner Groove Shape on Heat Transfer Performance of Heat Pipe", *Thermal Solution*, vol. 115, pp.6-9 (in Japanese).
35. Weislogel, M.M., "Passive oscillatory heat transport systems", (2002), *NASA Center, AIP Conference Proceedings*; vol.608, no.1, pp.241-249.

36. Yamamoto, K., Nakamizo, K., Kameoka, H., and Nanba, K., (2002), "High-Performance Micro Heat Pipe", *Furukawa Electric Review*, vol. 110, pp.73-76 (in Japanese).
37. Zou, L., Xu, Y., and Gu, J., (1999), "Experimental investigation on parallel connection module along the exhaust current direction for gravity type heat pipes", *Proceedings of 11th International Heat Pipe Conference*, Vol.1, pp.159-163.

38. **Adina P Cirtog.**, Sadanari Mochizuki, Akira Murata, Jaroslav Hemrle and Ioana Ionel, "Heat transport device with phase change using one way valves on parallel tubes", *Scientific Journal of University Politehnica Timisoara, Transactions on Mechanics*, Tom 50(64), Fascicola 2, 2005, pp. 19-23
39. **Adina P. Cirtog**, Sadanari Mochizuki, Akira Murata, Jaroslav Hemrle and Ioana Ionel, "Heat transport device with separated passages for vapour and condensate return flow", *Proceedings of COFRET'06*, Timisoara, Romania, 2006, Vol. 2, ISSN: 1224-6077, pp. 49-53.
40. **Adina P. Cirtog**, Sadanari Mochizuki, Akira Murata, "Heat transport device with boiling driven re-circulating flow", CD-ROM *Proceedings of 17th International Symposium on Transport Phenomena*, Toyama, Japan, 2006, ISBN 1-930746-03-2
41. **Adina P. Cirtog**, Sadanari Mochizuki, Akira Murata, and Ioana Ionel, "Heat transport device with phase change using two parallel tubes", *Proceedings of the 43rd National Heat Transfer Symposium of Japan*, Nagoya, 2006, Vol. II, ISSN 1346-1524, pp.519-520.
42. **Adina P. Cirtog**, Sadanari Mochizuki, Akira Murata, "Heat transport device with phase change using two parallel tubes" (part II), *Proceedings of the 44th National Heat Transfer Symposium of Japan*, Nagasaki, 2007, Vol. I, ISSN 1346-1524, pp.165-166.
43. **Adina P. Cirtog**, Sadanari Mochizuki, Akira Murata, "Characteristics of two-phase heat transport device with multiple parallel tubes", *Proceedings of Thermal Engineering Conference'07*, Kyoto, Japan, 2007, No.07-5, pp. 383-384.
44. **Adina P. Cirtog**, Sadanari Mochizuki, Akira Murata and Ioana Ionel, "Heat transport device with phase change using two parallel tubes", (short note),

Thermal Science and Engineering, ISSN: 0918-9963, Vol.15, No.4, 2007.10, pp.241-244

45. Jaroslav Hemrle, Tetsuo Onishi, **Adina P. Cirtog***, Sadanari Mochizuki and Akira Murata, "Quantitative description of the inner flow behaviour of two-phase heat transport device using image sequence processing", *Journal of Flow Visualization and Image Processing*, volume 14, issue 4, 2007, pp.417-430.
46. **Adina P. Cirtog**, Sadanari Mochizuki, "Heat transport device with boiling driven re-circulating flow", Akira Murata, *International Journal of Transport Phenomena*, (accepted for publication).

47. Bejan, A., Tsatsaronis, G., Moran, M., *Thermal Design and Optimization*, John Wiley and Sons, New York, USA, 1996
48. Briggs, A. and Rose, J. W., (2007), Condensation on Integral-Fin Tubes with Special Reference to Effects of Vapour Velocity, KEYNOTE Paper, Advances in Heat Transfer, Proc. 5th Baltic Heat Transfer Conf., St. Petersburg, Vol. 1, 96 - 116.
49. Briggs, A., Wang, H. S., Murase, T. and Rose, J. W., (2003), Heat transfer measurements for condensation of steam on a horizontal wire-wrapped tube, *J. Enhanced Heat Transfer*, 10, 355-362.
50. Cao, Y., Gao, M., Wickless network heat pipes for high heat flux spreading applications, *International Journal of Heat and Mass Transfer* 45 (2002) 2539-2547.
51. Zimparov, V.D. and da Silva, A.K. and Bejan, A., *Thermodynamic optimization of tree-shaped flow geometries with constant channel wall temperature*, *International Journal of Heat and Mass Transfer*, vol. 49 no. 25-26 (2006), pp. 4839 - 4849.

Publications:

- (1) **Adina P. Cirtog**, Ioana Ionel, Sadanari Mochizuki, "The effect of electrostatic field on the behaviour of airborne particles", *Proceedings of the 6th International Power Systems Conference*, Timisoara, Romania, Tom 50(64), 2005, Fascicola 1-2, ISSN: 1582-7194, pp.155-162
- (2) **Adina P. Cirtog**, Sadanari Mochizuki, Akira Murata, Jaroslav Hemrle and Ioana Ionel, "Heat transport device with phase change using one way valves on parallel tubes", *Scientific Journal of University Politehnica Timisoara, Transactions on Mechanics*, Tom 50(64), Fascicola 2, 2005, pp. 19-23
- (3) **Adina P. Cirtog**, Sadanari Mochizuki, Akira Murata, Jaroslav Hemrle and Ioana Ionel, "Heat transport device with separated passages for vapour and condensate return flow", *Proceedings of COFRET'06*, Timisoara, Romania, 2006, Vol. 2, ISSN: 1224-6077, pp. 49-53.
- (4) **Adina P. Cirtog**, Sadanari Mochizuki, Akira Murata, "Heat transport device with boiling driven re-circulating flow", CD-ROM *Proceedings of 17th International Symposium on Transport Phenomena*, Toyama, Japan, 2006, ISBN1-930746-03-2
- (5) **Adina P. Cirtog**, Sadanari Mochizuki, Akira Murata, and Ioana Ionel, "Heat transport device with phase change using two parallel tubes", *Proceedings of the 43rd National Heat Transfer Symposium of Japan*, Nagoya, 2006, Vol. II, ISSN 1346-1524, pp.519-520.
- (6) Jaroslav Hemrle, Tetsuo Onishi, **Adina P. Cirtog***, Sadanari Mochizuki and Akira Murata, "Quantitative description of the inner flow behaviour of two-phase heat transport device using image sequence processing", CD-ROM *Proceedings of 6th Pacific Symposium on Flow Visualization and Image Processing*, Hawaii, 2006 (*first speaker).
- (7) **Adina P. Cirtog**, Sadanari Mochizuki, Akira Murata, "Heat transport device with phase change using two parallel tubes" (part II), *Proceedings of the 44th National Heat Transfer Symposium of Japan*, Nagasaki, 2007, Vol. I, ISSN 1346-1524, pp.165-166.

- (8) **Adina P. Cirtog**, Sadanari Mochizuki, Akira Murata, "Characteristics of two-phase heat transport device with multiple parallel tubes", *Proceedings of Thermal Engineering Conference'07*, Kyoto, Japan, 2007, No.07-5, pp. 383-384.
- (9) ♠ **Adina P. Cirtog**, Sadanari Mochizuki, Akira Murata and Ioana Ionel, "Heat transport device with phase change using two parallel tubes", (short note), *Thermal Science and Engineering*, ISSN: 0918-9963, Vol.15, No.4, 2007.10, pp.241-244.
- (10) ♠ Jaroslav Hemrle, Tetsuo Onishi, **Adina P. Cirtog***, Sadanari Mochizuki and Akira Murata, "Quantitative description of the inner flow behaviour of two-phase heat transport device using image sequence processing", *Journal of Flow Visualization and Image Processing*, volume 14, issue 4, 2007, pp.417-430.
- (11) Ioana Ionel, Dan P. Oprisa-Stanescu, Corneliu Ungureanu, Sadanari Mochizuki and **Adina P. Cirtog**, "Numerical modelling as a possible analysing tool for coupling of a waste incinerator to an existing lignite fired boiler", *International Journal of Transport Phenomena*, vol.10, 2008, pp.63-72.
- (12) ♠ **Adina P. Cirtog**, Sadanari Mochizuki, "Heat transport device with boiling driven re-circulating flow", Akira Murata, *International Journal of Transport Phenomena*, (accepted for publication)

Note: ♠ extended version of the conference proceedings

Awards:

Best presentation award – from The Heat Transfer Society of Japan at the 44th National Heat Transfer Symposium, Nagasaki, Japan, 2007.

水の相変化を利用した並列細管熱輸送デバイスの実験的研究

発熱源Aから吸熱源Bへ効率よく熱を輸送する技術は、電子機器の冷却を始め様々な分野において強く求められている。そのための具体的方法としては、(1) AB間を熱伝導材でつなぐ、(2) AB間に流体を強制循環させる、(3) ヒートパイプを用いる、等が挙げられる。このうち、とくに(3)については、最近盛んに研究・開発がなされ一部実用化されつつある蛇行細管型ヒートパイプが、従来のヒートパイプを上回る熱輸送性能を示すものとして注目されている。

これらに対し、AおよびBにそれぞれ蒸発部および凝縮空間を設け、それらの間を複数の細管で結ぶだけの極めて簡単な構造を有するデバイスが、上述のいずれのデバイスよりも格段に高い熱輸送性能を発揮する可能性のあることが、論文提出者が現在所属する研究室において最近見出された。

本論文は、上述の背景の下に、より広範な条件下でも上記並列細管熱輸送デバイスが機能することを確認すると共に、何故そのような単純なシステムにおいて高い性能が得られるのかについてそのメカニズムを探るべく、数多くの影響因子について系統的な実験を実施し、その結果をまとめたものである。

本論文は英文で書かれ、4章よりなる。以下に、各章ごとの内容について要旨を記す。

第1章は序論である。研究の背景が述べられ、サーモサイフォン、ヒートパイプおよび蛇行細管などの既存の熱輸送デバイスについて説明がなされ、次いで本論文の研究対象である、並列細管熱輸送デバイスについて記述されている。本論文においては、基本構造が大きく異なる二つの並列細管熱輸送デバイスについて、研究を行っている。それらは、(1) エバポレータとコンデンサの二つの空間形状がいずれも円筒状で、それらを互いに内径の異なる2本の細管で連結する場合(二本の異径細管を有する場合)、および(2) エバポレータおよびコンデンサの形状が、電子機器の発熱・吸熱特性を考慮して、直方体で、複数細管を同径の5本で構成する場合(5本同径細管の場合)である。なお、本研究においては作動流体として水を用いている。

第2章は、二本の異径細管を有する場合について述べている。まず、実験装置および実験方法について、次にデータの整理方法および実験結果に対する不確かさの解析について記述されている。最後に、実験結果と考察が示されている。実験結果と考察においては、広範な条件のもとで系統的に行われた実験についての結果と詳細な考察が述べられている。主な結果を要約すると、(1) 本熱輸送デバイスは、従来のヒートパイプなどに比べはるかに高い熱

輸送性能を有する。(2)その理由は、径の大きい細管内を常に蒸気がエバポレータからコンデンサに向かって流れ、小さい方の細管内を凝縮液がコンデンサからエバポレータに向かって還流することにある。すなわち、エバポレータ⇨大径細管⇨コンデンサ⇨小径細管⇨エバポレータのように、流体の定常的な循環流が形成されることにある。(3)重力は性能に対して大きな影響を持つ。細管の傾斜角が90度(垂直配置)の場合に性能は最大になる。(4)垂直配置の場合、熱輸送に最大値を与える管長が存在し、その値は管長/管径が約20のときである。(5)作動流体の封入率も性能に影響を及ぼし、40%あたりに最適値がある。

第3章は、5本同径細管の場合について、実験装置と実験方法、データの処理と不確かさ解析、ついで実験結果と考察が記されている。実験は、(a)エバポレータおよびコンデンサを結ぶ5本の細管が全て直管でそれらが垂直に配置された場合と、(b)エバポレータは水平に置かれ、5本の細管を緩やかな局率で曲げてコンデンサをある角度で置いた場合について行われた。得られた結果を要約すると以下ようになる。(1)この場合にも並列細管熱輸送デバイスの性能は極めて高く、特に発熱・吸熱両熱源間温度差が大きい異場合には、非常に高い性能を示す。たとえば、純銅の熱伝導率の200倍以上の等価熱伝導率を示す。(2)流体の流動現象には、二つの明確に異なるパターンが存在する。ひとつは、低温度差時に現れる振動流(各細管内を流体が往復振動する)であり、他の一つは、高温度差時に現れる循環流(5本の細管のうちのある細管は蒸气流路、残りの細管は凝縮液戻り流路となる)である。(3)システムの配置が、既述の(a)の場合には高温度差域でエバポレータにドライアウト現象が生じるが、上記(b)の場合にはドライアウトは発生しない。

第4章は、本論文全体を通じての結論が述べられている。すなわち、本研究は、作動流体に水を用いた場合について、現象に影響を及ぼすパラメータを系統的に変化させた一連の実験により熱輸送特性を調べ、かつその機構の解明を試みたものであること。その結果、例えば、二本の径の異なる並行細管を用いると、径の大きい側が常に蒸气流の、小さい側が凝縮液の戻り管になり、極めて大きな熱輸送が実現されることなどがわかったこと。また、複数同径細管内の流動には熱輸送量の大小により二つの明らかに異なる流動パターン、すなわち、(a)低熱輸送量領域においては振動流が、また、(b)高熱輸送量領域においては循環流が発生することなどが再度述べられている。

Rezumat în limba română a tezei de doctorat

**“Contribuții la studiul fenomenului de trecere a căldurii
cu schimbare de fază, utilizând sisteme cu tuburi paralele”**

(Experimental Investigation of Parallel Tube

Heat Transport Devices using Phase Change of Water),

elaborată de domnișoara ing. Adina Petronela CÎRTOG

1. Importanța temei abordate în teza, scopul și obiectivele urmărite

Prezenta lucrare a fost elaborată în urma cercetărilor efectuate pe parcursul activității mele ca și doctorand în cotutelă în cadrul Departamentului de Mecanică a Universității de Agricultură și Tehnologie din Tokyo și la Universitatea Politehnică din Timișoara, Facultatea de Mecanică, Catedra Termotehnica, Mașini termice și Autovehicule rutiere. Lucrarea abordează o tematică de actualitate și interes ridicat din domeniul termodinamic, având ca scop dezvoltarea unor sisteme de răcire eficiente.

Datorită nevoilor actuale de protecție a echipamentelor electrice și electronice, au fost concepute diverse modalități de înlăturare a energiei degajate sub forma de căldură. Așa numitele « heat pipe » sau tuburi termice sunt cele mai cunoscute dispozitive utilizate pentru răcirea echipamentelor electronice, de exemplu pentru procesoare. Acestea sunt folosite și în navele cosmice datorită faptului că recircularea fluidului de lucru nu depinde de gravitație. Acest avantaj le este conferit de structura lor capilară, dar în același timp le și limitează performanța. Un alt sistem, menționat în literatura de specialitate și folosit în practică, este sistemul cu țevi sinuoase, a cărui structură și principiu de funcționare sunt diferite de cele ale tubului termic. Spre deosebire de aceste sisteme convenționale, instalația concepută pentru experimentele descrise în această lucrare prezintă o particularitate prin construcția geometrică. Aceasta se reflectă în modul de recirculare a fluidului de lucru și implicit a transportului de căldură de la sursa caldă la condensator. Instalația inițială a fost prevăzută cu două tuburi paralele simple de diametre diferite, conectate la un vaporizator încălzit electric și un condensator răcit cu apă.

Lucrarea in limba engleza are 110 pagini, 1 tabel, 98 figuri, 51 pozitii bibliografice, dintre care 9 proprii. Numerotarea figurilor in acest rezumat corespunde, pentru o mai usoara intelegere, cu cea originala, din teza redactata in limba engleza. Ea are urmatorul CUPRINS:

Mulumiri	3
Cuprins (în limba engleză).....	5
Rezumat (în limba engleză)	7
Notății	9
Capitolul 1: INTRODUCERE	11
1.1 Fundamentarea cercetării.Variante constructive.....	11
1.1.1 Termosifon.....	12
1.1.2 Tuburi termice	13
1.1.3 Sistem cu tevi sinuose	14
1.1.4 Conceptul sistemelor cu tuburi paralele	16
1.2 Obiectivele cercetării	17
1.3 Organizarea tezei	18
Capitolul 2: SISTEM CU DOUĂ TUBURI PARALELE DE DIAMETRE DIFERITE.....	19
2.1 Instalatia experimentală și procedeul de lucru	19
2.2 Prelucrarea datelor și estimarea erorilor	21
2.3 Rezultate obținute și interpretarea lor	23
2.3.1 Performanța sistemului propus	23
2.3.2 Mecanismul de recirculare a fluidului de lucru	24
2.3.2.1 Presiunile măsurate	24
2.3.3.2 Vizualizarea curgerii fluidului	26
2.3.3 Efectul orientării instalației	29
2.3.4 Efectul lungimii tuburilor	34
2.3.5 Efectul cantității de fluid	36
2.4 Analiza rezultatelor de vizualizare a curgerii	42
2.4.1 Metoda de estimare a vitezei fluidului	42
2.4.2 Analizarea rezultatelor	46
2.5 Concluzii	50

Anexa cap.2.....	.51
Capitolul 3: SISTEM CU CINCI TUBURI PARALELE	57
3.1 Instalatia experimentală și procedeul de lucru	57
3.2 Prelucrarea datelor	61
3.3 Rezultate obținute și interpretarea lor	62
3.3.1 Orientarea verticală a sistemului	62
3.3.1.1 Performanța sistemului	62
3.3.1.2 Relația între temperatura peretelui tubului și starea de agregare a fluidului de lucru din interior	65
3.3.2 Orientarea orizontală a sistemului	68
3.3.3 Tuburi cotate	69
3.3.2.1 Performanța sistemului	69
3.3.2.2 Comportarea fluidului sistemului.....	70
3.4 Concluzii	75
Anexa cap.3	76
Capitolul 4: CONCLUZII GENERALE ȘI CONTRIBUTII ORIGINALE	99
Concluzii ale cercetării. Contribuții originale.....	99
Bibliografie	102
Publicațiile autoarei	107
Rezumat în limba Japoneză	109
Rezumat în limba Română	111

2. Concepția unui sistem performant pentru transportul căldurii.

a) Generalități

În urma studiului din diferite reviste a literaturii de specialitate s-a constatat că este o nevoie acută de dezvoltare a unor sisteme de transport al căldurii cât mai eficiente, deși actualele sisteme au fost studiate și îmbunătățite de-a lungul ultimelor decenii. Analizând informațiile existente în literatură referitoare la avantajele și dezavantajele actualelor sisteme, precum și a nivelului actual de cunoaștere în domeniu, s-a conturat ideea necesității construirii unui nou sistem de transmitere a căldurii. Astfel a fost stabilită tema doctorală a cărei scop a fost de a contribui prin cercetare proprie la dezvoltarea principiului de funcționare al noii

instalații ce are la baza diferența de presiune dintre un recipient cald și unul rece (vaporizator și condensator), conectate prin intermediul unor tuburi paralele. Transferul căldurii este realizat prin schimbarea de fază a fluidului de lucru. Fluxul termic este transferat de la sursa caldă la cea rece are loc prin conducție și convecție (trecere de căldură). Aceste idei și scopul cercetării, în context actual al cunoașterii, au fost tratate în capitolul 1.

b) Identificarea principalelor caracteristici necesare asigurării unei răcirii eficiente

În concepția instalației au fost considerate următoarele aspecte:

- Asigurarea unui transport rapid de căldură,
- Costuri reduse ale instalației,
- Utilizarea unor agenți netoxici,
- Asamblarea cu ușurința a componentelor în cadrul laboratorului,
- Permitea repetării cu ușurința a experimentelor pentru validarea rezultatelor.

c) Variante constructive

Două instalații diferite au fost concepute, construite, și investigate experimental.

1. În prima fază a fost conceput un sistem cu două tuburi de diametre diferite. Pentru a asigura un transfer termic eficient recipientele (sursa caldă și sursa rece) au fost construite din alamă, iar tuburile au fost din cupru. Aceasta instalație a fost inițial prevăzută cu țevi de cupru, iar ulterior acestea au fost înlocuite cu tuburi de teflon pentru a permite vizualizarea curgerii fluidului de lucru cu scopul de a înțelege mecanismul de funcționare.
2. Ulterior a fost construit și investigat în diverse condiții experimentale un al doilea sistem, având cinci tuburi paralele de același diametru .

Prima instalație utilizată pentru cercetările experimentale este descrisă în capitolul 2 (fig. 2.1) al tezei și constă în principal din două tuburi de diferite diametre (3.5mm și 6.5mm), conectate la un vaporizator, încălzit electric, și un condensator, răcit cu apă. Inițial au fost folosite țevi de cupru, iar ulterior, pentru vizualizare, acestea au fost înlocuite cu tuburi de teflon. Înainte de a alimenta instalația cu fluidul de lucru (apa), întregul sistem a fost vidat până la o presiune absolută de aproximativ 2 kPa.

Lungimea tuburilor a variat între 215 mm și 750 mm, iar cantitatea de fluid între 0.26 % și 0.7 % din totalul capacității libere interne a instalației. Experimentele s-au planificat în așa fel încât să permită concluzii comparative, lucrându-se cu diverse înclinații ale echipamentului, de la 0 la 120° față de orizontală.

Temperaturile și presiunile în evaporator au fost măsurate și analizate, iar transportul de căldură a fost calculat utilizând următoarea relație :

$$\dot{Q} = \rho c_p \dot{V} (T_{w,out} - T_{w,in}) \quad (1)$$

Unde: ρ este densitatea, c_p este caldura specifica, \dot{V} debitul apei de racire, iar $T_{w,in}$, $T_{w,out}$ reprezintă temperatura apei de racire la intrare, respectiv la ieșire din sistem.

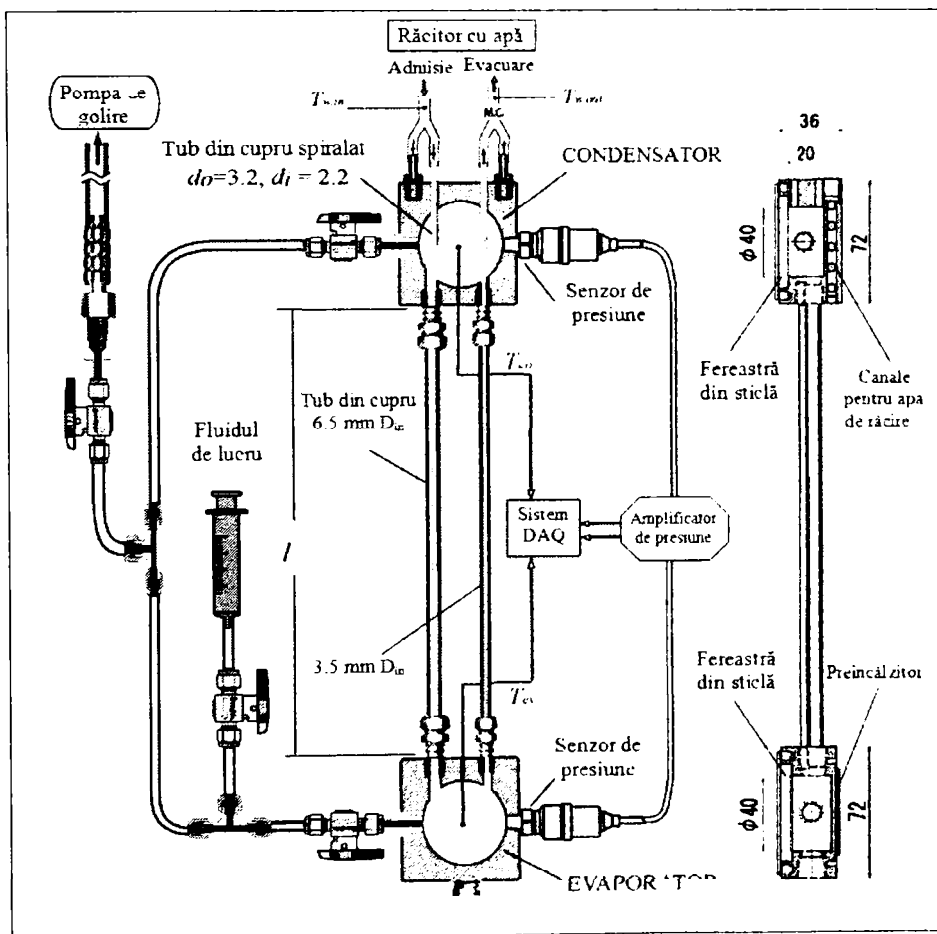


Fig. 2.1 Schița instalației cu două tuburi de diametre diferite

Obs: DAQ = achiziții date

Pe baza rezultatelor obținute, a fost concepută a doua instalație pilot. Investigațiile experimentale efectuate pe aceasta sunt prezentate în capitolul 3. Noua instalație a fost inițial prevăzută cu cinci tuburi paralele de același diametru 2.8 mm (fig.3.1). Experimentele s-au realizate pentru trei orientări ale instalației: verticala, orizontala și cazul tuburilor cotate, pentru care vaporizatorul este pe orizontala iar condensatorul pe verticala .

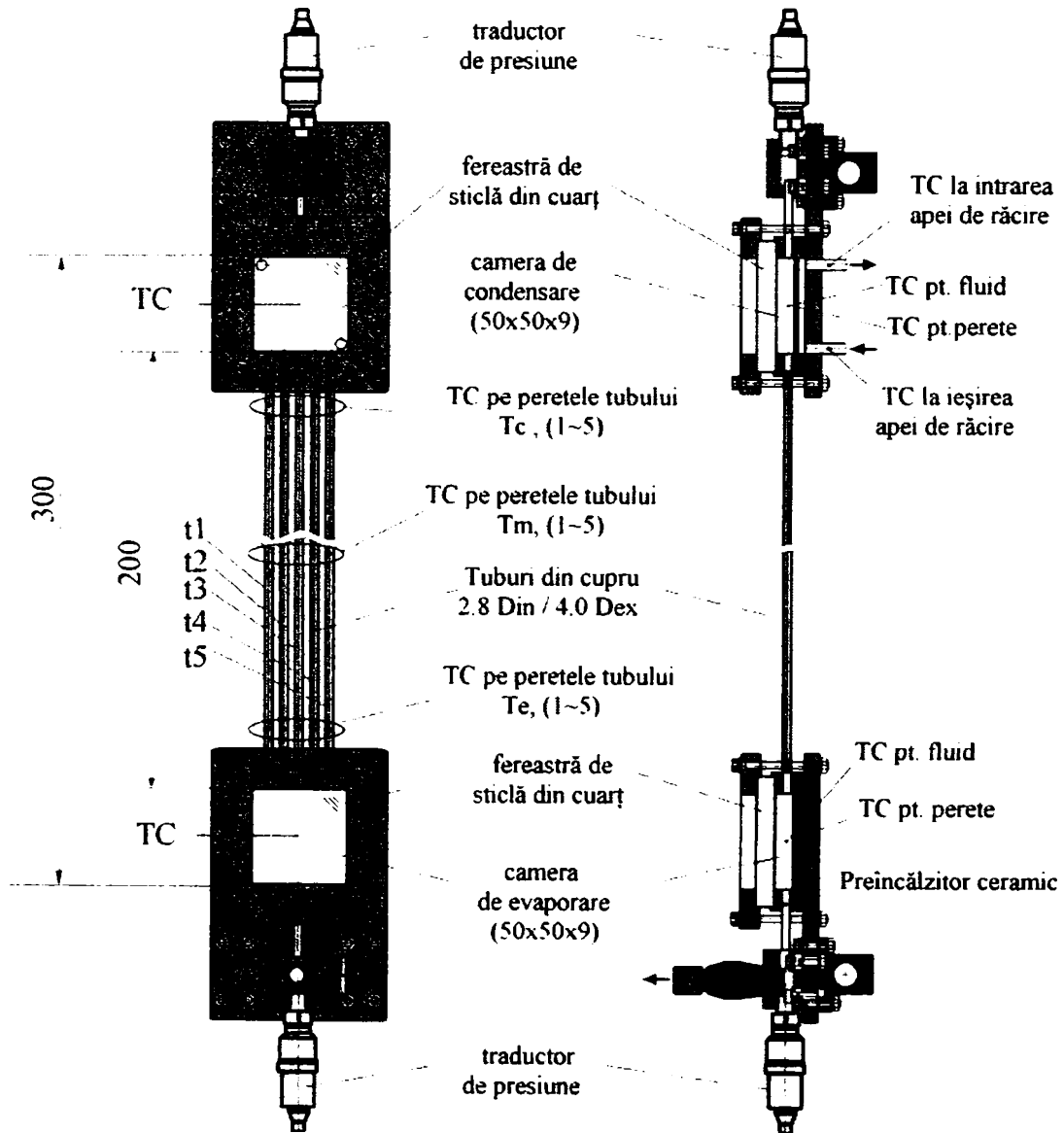


Fig. 3.1 Schița instalației cu cinci tuburi paralele

Observație: TC simbolizează poziționarea termocuplelor

3. Experimente vizând influența diferiților parametri asupra proceselor termo-dinamice

Datorită multitudinii de parametri care afectează sistemul, experimentele au fost efectuate sistematic, în diverse condiții. Au fost investigate efectele variațiilor unor parametri cum ar fi :

- orientarea spațială a instalației aleasă variabilă, cu înclinare la diferite unghiuri de la 0° la 120° față de orizontală;
- masa lichidă a fluidului de lucru, care a variat de la 20 % la 70 % din volumul total intern al sistemului;
- lungimea tuburilor, care a fost aleasă între 215mm și 750mm;
- nivelul temperaturilor de intrare (respectiv a fluxul termic introdus) între 20°C și 120°C (1W-1kW)
- debitul apei de răcire (reflectat în temperatura atinsă în condensator, respectiv fluxul termic evacuat), considerat în limitele domeniului $2 \times 10^{-6} - 10^{-5} \text{ m}^3/\text{s}$.

Pentru o mai bună înțelegere a fenomenelor generate prin acest sir de experimente logic programate s-au analizat și imaginile video înregistrate, cu viteze diferite. Ele au devenit apoi subiect de comparație cu datele prelucrate din măsurători. Faptul că s-a obținut o bună corelație între cele două metode de analiză a fost un argument puternic și temeinic care a permis interpretarea datelor, și extrapolarea concluziilor.

4. Rezultate obținute și interpretarea lor

În urma experimentelor efectuate și a rezultatelor obținute s-au conturat următoarele concluzii:

(I) Pentru instalația cu două tuburi de diametre diferite

a) - sistemul realizat și investigat poate transporta mai mult de 800 W, iar temperatura sursei de căldură (sursa caldă) este menținută sub 100 °C. Valoarea maximă a fluxului de căldură ce poate fi transportat de actualul sistem, nu a fost determinată datorită limitării puterii termice a echipamentelor utilizate (sursa de tensiune);

b) - pilotul conceput s-a dovedit a fi mult mai eficient (un flux termic de 3, 4 ori mai mare) comparativ cu sistemele convenționale de dimensiuni asemănătoare

in conditiile in care temperaturile sursei de căldură depășesc limita de 45 °C (Fig. 2.2).

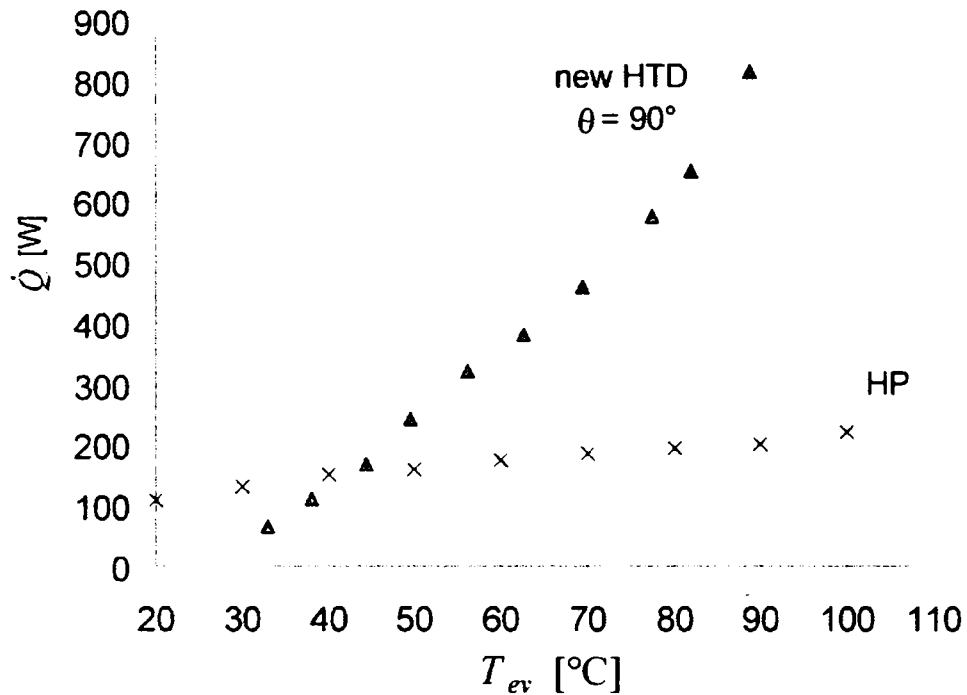


Fig. 2.2 Variația fluxului de căldură cu temperatura sursei calde (T_{ev}) comparată cu performanța unui tub termic convențional (HP) [15]

c) - performanța deosebită a instalației este atribuită mecanismului unic de funcționare. Recircularea fluidului datorată injectării intermitente a vaporilor în condensator prin tubul de diametru mai mare și întoarcerea condensatului în vaporizator prin intermediul tubului mai subțire (fig. 26, 27, 28), determină eliminarea frecării între cele două fluide ce curg în sens opus și coexistă în același mediu în cazul unui tub termic. Astfel, această limitare prezentă în cazul tuburilor termice este evitată în acest sistem. Funcționarea pilotului este dependentă de gravitație, aceasta având un rol important în recircularea fluidului și implicit a transportului de căldură. S-a demonstrat astfel că performanța cea mai bună se poate obține în condițiile în care se amplasează sistemul pe verticală, cu sursa caldă plasată la un nivel sub cel al condensatorului.

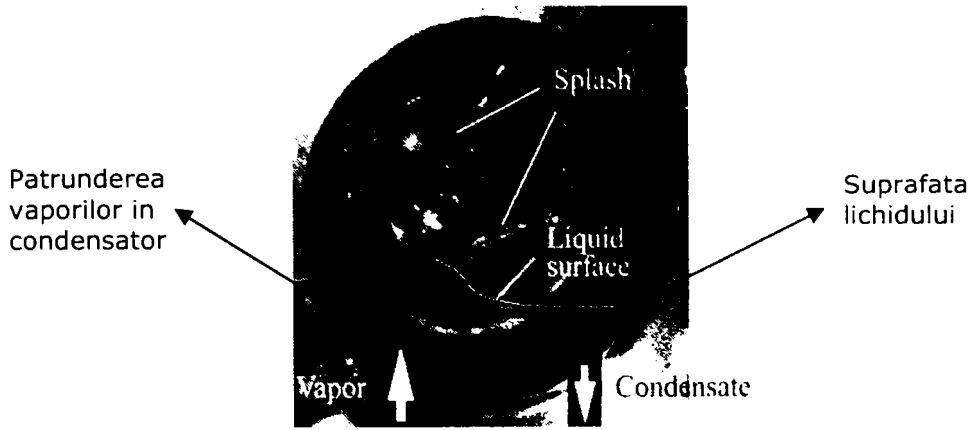


Fig. 2.6 Imagine ce evidentiaza curgerea fluidului în condensator

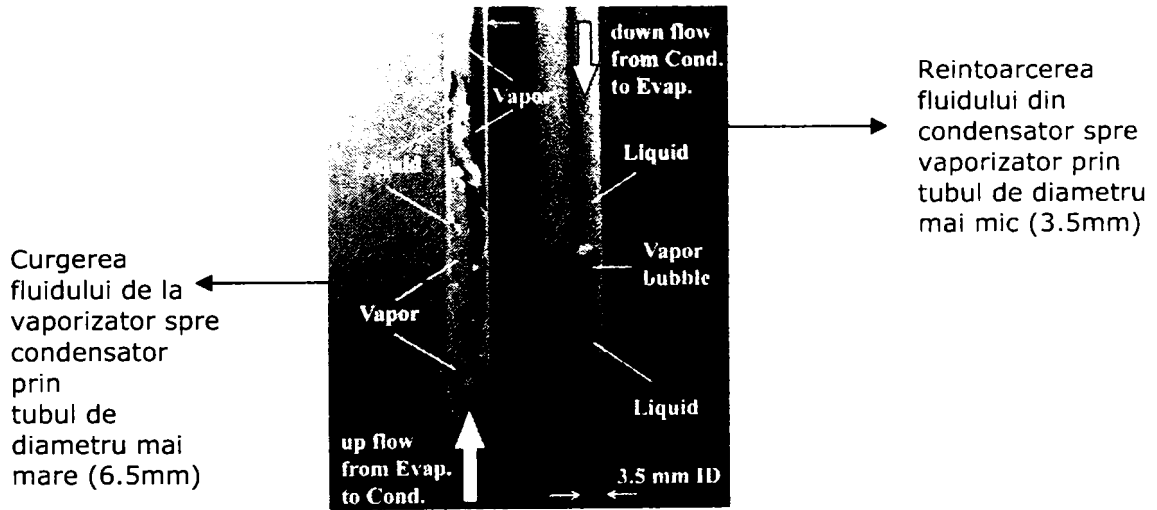


Fig. 2.7 Vizualizarea curgerii fluidului prin tuburile de teflon

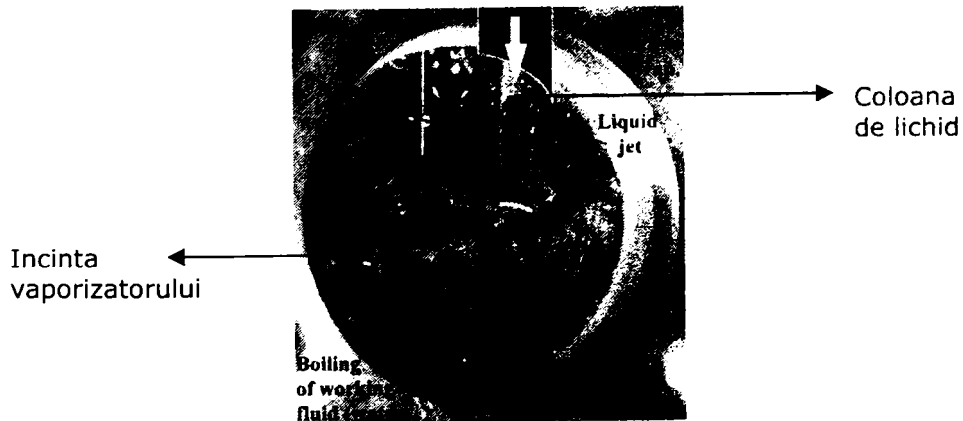


Fig. 2.8 Surpinderea pe pelicula a momentului in care se produce reîntoarcerea condensatului în vaporizator

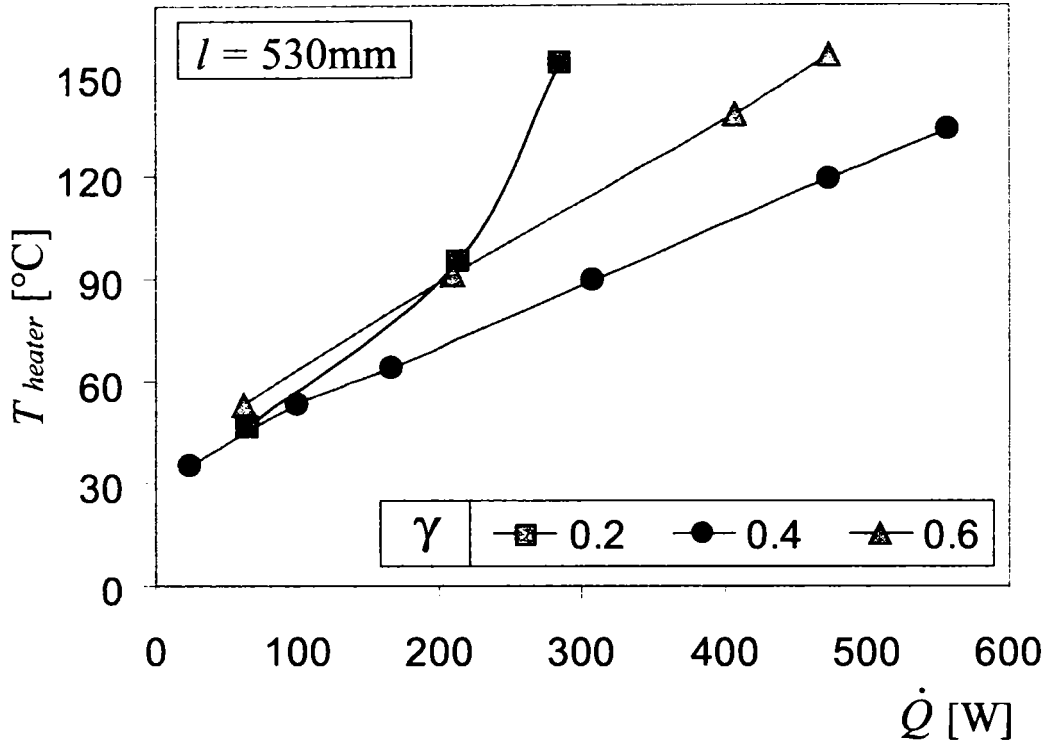


Fig. 2.21 Variația temperaturii T_{heater} cu \dot{Q} pentru parametrul γ (procentul volumic al fluidului de lucru)

d) - deși sistemul poate transporta eficient căldura pentru o gama largă a lungimii tuburilor, optimul a fost găsit pentru o lungime de 530 mm. Inițial, prin creșterea diferenței de presiune între cele două recipiente (vaporizator și condensator), recircularea fluidului s-a dovedit a fi mai intensă și automat transportul termic îmbunătățit. Ulterior însă s-a dovedit că în același timp, peste o anumită înălțime (în acest caz 530 mm), forța cu care vaporii sunt injectați în condensator scade și în acest caz performanța descrește.

e) - cantitatea de fluid utilizată are și ea un efect asupra performanței sistemului, și s-a demonstrat că valoarea optimă este un procent de circa 40 % din volumul total al instalației. În cazul unui procent mai mic, de exemplu 20 %, la temperaturi mai ridicate fierberea fiind foarte intensă, determină o rată de vaporizare foarte ridicată. Astfel, volumul de fluid este insuficient pentru a absorbi căldura produsă pe suprafața vaporizatorului, aceasta devenind astfel parțial uscată, adică necoperită de lichid. Acest fapt conduce la o creștere bruscă a temperaturii sursei de căldură și se reflectă într-o performanță scăzută a sistemului. Pe de altă

parte însă, dacă se injectează o cantitate de fluid de peste 60 % din volumul total intern al instalației, o parte din lichid se acumulează în condensator acoperind parțial suprafața acestuia, având ca și consecință reducerea performanța sistemului (fig. 2.21).

Contactul dintre fluidul de lucru și suprafața caldă (unde este generată fierberea) și de asemenea contactul cu suprafața rece (unde se produce condensul) are un rol important în performanța sistemului. Fenomenele prezente în sistem sunt complexe (fierbere, schimbare de fază și condensare), iar rolul determinant al acestora este greu de stabilit, fiecare având propria contribuție la întreaga performanță a sistemului.

(II) Sistemul cu cinci tuburi paralele de același diametru

În cazul orientării pe verticală, un fenomen interesant a fost observat și anume, modul oscilator de curgere a fluidului la temperaturi joase și stabilirea unui traseu în cazul temperaturilor ridicate. S-a constatat că neuniformitatea termică a peretelui condensatorului are o influență substanțială în modul de circulare a fluidului.

Performanța maximă obținută a fost de 600 W, sau exprimat în alți termeni, conductivitatea termică a fost de 200 de ori mai mare decât cea a cuprului. În acest sistem orientat pe verticală, maximum a fost atins când patru din cele cinci tuburi transportau vapor, iar doar unul din ele era pentru reîntoarcerea condensatului. Peste această valoare a puterii introduse în sistem, toate cele cinci tuburi au avut tendința să transporte vapor la un moment instantaneu, pentru un interval de câteva secunde. Acest lucru a condus la o creștere abruptă a temperaturii în evaporator și pentru a evita distrugerea componentelor instalației, măsurătorile au fost oprite în acest punct.

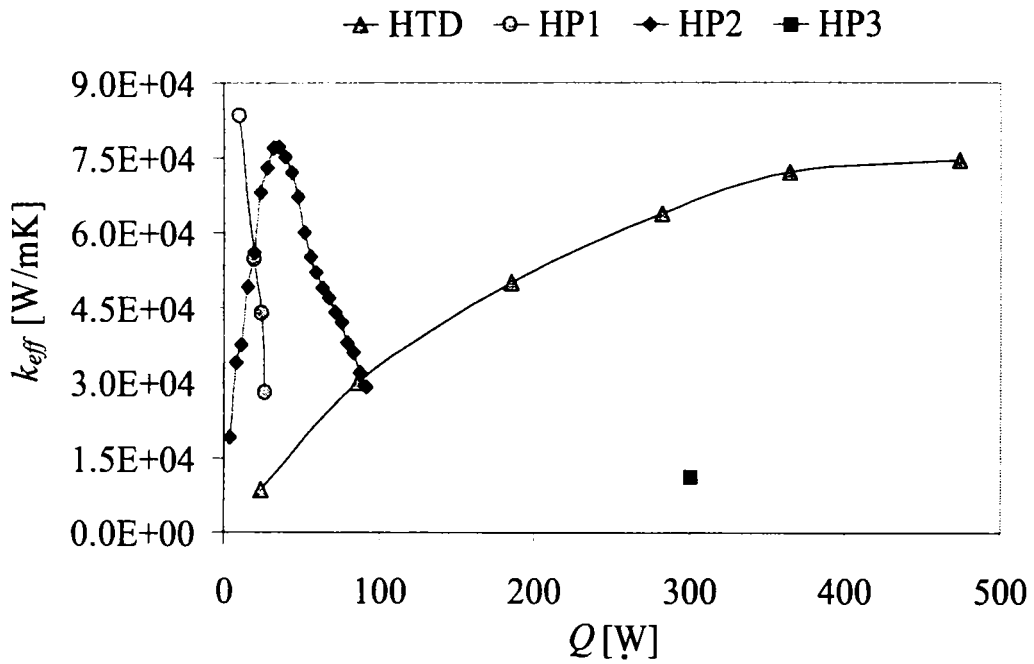
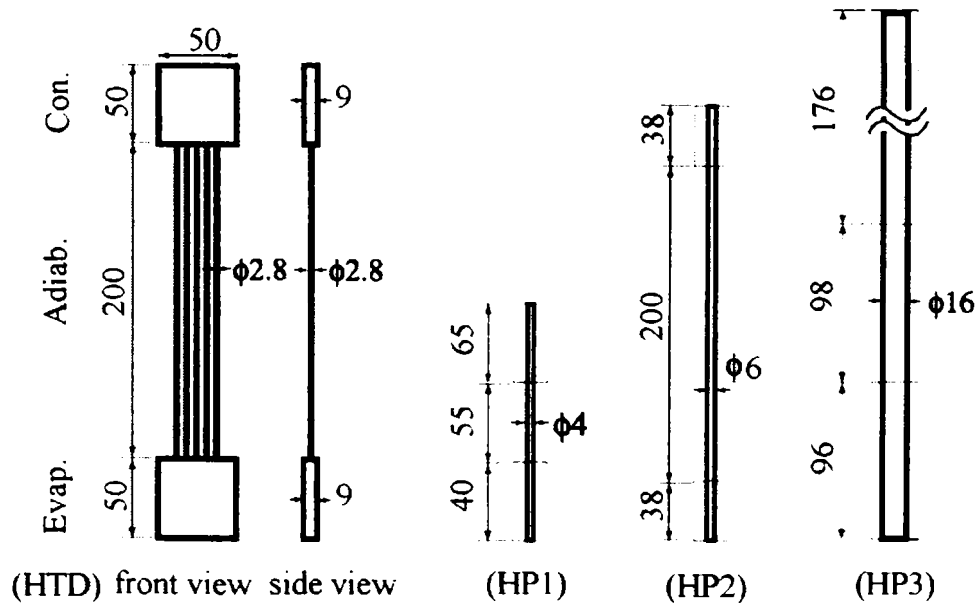
Fig.3.6 Variația conductivității termice efective în funcție de \dot{Q} 

Fig 3.7 Geometria unor tuburi termice (HP) din literatura [29, 34, 36] comparativ cu noua instalație originală propusă și experimentată (HTD)

Orientarea pe orizontală a instalației a condus la o performanță scăzută comparativ cu cea obținută în cazul orientării pe verticală și nu a fost abordată în continuare în amănunt.

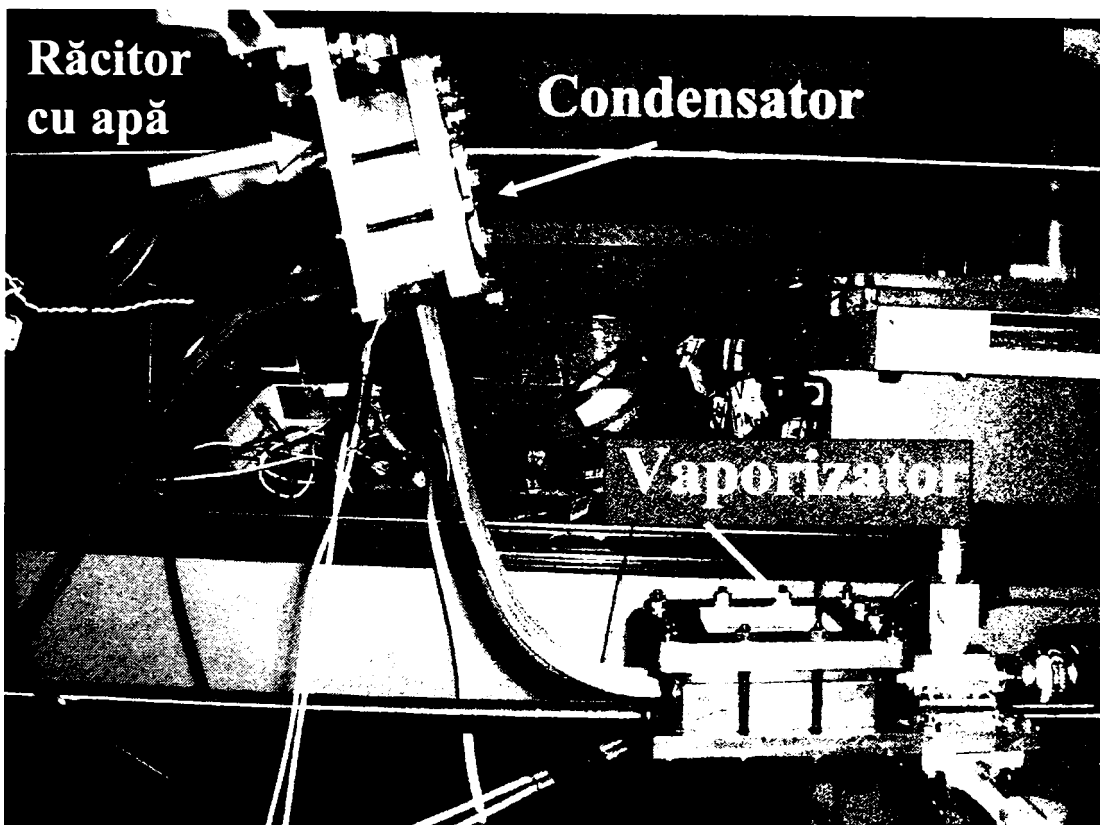


Fig. 3.3 Reprezentarea instalației cu cinci tuburi paralele și poziționarea pe orizontală a vaporizatorului

Deoarece s-a constatat din experimentele precedente cât de important este contactul dintre fluidul de lucru și suprafața caldă, respectiv cea rece, s-a realizat și experimentat o nouă poziționare a instalației (fig.3.3). Scopul în faza inițială a fost de maximizare a contactului dintre fluidul de lucru și suprafața de unde se preia căldura în sistem. Acest caz s-a dovedit a fi mai eficient decât simpla orientare pe verticală. Spre deosebire de cazul precedent, a fost evitată situația de « dry out » (apărută într-o fază incipientă în cazul anterior), iar performanța termică obținută a fost de 700 W.

A fost concepută o nouă metodă de estimare a stării fluidului în tuburile de cupru, care apoi s-a dovedit extrem de ingenioasă și a fost confirmată de a fi

credibilă, în baza unor repetate și numeroase măsurători. Astfel s-a arătat că prin măsurarea temperaturii peretelui tubului se poate estima cu bună relevanță care este faza de agregare a fluidului de lucru, adică dacă prin interiorul tuburilor curg vapori sau curge condensatul.



Fig. 3.15 Vizualizarea curgerii în condensator pentru $\dot{Q} \sim 100\text{W}$

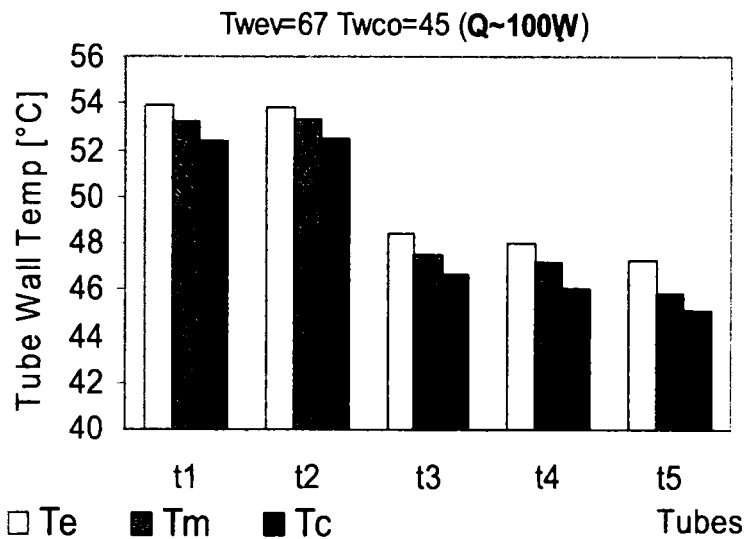


Fig. 3.16 Temperaturile medii a peretelui tubului pentru $\dot{Q} \sim 100\text{W}$



Fig . 3.17 Vizualizarea curgerii în condensator pentru $\dot{Q} \sim 200W$

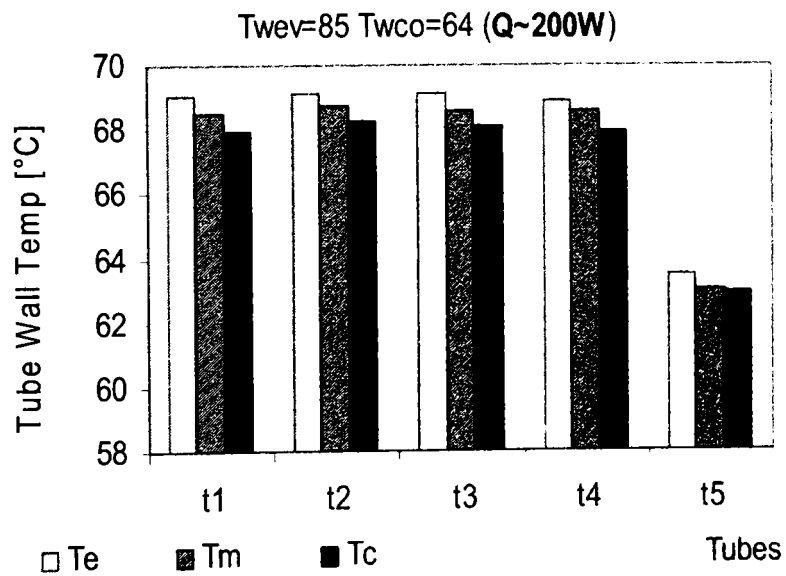


Fig. 3. 18 Temperaturile medii a peretelui tubului (în cele 3 locatii indicate in fig.3.1), pentru $\dot{Q} \sim 200W$

Utilizând o camera digitală a fost înregistrată și curgerea fluidului în condensator. Astfel prin intermediul ferestrei de sticlă prevăzută cu acest scop s-au luat imagini relevante și impresionante ale unor fenomene reale, care au contribuit ulterior și au permis, prin încetinirea frecvenței de proiectare, secvențializarea și etapizarea fenomenului complex. Între înregistrările video și măsurătorile efectuate s-a obținut o bună corelare (fig. 3.15, fig. 3.16, fig 3.17, fig 3.18).

5. Concluzii generale și contribuții personale

Aspectele tratate și prezentate prin redactarea lucrării de doctorat sunt novatoare și cuprind un număr mare de experimentări, efectuate cu forțe proprii, pe instalații de concepție originală. Se demonstrează că studiul fenomenelor de transport al căldurii prin schimbarea de fază a fluidului de lucru într-un sistem special conceput cu tuburi paralele contribuie la îmbunătățirea sistemelor de răcire convenționale. Rezultatele prezentate sunt bazate pe experimente efectuate în laborator, utilizând instalații pilot de scară redusă, special concepute pentru elucidarea problemelor și atingerea scopurilor de cercetare impuse de tematica tezei. Datele obținute au fost comparate cu cele ale echipamentelor de răcire convenționale existente și s-a constatat că instalațiile pilot concepute s-au dovedit mult mai performante. De asemenea, eficiența acestora este explicată și argumentată de unicitatea fenomenelor observate. Ideea novatoare a sistemelor de transport a căldurii, utilizând tuburi paralele interconectate la ambele capete prin două rezervoare, a fost pusă în aplicație pentru prima oară în cadrul Laboratorului Mochizuki din Universitatea de Agricultură și Tehnologie din Tokyo. Spre deosebire de multitudinea cercetărilor efectuate pentru înțelegerea mecanismului de funcționare și îmbunătățire a performanței tuburilor termice (heat pipe) și a buclelor spiralate închise (meandering closed loop), în literatura de specialitate analizată pentru documentare nu s-a identificat nici o referință legată de un sistem asemănător cu noul concept dezvoltat în cadrul cercetărilor doctorale prezente. Singurele publicații disponibile în domeniu au fost cele ale lui Onishi [27, 28] și cele ale autoarei acestei teze, Cîrtog [38, 39, 40, 41, 42, 43, 44, 45, 46]. Pentru a ajunge la această concluzie însă s-au parcurs numeroase titluri bibliografice [1-26, 29-37, 47-51] din toate extragându-se avantaje, idei care au indus apoi altele și dezavantaje care trebuiau evitate.

Instalațiile prezentate în aceasta lucrare au fost concepute, realizate, asamblate și utilizate doar de autoarea acestei teze. De asemenea, construirea echipamentelor auxiliare, stabilirea parametrilor de lucru, experimentele, măsurătorile și analizarea datelor au fost efectuate și integral planificate de către autoare. Diversele soluții constructive precum și metode de verificare a rezultatelor au fost elaborate și testate. De exemplu, o îmbunătățire adusă celui de-al doilea sistem prezentat în această lucrare, a constat din sudarea țevelor de cupru și eliminarea conectorilor folosiți în cazul primei instalații, pentru a atinge și asigura o mai bună etanșeitate în timp. Nu au existat colaboratori în tot lanțul de cercetări întreprins. Ideile sunt originale, iar etapele de lucru au fost stabilite sistematic. Inițial s-a plecat de la ideea creșterii performanței sistemelor de răcire prin separarea celor două faze ale fluidului de lucru în cele două tuburi ale instalației pentru obținerea unei recirculări continue și astfel evitarea situației de uscare a vaporizatorului « dry out ».

Lucrarea de față tratează modalități de îmbunătățire a sistemelor de transport a căldurii. Două instalații nou concepute au fost investigate experimental și ambele s-au dovedit a fi eficiente în transportul căldurii de la sursa caldă la cea rece. Toate etapele, de la construirea instalației până la punerea într-o formă finală a rezultatelor este contribuția proprie a autoarei acestei teze. Fenomenele observate sunt unice și au fost pentru prima dată descoperite de către autoare. Faptul că rezultatele prezentate în această lucrare au fost anonim recenzate și public dezbatute sau prezentate la conferințe internaționale și publicate în jurnale de prestigiu [38, 39, 40, 41, 42, 43, 44, 45, 46] este încă o dovadă a recunoașterii științifice și corectitudinii teoriei dezvoltate și a concluziilor trase din experimentări și analizele teoretice.

Comparativ cu sistemele convenționale existente, ambele instalații pilot de laborator au dovedit o performanță termică mai ridicată, fiind capabile să transporte eficient fluxuri de până la 800 W și respectiv 700 W. Instalațiile nu au fost de la bun început concepute cu un scop aplicativ concret, ci pentru a studia școlastic și în amanunt fenomenele ce apar în cadrul transportului de căldură, pentru a le înțelege mecanismul de funcționare. Doar după o analiză amănunțită a tuturor factorilor ce influențează performanța sistemului, acesta a putut fi îmbunătățit, ceea ce de fapt s-a și dovedit prin cele două instalații concepute, cu particularitățile lor distincte.

După îndelungi teste și combinând serii de parametri ce induc influențe, au fost identificate, explicate și apoi descrise condițiile optime de funcționare. Dacă în faza

inițiala cercetările au fost derulate mai mult pe intuiție sau pe ipoteze și presupuneri teoretice, ulterior s-au concretizat rezultate practice și s-a putut descrie destul de simplu un fenomen complex. Remarc și faptul că, unele aspecte fenomenologice observate au fost cu totul neașteptate, fără putinta unei anticipări. Lucrarea de față, prin rezultatele prezentate, aduce o nouă și certă contribuție atât teoretică, cât și practică în domeniul transportului de căldură. Tematica abordată este de interes și are deschidere spre continuare. Se considera că primii pași au fost făcuți într-o nouă direcție iar orizontul este deschis pentru continuarea lor.

Titluri recent publicate în colecția „TEZE DE DOCTORAT” seria 9: Inginerie Mecanică

1. **Gheorghe-Vasile Abrudan** – *Contribuții teoretice și experimentale privind aplicarea șocurilor în procesul de lucru al separatorului cu bandă, de la mașinile de treierat mazăre, ISBN 978-973-625-567-0, (2007);*
 2. **Ioan Goia** – *Studiul influenței ansamblului roată – șină în condiții de exploatare asupra structurii liniei de tramvai, ISBN 978-973-625-582-3, (2007);*
 3. **Adrian Aristide Voicu** – *Studiul biocompatibilității implantelor chirurgicale din aliaje de titan în organismul uman, ISBN 978-973-625-502-1, (2007);*
 4. **Alin-Daniel Rus** – *Studii și cercetări asupra comportării mecanice a unor materiale compozite pentru frânarea vehiculelor feroviare, ISBN 978-973-625-596-0, (2008);*
 5. **Luisa-Izabel Dungan** – *Contribuții la studiul și cercetarea comportării arcurilor de tip flexicoil de la locomotiva electrică CFR 060-EA de 5100 kW, ISBN 978-973-625-599-1, (2008);*
 6. **Gabriel-vasile Ursu-Neamț** – *Contribuții la optimizarea parametrilor cuplei elastice și a influenței acesteia asupra circulației în curbă a locomotivelor cu boghiuri articulate, ISBN 978-973-625-602-8, (2008);*
 7. **Gheorghe Cornea** – *Cercetări asupra rigidității unei mașini pentru încercări de conductori și cabluri cu lungimi de peste 10m, (2008);*
 8. **Ionică Cărăbaș** – *Contribuții privind biomecanica și recuperarea postoperatorie a articulației genunchiului cu implant restaurador total, ISBN 978-973-625-636-3, (2008);*
 9. **Lelia Dobjanchi** – *Contribuții privind aportul centralei pe cărbune ROMAG TERMO la poluarea aerului și măsuri pentru reducerea acesteia, ISBN 978-973-625-628-8, (2007);*
 10. **Gheorjon Lorand Toth** – *Studiul influenței construcției și condițiilor de utilizare asupra fiabilității cablurilor de oțel, ISBN 978-973-625-539-7, (2007)*
-



EDITURA POLITEHNICA